Humboldt-Universität zu Berlin – Geographisches Institut

Dissertation

Quantification of soil properties for analyzing surface processes using spectroscopy and laser scanning

zur Erlangung des akademischen Grades
doctor rerum naturalium

eingereicht von
Sören-Nils Haubrock

an der Mathematisch-Naturwissenschafltiche Fakultät II
Dekan: Prof. Dr. Wolfgang Coy

Gutachter:

Prof. Dr. Patrick Hostert

Prof. Dr. Hermann Kaufmann

Prof. Dr. Eyal Ben-Dor

eingereicht: 8. Dezember 2008
Datum der Promotion: 23. April 2009

Acknowledgments

This thesis is the result of several years of research performed at the German Research Centre for Geosciences (GFZ). There are many people that supported me in various ways, but special thanks go to my colleagues, friends and family for their very own contribution to this work.

Hermann Kaufmann and *Patrick Hostert*, for their support, encouragement and patience during the last years. *Charly*, thank you for giving me the opportunity to find my way back to the research community after years working in the industry. You offered me a perfect framework for developing my scientific skills while making best use of my former experiences. You made working in your lab not only interesting, but also enjoyable, not least due to your Bavarian brand mark. *Patrick*, you were an invaluable help for improving the science in my work, providing me the opportunity to work with your team and by helping me in organizing the formal matters. When I needed your support, I could always rely on your competency, open mind and confidence.

Eyal Ben-Dor for interesting discussions with you in Warsaw and at GFZ, for asking challenging questions about my work and for developing interesting ideas with me for future publications. I thank you for your uncomplicated and spontaneous consent to be reviewer of this thesis.

Sabine Chabrillat. From the first day on that I worked for this project, you were an excellent coach for me, always taking your time and giving me the support that I needed to improve the way I was doing research, while leaving me the opportunities to „cut my own path“ through the world of science. Even in those difficult moments where progress was not visible, I was sure that I could count on your support. Working with you was not only successful, I also enjoyed the time together at conferences, workshops and during field trips. Sabine, you probably know how important your role for this thesis is. Thank you so much!

Matthias Kuhnert and *Christine Lemmnitz* for the great collaboration within this interdisciplinary project. Thank you both for your willingness to share resources and results as well as for the time you spent with me collecting data, testing and improving our methods. *Matthias*, it was a pleasure to work with you and to share successful and difficult moments. Your fascination about doing research out in the field, your ideas and motivation deeply impressed me. Thank you also for introducing me into the culinary culture of Lower Lusatia. It was great fun to work with you!

My colleagues from the remote sensing lab at GFZ *Karl Segl, Sylvia Magnussen, Jan Anderssohn, Sibylle Itzerott, Daniel Spengler, Hans-Ulrich Wetzel, Mathias Bochow, Nicole Richter* and *Sigrid Rössner* for always being welcome when I needed your help or a cup of coffee. *Sylvia and Karl* for your invaluable and prompt technical support and for your assistance with the more complex software systems whenever needed. *Jan* for the enjoyable time that we shared in our office and for the various offers to improve my sailing experience on your boat – I'm sure that we will finally manage to spend some time on the water. *Daniel* for the work together in the laboratory and field and the support in analysing various datasets. *Sibylle* for your ideas, discussions and openness when I was struggling to justify new and uncommon ideas. *Uli*, I appreciate your open-minded character and commitment for your colleagues. And I am still impressed by your indescribable historical knowledge that you shared with us junior scientists during numerous walks to the canteen.

Ramona Baran, *Katrin Zabel* and *Steffen Leider* for your work in laboratory and field with the laser scanner, and especially for carrying out large parts of the intense data processing tasks.

Heiko Thoss, *Andreas Güntner* and *Benjamin Creutzfeld* from the Hydrology lab at GFZ for the efficient and diversified work together in the field and for having a great time together during and beyond office hours.

Doris Dransch for your indefatigable support allowing me to finish working on this thesis parallel to my every-day-business at GFZ.

The colleagues from the Humboldt University Geomatics group, especially *Tobias Kümmerle* and *Sebastian van der Linden,* for their kindness and support in organizational and technical issues as well as the great work on the final document template!

Sonja Germer for her proofreading at the very end of the writing stage.

The people who gave me the most valuable support were the closest ones around me. I deeply thank my parents for doing everything they could to allow me getting this far.

Jenny and Malik - thank you so much for your love and support that I have felt every single day. Now it's your turn, and I will try to give it all back to you…

Abstract

Soil processes taking place in the context of erosion and land degradation are highly dependent on the properties of the surface. While the causes and effects of such processes are commonly well understood on a conceptual level, there is a lack of adequate data sources allowing for their quantification at various spatial scales. The main goal of this thesis was to assess the role of state-of-the-art remote sensing methods for the quantification of soil properties with the aim to improve the understanding of surface processes taking place in a degraded landscape. The chosen study area of 4 ha size located in a lignite mine in eastern Germany allowed for a comprehensive, interdisciplinary and multi-temporal analysis of surface properties based on remote sensing, pedological and hydrological measurements over the years 2004 and 2005. The quantification of surface soil moisture as an important variable for infiltration and runoff processes has been the objective in laboratory and field spectroscopic experiments as well as in airborne hyperspectral measurements. The newly developed *Normalized Soil Moisture Index (NSMI)* was identified as the most robust quantifier for surface soil moisture in sandy substrates in the field. Surface roughness was successfully quantified at high precision in form of novel multiscale indices derived from datasets collected with a stationary laser scanning device. The analysis of spatiotemporal roughness distributions allowed for the detection of distinct patterns that developed under the influence of soil erosion in the field. Observed substrate movements could be linked to the changes in both surface properties that were quantified in this study based on remote sensing technologies. The thesis developed a set of methods and indices that successfully implement the quantification of surface soil moisture and roughness in the field. For an increasing number of regions in the world suffering from land degradation, the application of these methods promises further insights into the details of soil erosion processes taking place as well as the collection of invaluable datasets to be used for soil erosion monitoring and modeling campaigns in the future.

Zusammenfassung

Oberflächennahe Bodenprozesse werden durch die dynamischen Eigenschaften der Bodenoberfläche besonders beeinflusst. Zwar sind die kausalen Zusammenhänge dieser Prozesse weitestgehend bekannt, doch gibt es einen Mangel an verfügbaren Datenquellen und Erhebungsmethoden, die es erlauben, die Prozesse auf unterschiedlichen Skalen zu quantifizieren. Das Ziel dieser Arbeit bestand darin, das Potential ausgewählter moderner Fernerkundungstechnologien zu bewerten, relevante Bodeneigenschaften zu quantifizieren und damit das Verständnis von oberflächennahen Prozessen in degradierten Landschaften zu verbessern. Das Studiengebiet befand sich in einer Rekultivierunglandschaft des Niederlausitzer Braunkohletagebaus Welzow-Süd. Die Größe von 4 ha ermöglichte eine umfassende, interdisziplinäre und multi-temporale Analyse der Bodeneigenschaften auf Grundlage von Fernerkundungsmethoden sowie hydrologischen und bodenkundlichen Feld- und Labormessungen in den Jahren 2004 und 2005. Die Quantifizierung der Bodenfeuchte als eine entscheidende Variable für Infiltrations- und Abflussprozesse war das Ziel von labor- und feldspektroskopischen Messungen sowie von hyperspektralen Flugzeugscanner-Messungen. Der hierbei entwickelte *Normalized Soil Moisture Index (NSMI)* wurde als optimales Quantifizierungsmodell für Oberflächen-Bodenfeuchte in den sandigen Substraten im Feld ermittelt. Bodenrauhigkeit wurde in hoher Präzision durch Anwendung eines stationären Laserscanners gemessen und in Form neuartiger multi-skalarer Indizes quantifiziert. Die Analyse der raum-zeitlichen Verteilungen ermöglichte die Identifizierung von Rauhigkeitsmustern, die unter dem Einfluss der Erosion im Feld entstanden. Beobachtete Substratverschiebungen wurden durch beide angewandten Methoden erkennbar. Diese Arbeit entwickelte neuartige Methoden und Indizes zur Quantifizierung von Oberflächen-Bodenfeuchte und Rauhigkeit im Feld. Für die zunehmende Zahl an degradierten Regionen auf der Erde verspricht deren Anwendung die Entwicklung eines tieferen Verständnisses von Bodenerosionsprozessen sowie die Sammlung wertvoller Daten für zukünftige Monitoring- und Modellierungskampagnen.

Contents

List of Figures

List of Tables

Chapter I:
Introduction

1 Soil surface processes in the context of global change

The surface of planet Earth has undergone significant changes since the time of the industrial revolution in the 19th century (Steffen et al. 2004). Drastic changes in climate, land use forms, settlement distribution as well as extensive pollution have formed significant pressure on ecosystems at local to global scales. Today, no place on Earth remains unaffected by human living (Vitousek et al. 1997), either directly through land use and exploitation, or indirectly due to climate change responses and pollution. With ongoing trends expected for the near future, a need for monitoring and understanding their consequences for natural environments at the local scale has been recognized. The integrative nature of climate change problems requires science to include integrative elements in the search for solutions: a willingness to apply interdisciplinary science and a strengthening of the interface with decision-makers (Howden et al. 2008).

Land degradation, commonly defined as the temporary or permanent decline in the productive capacity of the land (Food and Agriculture Organization of the United Nations), caused directly or indirectly by human influences, reflects global change patterns on land surfaces. In dryland regions, where land degradation is referred to as desertification, the impact for ecosystems and human life is particularly severe. The awareness of an ongoing large-scale desertification process emerged for the first time between 1968 and 1973, when the African Sahel region was seriously affected by an extreme drought (Babaev 1999). Today, drylands cover about 41% of Earth's land surface and are inhabited by more than two billion people (Adeel et al. 2005).

In the last years, the controlling factors of land degradation processes were analyzed in various studies covering semi-arid and arid regions of the world (Howden et al. 2008; Marker et al. 2008; Wang et al. 2008), generally confirming the assumption that climate change and direct human influence are significant drivers of this process. The hydrological cycle, especially its terrestrial sphere, has been identified as one of the most impacted components of the Earth system by ongoing global change trends (Steffen et al. 2004). Climatic change acts upon the underlying processes by e.g. more intense precipitation events, droughts, and subsequent loss of vegetation. In combination with land degradation phenomena, local processes in the hydrological cycle are increasingly imbalanced and often result in soil erosion.

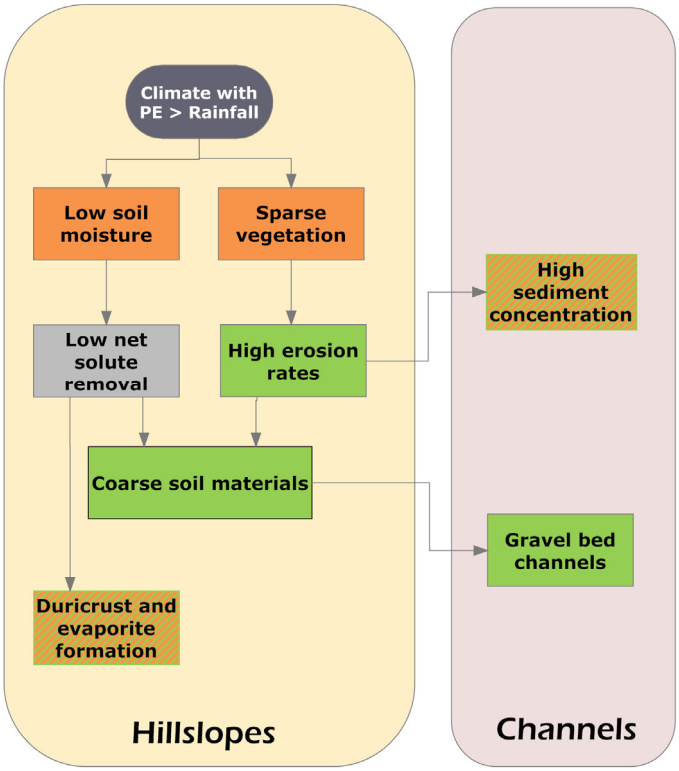

Figure I-1 Dominant geomorphologic processes and impacts in dryland environments. (Bull and Kirkby 2002)

A thorough understanding of surface processes in space and time is crucial for coping with challenges arising from an increasingly significant impact of soil erosion in many regions of the world. Today it is known that different soil surface characteristics control runoff, infiltration, soil moisture and temperature regimes, and are important factors governing badland evolution and geomorphologic behavior (Gallart et al. 2002). Bull and Kirkby (2002) gave a conceptual overview of surface processes and their impacts in dryland environments with respect to soil erosion (Figure I-1). Typical scenarios of local soil surface processes in dryland environments are triggered by system states in which evapotranspiration exceeds precipitation throughout the year, soil moisture is low, and vegetation cover is sparse. Overland flow and hillslope erosion by wash processes are a consequence of occasional intense rainfall events, resulting in erosion and subsequently in heterogeneous surface conditions with respect to substrate and grain size distribution, duricrust and channel formation.

While the causes and effects in these geomorphologic process chains are well comprehensible at the conceptual level, the detailed processes taking place at the small scale are very complex and not yet fully understood. Several factors make the appreciation of local surface processes challenging. Firstly, soils and especially soil surfaces are highly

heterogeneous due to dynamic influences by external forces from the hydrosphere, atmosphere, biosphere and lithosphere. The uppermost soil layer is hereby not only the most dynamic part of the pedospheric system, it is also the most vulnerable compartment to soil degradation processes (Marques et al. 2008). Additionally, surfaces of the pedosphere underlie significant temporal changes, in time spans ranging between seconds (like substrate displacement due to wind erosion) and some 100 years (weathering and subsequent soil formation). Secondly, in natural environments, surface processes are challenging to comprehend due to the abundance of influencing factors as opposed to a general lack in data due to laborious measurement techniques. In response to this discrepancy, the modeling of the processes can either be generalized resulting in a loss of accuracy and process understanding, or a significantly larger data basis and model complexity needs to be provided.

Soil surface properties playing a crucial role in these processes according to Figure I-1 are soil moisture, (micro-) topography incl. grain size distributions, and crusts. These soil properties are dynamic in their spatiotemporal distribution, so a high temporal resolution of measurements would be necessary to monitor them in the field and to assess their role in surface processes quantitatively.

2 Prospects of contemporary remote sensing technologies

In the context of soil surface process studies, remote sensing technologies bare high potential for collecting data used for analysis and monitoring purposes in an efficient way. While in-situ physical measurements have been applied for many years in soil science and hydrology to analyze soil properties and processes, their application is associated with certain limitations and side effects. Firstly, data collection in the field is in most cases performed through physical contact of the sensor with the surface. The property of the surface is hereby often changed and will therefore potentially affect surface processes taking place afterwards. This is particularly relevant when processes at the microscale are of interest. Measuring for example soil moisture with a physical device will leave behind a soil layer affected by the instrument, which in turn can modify future soil moisture values. When in-situ data collections cannot be performed directly, sampling in the field and subsequent analysis in the laboratory is a common procedure. The surface and deeper layers in the soil column are often severely affected around the sampling locations.

Secondly, in-situ measurements and sampling are in most cases restricted to single spots rather than covering continuous areas. With increasing density and number of point measurements, an approximation of two-dimensional data sets can be achieved. This approach is, however, often not practicable, laborious and expensive and might result in overly surface disturbances. Moreover, characterization of the spatial variability exclusively based on point sampling and analysis is insufficient.

Thirdly, the quantification of surface properties makes sampling and measurements of the uppermost layer necessary. Separating the very surface from deeper layers is hard to achieve based on sampling or measurements using physical devices. Especially under field conditions, side-effects like surface crusts and organic matter can make this separation impracticable.

Finally, measuring from airborne or spaceborne platforms bares the potential to collect data covering remote regions in the world in the case that the spatial resolution and coverage of the measurements correspond with the scale of the soil properties under survey.

Optical methods provide a means to overcome the challenge of collecting data on surface properties in an efficient – and by avoiding local disturbances – sustainable way. Over the years, remote sensing techniques have continuously improved and expanded to the point, that they now have the potential to cover most parts of the electromagnetic spectrum relevant for environmental surveys at high resolutions. Different sensor types are nowadays able to provide unique information about properties of the surface or shallow layers of the Earth at various spatial scales.

The variables in Figure I-1 are colored according to their measurability characteristics: (1) surface properties reflecting physico-chemical constituents (red color) and (2) properties of the topographical surface structure (green color). Optical methods are particularly suitable to measure physico-chemical surface properties, i.e. soil moisture, vegetation cover and crusts (due to their mineralogy and organic matter). Reflectance values and their relation to surface materials, properties and structures have been studied since the 1920s (Angström 1925). Spectroscopy has been used in laboratory studies of various disciplines, such as physics, chemistry, and biology, to investigate material properties making use of the interaction of electromagnetic radiation with matter (Green et al. 1998). Baumgardner (1985) summarized typical reflectance properties of natural soils based on laboratory measurements. In the last couple of years, various studies examined soil parameters in laboratory and field measurements based on high-resolution spectroscopy covering the

visible (VIS) to shortwave infrared (SWIR) spectral range (350 to 2500 nm) at spectral resolutions as little as 1 nm. Relevant variables for soil erosion included surface crusts (Goldshleger et al. 2001; Goldshleger et al. 2002; Eshel et al. 2004; Goldshleger et al. 2004a) and soil moisture (Muller and Décamps 2000; Lobell and Asner 2002; Weidong et al. 2002; Weidong et al. 2003; Bogrekci and Lee 2004).

Imaging spectroscopy – the transfer of laboratory and ground based spectroscopy technology to airborne and spaceborne remote sensors – has gained widespread interest in the past 10 to 15 years as a remote sensing technique that allows for quantitative determination of the abundance and composition of Earth surface materials at the subpixel resolution level (Goetz et al. 1985; Goetz and Curtiss 1996). Airborne hyperspectral data have been applied to measure various natural land cover constituents, like vegetation, soil or water bodies, generally demonstrating its great potential considering their quantification. Many measurements that are impractical or impossible to perform with a multispectral sensor system can be accomplished with imaging spectroscopy, as studies on geological mapping and lithological discrimination (Farrand and Harsany 1995; Kruse 1997; Chabrillat et al. 2000; Schodlok 2004) or the analysis of biophysical properties like canopy water content, chlorophyll content or leaf biochemistry (Ustin et al. 2004) show.

Just recently, Ben-Dor et al. (2008) gave a detailed overview of state-of-the-art case studies applying imaging spectroscopy for soil science studies. They found that this technology has already successfully been applied to measure soil properties like salinity, chemistry, or contamination. By combining different quantification models on the abundance of the soil's constituents, soil classifications in general are believed to be feasible when background information about the properties of these soil classes is given. The authors concluded that soil scientists have recognized the potential of this novel technology in their field. However, their use remains undeveloped and seldom reported in the literature.

While reflectance measurements can be linked to surface properties that represent biochemical and physical characteristics, they need to be supplemented when microtopography of soil surfaces is of interest. In the context of soil erosion studies, surface patterns that are represented by microtopography models are crucial and need to be detected and quantified for understanding the underlying processes. The spatial distribution of elevation, slope and roughness is important for erosion phenomena (Kirkby 2001). When applying multi-temporal monitoring, these spatial patterns can even be linked to corresponding processes like the segregation of fine and coarse material, the identification

of erosion and accumulation zones as well as the differentiation of zones (e.g. rill and interrill areas). Laser scanning represents a technology that is suitable for deriving surface elevation models at various spatial scales. For monitoring processes at the microtopography scale, stationary devices offer a way of delivering models in sub-millimeter resolution (Huang and Bradford 1992).

While point laser instruments with a much broader spatial resolution have been applied in several laboratory (Bertuluzzi et al. 1990; Huang and Bradford 1990; Römkens et al. 2001) and some field studies (Solé-Benet et al. 1997), the potential of devices generating three-dimensional datasets based on triangulation methods has been discovered just recently (Schmid et al. 2004; Bryant et al. 2007). However, the suitability of these instruments to quantify soil properties related to erosion in the field has yet to be analyzed.

In summary, recent studies have proved that state-of-the-art remote sensing represents promising technologies when surface characteristics of soils need to be measured in a comprehensive and efficient way. Their potential to complement or even substitute in-situ data collection procedures has, however, only marginally been analyzed in interdisciplinary field studies. Instead, many research results so far have been confined to laboratory experiments or tried to quantify small scale processes with broad scale methodologies. For understanding surface processes emerging in the context of soil erosion and land degradation, a more comprehensive view on the complexity of these processes and phenomena is necessary. Recent studies analyzing the opportunities of remote sensing for monitoring dryland regions were mostly focused on the assessment of vegetation cover (Okin and Roberts 2001). The analysis of soil properties is, however, important for the understanding of the soil surface processes, and field studies are in particular necessary to take into account the spatial and temporal heterogeneities of soil properties and resulting influences by covariates. The potential and limitations of contemporary remote sensing technologies in quantifying soil properties while coping with disturbances need to be further analyzed in the context of interdisciplinary case studies.

3 Research questions and approaches

Against the background of the successful application of remote sensing methods in other research domains and recent technological developments, their potential to provide data for a better understanding of soil surface processes is obvious. *The overall goal of this thesis is therefore to develop quantification models based on state-of-the-art remote sensing technologies to monitor soil surface properties in a confined study site exhibiting soil erosion, and to assess the potential and limitation of these methods to contribute to an improved understanding of surface processes in field studies in general.*

This thesis is an integrative part of an interdisciplinary study focusing on the quantification of near-surface processes for the characterization of soil properties, erosion and water regime (Kuhnert et al. 2004). The approach of this thesis is therefore characterized by monitoring and analysis activities at the test site Welzow-Süd. The quantification of soil surface properties, their spatial distribution and change in time are of specific interest here. The study site provides unique opportunities to perform research on soil surface and near-to-surface processes over multiple hydrological seasons. Coupling remote sensing measurements with field data and experiments as well as sampling and subsequent laboratory analyses allowed for deriving information about soil properties and surface processes over the years 2004 and 2005 taking place at the micro- to hillslope spatial scales. According to Gallart et al. (2002), the approach followed here to monitor erosion processes can be classified as short-term method (1-10 years) with respect to the temporal scale. Conformant with this classification, the study involved a monitoring program, but used – in contrast to traditional approaches – in large part remote sensing technologies instead of in-situ devices.

With respect to the paramount surface processes taking place in dryland regions according to Figure I-1, the potential of state-of-the-art remote sensing technologies for a better understanding of these processes was analyzed. Firstly, the possibility of extracting surface soil moisture values from high spectral-resolution reflectance data has been scrutinized and resulted in

Research question I: What is the potential of reflectance-based soil moisture quantification models in natural environments and how are they affected in comparison with laboratory set-ups?

Measurements in natural environments generally have to deal with much higher heterogeneity and significant side-effects compared to laboratory studies. However, the influence of these factors on reflectance values has been neglected in many studies, in which analyses were performed on cleaned and further manipulated soil samples in the laboratory. In order to find a quantifier that can be applied in the natural environment, the difference between model outcomes when being applied in these traditional laboratory set-up on one side and with unprepared samples on the other needs to be analyzed. This is especially important in the context of soil erosion analysis, since covariates like substrate compositions, surface crusts, roughness and vegetation cover act upon reflectance values and need to be taken into account.

Research question II: *Are soil moisture quantification models applicable to airborne hyperspectral sensors (imaging spectroscopy) and under which terms can the resulting data sets be integrated into surface process analysis?*

For quantification models that generate appropriate results under laboratory and field conditions, additional challenges arise when measurements are performed from remote sensors, such as dealing with spatial heterogeneity, contamination of the atmosphere, and low signal-to-noise ratios (Ben-Dor et al. 2008). With larger scales, the heterogeneity of each image pixel and likewise the effect of covariates are likely to increase, which makes the analysis of the effect of lower spatial and spectral resolution necessary.

At the same time, airborne sensors are a promising approach for quantifying soil moisture over larger continuous areas and are therefore of special interest for hydrologists to calibrate and validate their surface process models. An important task therefore is to identify the constraints for deriving valid and usable data sets from the reflectance-based quantification models applied to airborne or spaceborne remote sensing datasets.

Research question III: *Are in-situ laser scanner measurements suitable for deriving soil microtopography models to be used for the quantification of surface roughness and the monitoring of substrate movements?*

Laser scanner devices with high spatial two-dimensional resolution have traditionally been used in laboratory environments to derive three-dimensional models of objects or surfaces. In the context of soil erosion, these instruments have been applied in very few cases only, although their high potential for generating microtopography models is obvious. The application of a stationary two-dimensional laser scanner device with high spatial resolution in the field has therefore been under survey here. Based on multi-temporal

measurements over two years, the suitability of the approach to generate microtopography models and derive information on the following variables of interest was examined: surface roughness representing the spatial distribution of grain sizes, identification of substrates and detection of substrate movement patterns.

All three research questions are finally to be discussed against the background of the overarching goals of this thesis, namely to develop, assess and discuss the general applicability of remote sensing methodologies for monitoring soil surface properties to help understanding surface processes in the context of soil erosion.

Each research question was condensed into more specific objectives to be fulfilled in the framework of this thesis.

The main objective concerning *Research Question I* was to

(1) develop a surface soil moisture quantification model, which can be applied under field conditions specific to the test site using spectral instruments.

Research Question II goes one step further by following the objective to

(2) adapt, apply and evaluate the initially developed soil moisture quantification model with an airborne imaging spectrometer.

Finally, *Research Question III* results in the third objective to

(3) develop a methodology to generate microtopography datasets in the field using a stationary laser scanner device that allowed to derive surface roughness patterns.

4 Study area

Soil properties and surface processes were studied in a reclamation area located in the lignite mine Welzow-Süd, south of Cottbus, Brandenburg, Germany. Welzow-Süd is one of the largest among several surface mines established in the coal-rich region of Lower-Lusatia. Digging started in 1966, and in 2004 approximately 20 million tons of coal were mined (Vattenfall, pers. comm.). The overall size of the surface mine was 67.7 km² in the end of 2004. While the coal itself is carried to nearby power stations, the overburden is heaped up next to the open coal bed in order to refill the area. A small part of these substrates was also used for setting up the reclamation area, where the test site of this study was located (Hanschke 2002). The area was chosen as study site on the basis of several criteria, which are described in detail in the following.

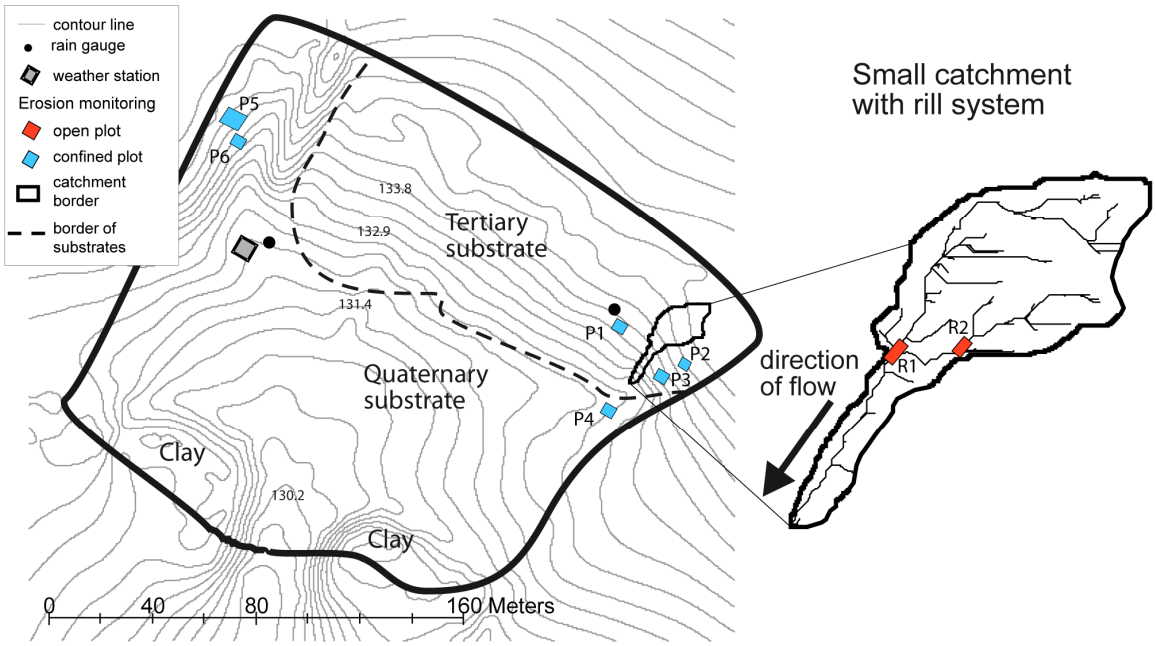

Figure I-2 Overview map of the test site Welzow-Süd.

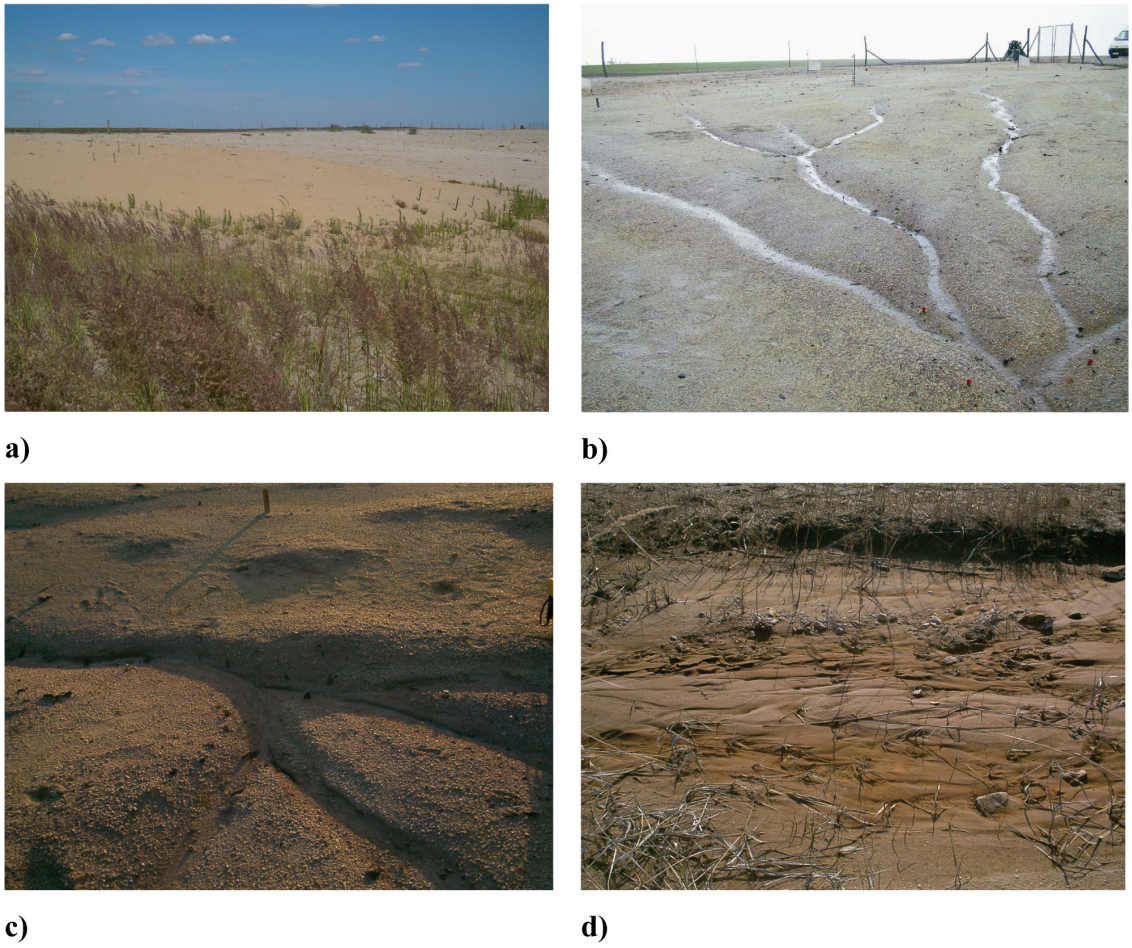

Figure I-3 Heterogeneous surface structure of the test site Welzow-Süd: a) vegetated vs. non-vegetated areas , b) erosion rills in the tertiary substrate during a precipitation event, c) the same erosion rill in dry conditions, d) accumulation area in the quaternary substrate. (Photos by S. Haubrock, M. Kuhnert, R. Baran and K. Zabel, pers. comm.)

Scale

Since surface change patterns are heterogeneous in time and space, monitoring and assessing soil processes in high spatial and temporal resolution is costly and requires the installation of a dense measurement network.

The relatively small size of the test site (4 ha) allowed for analyzing surface properties and processes in high spatial and temporal resolutions covering the whole area. This is particularly important when soil properties at the plot or micro-catchment scale are of interest, and remote sensing datasets need to be examined on a pixel-by-pixel basis in order to validate them against in-situ data.

Substrates

The whole reclamation zone is covered with mainly three different substrates: tertiary sand, quaternary sand and clay. These substrates differ mainly in terms of their grain size distributions, mineralogy and organic matter content (Lemmnitz et al. 2007). When the substrates were dumped in 2002, each of them was located in a different location, resulting in three homogeneous zones (see **Figures I-2 and I-3**).

Field studies were focused on the sandy parts for two reasons: firstly, areas covered by sand proved to be more susceptible to erosion processes at the study site, and secondly, the absence or lack of vegetation made research on soil parameters and processes more promising here. The effect of two different sandy substrates, slopes and vegetation on surface properties and processes could be analyzed in the field. Due to its physico-chemical properties, in the tertiary sand virtually no vegetation could establish between 2002 and 2005, whereas only sparse vegetation evolved in the quaternary sand.

Climate

The lignite mine Welzow-Süd is located in the southeast of Brandenburg near the borders to Saxony in the south and Poland in the east. Brandenburg is characterized by a transition from oceanic climate in the west to humid continental climate in Eastern Europe. Mean annual precipitation in south-eastern Brandenburg was below 600 mm for the period from 1951 to 2000 (Gerstengarbe et al. 2003), while mean annual temperature ranged between 8.5 and 9.5 °C.

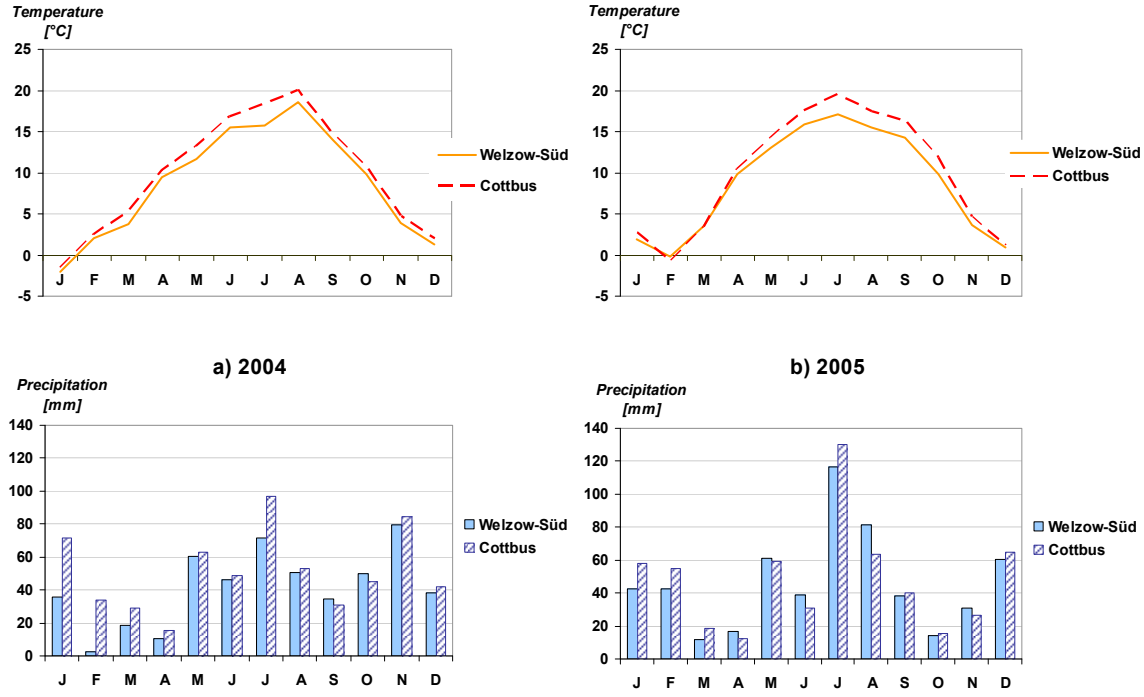

Figure I-4 Climate at Welzow-Süd and at the closest weather station run by the German Meteorological Service (DWD) in Cottbus.

Weather stations located at the test site collected temperature and precipitation data in 10 min intervals during the time of the study in 2004 and 2005. Local climate turned out to be drier than long-term averages with precipitation amounts of 432.7 mm in 2004 and 483.9 mm in 2005, while mean annual potential evaporation was lower than average in 2004 (582 mm) and higher in 2005 (735 mm).

Compared to the meteorological measurements collected at the official climate station in Cottbus (Station No. 23001), located about 25 km from the test site, two distinct patterns occur. Firstly, the local climate in the lignite mine is characterized by lower mean temperatures. Secondly, precipitation amounts are generally lower (in 17 out of 24 months). Both phenomena correspond with the findings from (Biemelt 2000), describing similar local climate particularities for the lignite mine Schlabendorf-Nord, about 35 km northwest of Welzow.

Predominating surface processes

The composition of the prevalent substrates, absent vegetation and slight to medium slopes to the southwest made the test site particularly susceptible to a variety of surface processes that were monitored and analyzed over two years. Soil erosion by wind and water as well as accumulation were among the most dominant phenomena visible in the field. Mainly

tertiary substrates eroded from the north of the site and accumulated further south where the slope decreased. The formation of distinct microtopography patterns with rill and interrill areas, as well as increasingly heterogeneous substrate compositions and chemical surface properties including temporal crust formation were the consequence. In addition, changes in soil water repellency were determined based on measurements in the field (Lemmnitz et al. 2007). The increase in vegetation cover was marginal on sandy substrates, while the clay hills were covered with herbaceous plants and shrubs already in 2004.

Parallels with dryland regions

While the genesis and local conditions of the test site have been very specific, this study also aimed at developing methodologies that bare the potential to be applied in other regions in the world with different local conditions, but similarities in terms of substrate grain size, vegetation cover and partially climate conditions. For semi-arid regions, where bare sandy substrates prevail, parallels can be identified.

As in dryland regions, runoff processes taking place at the test site are highly variable in time. Precipitation events occasionally caused rapid runoff dominated by Hortonian overland flow, which was also highly variable in space due to heterogeneous surface properties such as crusting, vegetation, and microtopography, corresponding with observations made in dryland areas (Bull and Kirkby 2002). As is typical for uncultivated soils in dryland regions, flow paths of surface runoff persisted over years in the test site.

However, although parallels with dryland regions exist, the specificity of this overburden reclamation zone needs to be taken into account when analyzing the transferability of the results. The main difference to surfaces in natural environments and particularly in dryland regions is the relatively low compaction of the soil layer resulting in loose grain structures.

Isolation

To be able to receive unaltered multi-temporal erosion measurements over multiple years, it is helpful to work in a confined area with no direct anthropogenic influences. The test site met this requirement by being fenced in and as such being inaccessible by other people or animals.

In summary, the test site bares high potential to analyze soil properties and surface processes in detail, while the methodologies developed and applied in the context of this thesis aim to be transferable to other study regions.

5 Structure of the Thesis

The structure of this thesis represents the main objectives associated with the research on soil surface properties performed in this study. Three main sections (Chapter II-IV) each deal with the analysis of quantifiers derived from remote sensing data, their validation and potential for application in the context soil surface process analysis.

In Chapter II, different reflectance-based surface soil moisture quantification models were developed, applied to field samples in laboratory measurements and compared to each other. Specific to this approach was to find a quantifier that is able to deal with unprepared natural field samples being affected by several covariates like substrate heterogeneity, organic carbon content or crusts.

Chapter III is based on the initial results by transferring the spectral feature identified as the optimum quantification model to the remote sensing scale. Airborne hyperspectral HyMap datasets from 2004 and 2005 were used to set up surface soil moisture maps, which were validated by pixelwise comparison with in-situ data. The major aim hereby was to answer the question under which pre-conditions the reflectance-based model is suitable for surface soil moisture quantification in natural environments.

In Chapter IV, soil surface processes were investigated in detail at the plot scale. In both sandy substrates present at the test site, micro erosion plots and rills were monitored over two years by collecting high-precision microtopography data, which were analyzed applying novel multiscale roughness indices.

All chapters were written independently from one another as manuscripts to be published in peer-reviewed journals. Each chapter is therefore subdivided into the subsections Introduction, Data/Methods, Results/Discussion and Conclusion/Outlook. Some limited material, especially in the introductory subsections, recurs throughout this thesis.

The three following chapters were submitted or published as follows:

Chapter II: Haubrock, S.N., Chabrillat, S., Lemmnitz, C., & Kaufmann, H. (2008b). Surface soil moisture quantification models from reflectance data under field conditions. *International Journal of Remote Sensing, 29*, 3-29.

Chapter III: Haubrock, S.N., Chabrillat, S., Kuhnert, M., Hostert, P., & Kaufmann, H. (2008a). Surface soil moisture quantification and validation based on hyperspectral data and field measurements. *Journal of Applied Remote Sensing*, *2 (023552), 1*.

Chapter IV: Haubrock, S.N., Kuhnert, M., Chabrillat, S., Güntner, A. & Kaufmann, H. (2008c). Spatiotemporal variations of soil surface roughness from in-situ laser scanning. *Catena*, in print.

Chapter II:
Surface soil moisture quantification models from reflectance data under field conditions

International Journal of Remote Sensing 29/1 (2008) 3-29

Sören-Nils Haubrock, Sabine Chabrillat, Christine Lemmnitz and Hermann Kaufmann

doi: 10.1080/01431160701294695
Received 25th May 2006; revised 17th February 2007; accepted 18th February 2007.

Abstract

A new approach to estimate surface soil moisture from reflectance data in the solar spectral range (350–2500 nm) is presented, called the Normalized Difference Soil Moisture Index (NSMI). The motivation for this new index is to make use of spectral features that fulfill the criteria of robustness against covariates, physical comprehensibility and easy applicability in the field and from remote sensing platforms. Spectral measurements were taken in the laboratory from 121 prepared as well as 467 natural soil samples consisting of different sands and clayey substrates originating from a lignite mine reclamation site. While the preparation procedure performed on samples from the first group removed the covariates' influence on the reflectance spectra, the natural samples in the second group maintained the influencing factors like impurity, crusts, and organic matter. In a systematic way all wavelengths were combined in different spectral feature approaches and optimum bands or band combinations were found for linear correlation with soil moisture. For the natural samples, the NSMI achieved best results in this study with R^2 of 0.61 by combining reflectance values at 1800 and 2119 nm. This value increased to 0.71 when samples with significant xylite proportions had been removed. Analyses on the effect of single covariates showed that neither surface crusts nor substrate heterogeneity changed the correlation between soil moisture and the NSMI significantly. The NSMI can therefore be seen as a new index for quick assessment of surface or near-surface soil moisture directly in the field using spectral instruments.

1 Introduction

Surface soil moisture is a significant parameter triggering processes in environmental systems. In the context of soil erosion, land degradation and desertification, the monitoring and modeling of these processes makes a universal approach necessary for estimating this variable at the mesoscale. A large number of research projects are dealing with the potential of different remote sensing technologies for estimating surface soil moisture. Approaches have primarily been focused on the microwave part of the spectrum, based on the facts that moisture strongly affects soil dielectric properties and longer wavelengths make a relatively deep penetration into the ground possible (Bryant et al. 2003). The European Space Agency started recently the Soil Moisture and Ocean Salinity (SMOS) mission designed to observe soil moisture over the earth's landmasses (Berger et al. 2003).

Surface soil moisture estimations gained from optical measurements in the visible/near-infrared (VNIR) to short-wave infrared (SWIR) part of the spectrum (350–2500 nm) are important in two different contexts. For many environmental surveys, surface soil moisture data are needed. The calibration and driving of hydrological models at different scales is a challenging domain for remotely sensed soil moisture quantifications. When parameters like surface hydrophobicity are of interest for e.g. modeling soil erosion, information on soil moisture of the uppermost surface is crucial (Doerr et al. 2000). Especially in dry regions of the world, the surface soil moisture is a dynamic variable at a relatively low level, making an optical remote sensing approach useful for the assessment of degradation processes. Secondly, when high-spectral resolution measurements are necessary for the determination of ground cover properties (e.g. minerals, soil type), soil moisture severely influences the background reflectance and therefore affects the classification accuracy. By estimating soil moisture from the reflectance measurements before quantifying the parameter of interest, this effect can be taken into account and decreased. The presence of soil moisture causes distinct effects in reflectance in the VNIR to SWIR spectral range. The most dominating effect can be described as an overall decrease in reflectance with increasing soil moisture (Baumgardner 1985; Lobell and Asner 2002; Weidong et al. 2002). While this rule holds for the range from 350–2500 nm and small to medium soil moisture percentages (Weidong et al. 2002), some parts of the spectrum show more pronounced absorption quantities than others. Especially the overtone and combination absorption bands of molecular water around 900 nm, 1400 nm and 1900 nm as well as the

fundamental absorption band around 2800 nm are sensitive regions for soil moisture variability (Weidong et al. 2003). Due to the impracticability of measuring soil reflectance in the field directly from these bands caused by atmospheric absorption, Beck et al. (1976) suggested analyzing wavelengths in the region from 1500 to 1730 nm, whereas other authors made use of reflectances in the SWIR part of the spectrum. Several approaches for soil moisture estimations from reflectance measurements have been established and show promising results for different types of soils. The measurements were mostly conducted in the laboratory where the environment can be controlled and the spectral effect of soil moisture can be isolated from potential covariates, i.e. different physical and chemical soil characteristics (Lobell and Asner 2002; Weidong et al. 2002; Weidong et al. 2003; Whiting et al. 2004). In contrast to other soil properties, where quantification can be directly deduced from spectral measurements due to very specific absorption characteristics (e.g. (Cloutis 1996), the covariates make a determination of soil moisture more challenging. Soils are complex systems consisting of varying proportions of soil matrix, water and air (Scheffer and Schachschabel 2002). Inorganic and organic substances within the matrix generally follow soil type-typical vertical distributions. Soils are highly heterogeneous in their physical properties and chemical composition and highly variable in their spatial distribution. Additionally, the surface of the soil is prone to weathering and erosion effects by wind, water and insolation. These factors trigger processes that may result in surface crusts and/or bleaching (Karnieli et al. 1999; Goldshleger et al. 2001; Goldshleger et al. 2002; Ben-Hur and Wakindiki 2004). As a consequence, the uppermost surface often differs significantly from the lower parts of the soil column with respect to physical features and biochemical constituents. As a consequence, soil parameter estimations based on reflectance measurements from the surface often do not give information about the properties of lower soil layers. The spectral features caused by soil moisture are severely influenced by the previously mentioned soil-specific chemical and physical properties, such as organic matter, mineralogy, crusts or grain size (Ben-Dor and Banin 1994; Krüger et al. 1998; Ben-Dor et al. 1999; Engman 2000; Goldshleger et al. 2001; Goldshleger et al. 2004b). In the context of remote sensing applications these natural conditions are present and therefore need to be investigated. The aim of this study is to take a step towards finding a robust, comprehensible and easily applicable model for the determination of surface soil moisture, which can be applied not only under laboratory, but also under field conditions despite the natural heterogeneity. An analysis of several existing soil moisture estimation models when being applied with unprepared field samples was performed. In

order to find an optimum quantification model, the methods applied here analyzed the full spectral resolution from the visible to the SWIR spectral range. Important approaches found in the literature were evaluated and further supplemented with spectral feature analyses like absorption depths or shapes of the spectrum curve at certain regions, which have been successfully applied in other application domains (e.g. mineralogy) (Cloutis 1996; Krüger et al. 1998). Analyses of the effect of covariates are shown and limitations of the model are discussed.

2 Background

Most approaches estimating surface soil moisture from reflectance are based on the fact that increasing soil moisture up to a certain level leads to a decrease in reflectance values over the VNIR to SWIR part of the spectrum.

One of the earlier works in this domain showed this effect by wetting soils artificially and measuring the decrease in reflectance (Angström 1925). He ascribed it to total internal reflections of the reflected radiation in a water layer covering the soil. Planet (1970) later called this effect visual darkening. He stated that with knowledge of the dry soil reflectance spectrum and the index of refraction of the liquid, it becomes possible to predict the visual reflectance of the same sample under saturated conditions. He further mentioned that physical changes of the soil surface caused by water and impure materials, have a severe effect on reflectance and can therefore affect the accuracy of the soil moisture estimation.

While Planet (1970) deduced his reasoning from only two different soil moisture states, dry and saturated, Weidong et al. (2002) prepared their soil samples with up to 18 different moisture levels. They found out that a decrease in reflectance with increasing soil moisture is not necessarily the case for wet soils. Moreover, beyond a critical soil specific moisture ratio, which is closely related to field capacity, this relationship was reversed in their studies, such that a further increase in moisture led to an increase in reflectance. Thus, when dealing with the estimation of soil moisture values from reflectance, their range has to be taken into account.

Similarly to Weidong et al. (2002), Lobell and Asner (2002) used the a priori information of dry spectra for each soil sample. Consequently, the type of soil needed to be known before applying the estimation model in order to choose the correct dry reference spectrum.

2.1 Single-band reflectance approaches

Weidong et al. (2003) compared several approaches for surface soil moisture estimation from reflectance data based on laboratory analyses in order to investigate the potentials of the optical domain for soil moisture estimation. In the scope of their work, relative reflectance parameters were among the indices approaches and have been calculated from 18 soil samples. The approach is based on single-band reflectance values (Weidong et al. 2002). The specific characteristics of different soil types are taken into account by regarding the relativity, i.e. the ratio of the measured reflectance and the reflectance of the corresponding reference sample under dry conditions. The results of applying this approach in the laboratory showed that best results could be achieved in the major absorption band around 1944 nm. Under field conditions these absorption bands cannot be used as they are masked through atmospheric absorption. In the context of fieldwork, the relative reflectance approach can therefore not be applied in the spectral regions where it showed best results.

The determination of relative reflectance values also implies that for each type of soil a dry reference spectrum is available, so each further soil moisture estimation based on the relative reflectance approach relies on the existence and accuracy of the reference spectrum's reflectance. In natural heterogeneous environments, the definition of a single reference spectrum seems problematic when spatial variability is high and homogeneous substrates are rare. In order to extend this method to outdoors application, more soil type independent approaches extending the relative reflectance approach are necessary, including parameter calculations of certain spectral features based on two or more wavelengths.

2.2 Multi-band spectral feature approaches

While the former methods are based on single reflectance values, most approaches in spectroscopy rely on a set of multiple reflectance values for classification and quantification purposes in order to take advantage of the high spectral dimensionality. The incorporation of multiple bands generally makes regression models more robust against covariates, since absolute measurement values can be set in relation to each other, reducing the effect of the overall albedo. In contrast to single reflectance models, this relativity is not dependent on a priori information (i.e. spectra of corresponding dry soils). Instead, for each sample spectrum the reflectance values at different wavelengths can be set in relation to each other.

As some regions in the spectrum are more sensitive to changes in substrate properties than others, relating sensitive parts to invariant parts of the spectrum is a feasible approach, implemented in the form of distinct types of band combinations, e.g. ratios or gradients. The approach by Bogrekci and Lee (2004) uses a combination of the wavelengths 340 nm, 1450 nm, and 1940nm to estimate soil moisture. Bryant et al. (2003) applied the WISOIL index, a ratio between 1450 and 1300 nm, but needed to normalize this estimate against the dry reference spectrum of the corresponding soil.

Around the overtone water absorption bands, the gradient between reflectance values proved to be an appropriate measure for soil moisture quantification under laboratory conditions. Weidong et al. (2003) proposed an approach, in which the first derivative is calculated as the difference in reflectance between two consecutive bands. As a generalization of this, they also generated the reflectance difference between two arbitrary bands for all wavelength combinations and established a linear regression between these differences and the soil moisture values. As a result, this approach generated better correlations compared to the relative reflectances and reflectance derivatives applied in their studies.

While absorption depth and asymmetry measures are common analysis techniques for hyperspectral data (van der Meer 2004), these features are rarely applied in soil moisture quantification approaches. Indeed, the absorption depth cannot be used where it promises best results, since these regions are within atmospheric absorption bands.

The advantage of multi-band spectral features towards single reflectance values is the relative stability between different soil types. However, most studies still faced difficulties in finding robust spectral features when regarding e.g. multiple soil types with different characteristics (e.g. Weidong et al. 2002).

One further advantage of multi-band spectral features is the fact that their best results are not necessarily directly in the water absorption bands. In the context of developing an outdoor methodology that may be applied from airborne and spaceborne sensors, this advantage becomes crucial.

2.3 Spectrum modeling approaches

In recent studies, some authors go a step further towards an optimum use of information provided by the spectra. Gaussian approaches have been successfully applied for the deconvolution of mineral absorption bands (Clark and Roush 1984; Sunshine et al. 1990).

In the context of soil moisture, Whiting et al. (2004) proposed the fitting of an inverse Gaussian function to the SWIR part of the spectrum and called this approach the Soil Moisture Gaussian Model (SMGM). The overall idea is to take into account the reflectance decrease towards the water absorption band at 2800nm. In a first step, the spectra are logarithmized and normalized by scaling all reflectance values such that the maximum reflectance of a spectrum is set to 1. As a result, the influence of different albedos between the spectra is reduced. The convex hull of the resulting normalized spectra is used to fit the inverted Gaussian function with the aid of pre-defined base points (described in Whiting et al. 2004). Specific function parameters like the area under the resulting curve are then correlated with the soil moisture percentage.

Characteristic of this approach is the evaluation of the whole SWIR part of the spectrum. The fundamental water absorption band around 2800 nm spreads towards the measurable shorter wavelengths, and the method showed a feasible way to take advantage of this effect.

The creation of the convex hull makes additional pre-processing of the spectra necessary for reducing the noise in the SWIR around 2400 nm, which is essential for deducing correct hull points and fitting the Gaussian function to the vertices of the hull. A very strong advantage of this multi-step method is the fact that no a priori information about the soils is necessary. The study showed as well that best results can be achieved when stratifying the model to soil groups. The applicability of this method with natural soil samples has yet to be analyzed.

Table II-1 gives an overview of important soil moisture quantification approaches from reflectance data and their characteristics.

2.4 Application domain

While the given approaches led to appropriate results in their application contexts, some major questions remain when being applied under natural field conditions. In most cases, the soil samples were taken to the laboratory and thoroughly prepared. These preparations include drying and sieving, resulting in the destruction of a potential crust, or more generally in a reduction or removal of natural heterogeneities. As a result, the direct effect of soil moisture could be isolated from all covariates in order to diminish their potential effect, but the approaches' applicability under field conditions could not be proved.

Table II-1: Overview of common soil moisture indices from reflectance data. R^2-values are given for combined analysis of different soils (without stratification). All analyses were performed on prepared samples in the laboratory.

Approach	Reference	Wavelengths	R²/RMS	Methodology and results
Exponential model	Weidong et al., 2002	350-2500 nm	not provided	Soils were considered separately, normalization against dry reference soils
Relative reflectance	Weidong et al., 2002	1998 nm	0.84/0.04	High moisture values applied, normalization against dry reference soils, critical moisture ranges for regression functions found
	Weidong et al., 2003	1944 nm	0.68/0.08	Reference spectra necessary, wavelengths in water absorption band
First derivative	Weidong et al., 2003	1834–1836 nm	0.63/0.08	Wavelengths in water absorption band
Reflectance difference	Weidong et al., 2003	2250–2062nm	0.69/0.076	Difference measured as absolute value
Ratio (WISOIL)	Bryant et al., 2003	1450 vs.1300 nm	0.76–0.96/–	Soils were considered separately, normalization against dry reference soils
MDR	Bogrekci and Lee, 2004	340, 1290 and 1940 nm	not provided	Absorbance values used, analysis focused on phosphorus concentrations with soil moisture being a covariate
SMGM	Whiting et al., 2004	1200–2500 nm	0.92/0.027	Samples prepared, complex method, high correlations

Most of the methods show difficulties when being transferred from one type of soil to another or if certain covariates are not invariant. In order to make the results applicable in the field, all these covariate effects need to be taken into account. One crucial question is therefore, which methods are robust against heterogeneous field environments.

3 Methods

3.1 Field and soil type description

In the scope of this work, soil moisture was measured in the laboratory over field soil samples. Samples were taken from a reclamation site at the lignite mine Welzow-Süd near Cottbus, Germany. After the mining activities were finished at the test site in 2002, different substrates have been refilled and nowadays form the In the scope of this work, soil moisture was measured in the laboratory over field soil samples. Samples were taken from a reclamation site at the lignite mine Welzow-Süd near Cottbus, Germany. After the mining activities were finished at the test site in 2002, different substrates have been refilled and nowadays form the reclamation zone (Hanschke 2002). Undisturbed conditions, a relatively harsh climate and the lack of vegetation make this area ideal for the

research on soil parameters. Since the time of the refill, severe erosion processes have taken place. changes in physical and chemical soil properties have been monitored between 2003 and 2005 with the aid of spectroscopic measurements in the field.

Generally speaking, three different groups of substrates were analyzed. The northernmost part of the test site is covered with a substrate labeled tertiary sand. This substrate is characterized by its bright-grayish color. The relatively large grain size gives it a poor water storage capability (field capacity). Due to its low pH-value (around 3.1), vegetation is very sparse on this ground. From the analysis of reflectance spectra taken in the field, this substrate has very little organic matter content, no carbonate, and is kaolinite-rich (Chabrillat et al. 2003).

In the adjacent area substrates summarized as quaternary sand are predominating. The slightly acid character (around 5.6) and small to moderate field capacity separates those sands from the tertiary sands.

Severe erosion activities from the tertiary and quaternary areas resulted in an accumulation of substrates with very distinct chemical properties in the southern part of the test site, where an erosion channel has formed between two hills consisting of mainly clayey substrates.

3.2 Laboratory analyses

In order to analyze and compare different soil moisture estimation approaches for substrates originating from the field, in a first step the effect of soil preparation on soil moisture estimation accuracy has been surveyed. Therefore, artificially prepared samples were compared to natural field samples, i.e. samples, which have been measured in the same state as they were collected in the field.

Artificially wetted samples

For the first group, samples from 11 different spots at the test site were analyzed in the laboratory. These spots were chosen after prior analyses of substrate variations, so they represent the range of present soils appropriately. The processes of soil erosion, weathering and vegetation taking place since 2002 have led to a formation of spatially distributed substrate patterns, which can be best described as sub-categories of the two sands (Table II-1). The samples represent these sub-categories, based on their location and the visual appraisal of crusts and organic layers. Grain size compositions were determined

for a collection of representative samples in the tertiary and quaternary substrates. The samples were collected over the summer season 2005.

The preparation steps for these 11 samples from the field comprised stirring, large grain and vegetation removal as well as oven-drying at 105 °C for 24 hours.

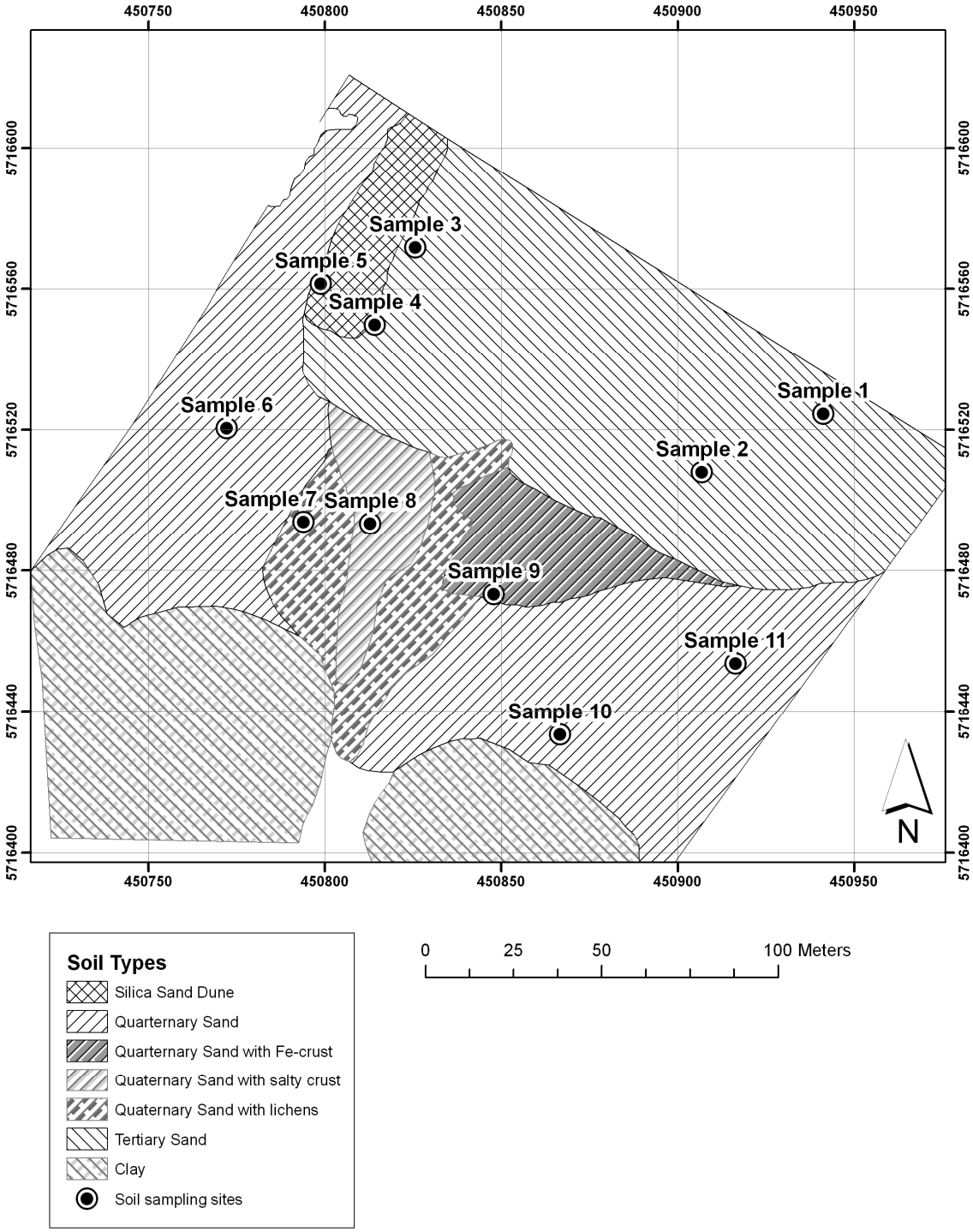

Figure II-1 Test site and field sampling locations. (Spatial reference system: UTM33N, WGS 1984)

The resulting homogenized substrates were then subdivided into smaller samples. Each of the dry sub-samples was put into a petri-dish of 1cm thickness. The masses of all sub-samples were measured. The soils were then wetted using a spray bottle. Each of the 11 samples was artificially wetted in steps of 2% until saturation (near field capacity), which ranged between 18 and 24% depending on the soil sample. The fractions of water put onto these samples were determined by measuring the masses of the wetted samples, and subtracting the masses of the dry samples and the petri-dishes using a balance of 10 mg accuracy. The soil moisture was calculated in mass of water per mass of soil matrix (gravimetric soil moisture). The soil samples were covered for at least 30 minutes to gain constant soil moisture over the whole sample. Afterwards, the masses were measured again to make sure no water has volatilized from the dishes. Reflectance spectra were then acquired over the wetted samples using a spectroradiometer ASD FieldSpecPro FR® with 8 ° foreoptic. An artificial light source with 2000 W illuminated the samples from a 60 ° viewing angle, while the spectrometer measured from nadir. White references were taken after every ten measurements using a Spectralon® plate.

Since each set of sub-samples originated from the same sample and the subsamples only differed in their amount of soil moisture, a direct effect of this parameter could be analyzed per sample. For analysis of the grain size fractions, multiple samples were collected over the summer season 2005 from chosen spots, oven-dried and sieved in the laboratory (Kuhnert, pers. comm.).

Soil samples in natural conditions

In a next step, spectra from field soil samples with their natural soil moisture rates were measured in the laboratory and correlated with gravimetric soil moisture values. In contrast to the first approach, the sub-samples originate from different sources, which were collected over more than a year. Similar to the artificially wetted samples, they represent the different substrates present in the field. Furthermore, soil moisture conditions exhibited the original field status. Thus, other physical and chemical parameters affected the spectra and consequently the determination of soil moisture as well.

Soil cores of 8 cm in diameter and 5 cm in depth were used for sampling in the field. Between April 2004 and October 2005, 96 soil cores were taken from all over the test site. The sealed soil cores were kept in a cool place between two and 24 hours for transport and storage before being analyzed in a laboratory of the BTU Cottbus. For analysis, the samples were subdivided into five layers (sub-samples) of 1cm thickness and placed on

petri-dishes with the aid of a trowel. Immediately afterwards, they were measured with a spectroradiometer ASD FieldSpecPro FR® (8 ° foreoptic) from nadir. For each sample, multiple spectra were taken and averaged later on. The artificial light source of 2000 W was positioned 80 cm from the samples with a 60 ° incident angle. After the spectral measurements, gravimetric soil moisture values were determined applying the conventional method of oven drying for 24 hours at 105 °C. The decrease in weight represents the initial mass of water in the sample used for calibrating the regression functions.

Altogether, 467 sub-samples of 1 cm depth were extracted from the cores. From these layers, 125 were classified as pure quaternary sand and 120 as tertiary sand. 32 layers can be described as clayey substrates, while the remaining samples originated from areas where different substrates formed heterogeneous samples and were partly affected by significant amounts of xylite.

Due to the sampling method it was possible to analyze for each of the samples the vertical heterogeneity, such that a distinction between reflectance properties at the very surface (uppermost soil layer) and the lower parts could be realized. Consequently, the effect of the potentially existing soil crust for one fifth of the sub-samples were analyzed in a separate step.

3.3 Soil moisture estimation

Spectral features

In the scope of this work, different soil moisture estimation approaches based on spectral reflectance data were compared to each other in terms of their applicability under natural heterogeneous conditions. These approaches comprise some of the most promising procedures found in the literature: single absolute reflectance values, absorption depths, areas of certain spectral regions, and normalized differences.

In a first approach, single absolute reflectance was measured normalized to the white reference standard with known reflectance characteristics. Since overtone water and also mineral absorption bands are known to be very sensitive to a variation in soil moisture, in a next step the depth of absorption bands was evaluated as potential spectral feature for soil moisture estimation. In the case that absorption depth is used for the quantification of a substance, the continuum has to be removed initially, yielding the relative absorption band

depth. The absorption band depth applied here is a minor modification of the approach published by (Clark and Roush 1984). Here, the band depth is measured in the middle between two wavelengths rather than at an arbitrary position of the continuum removed spectrum. In Eq. 1, which has been applied here, the depth D is calculated for an absorption band between wavelength i and wavelength j where R[i] denotes the reflectance at wavelength i.

$$D = 1 - \left[\frac{R\left[i + \frac{j-i}{2} \right]}{\frac{R[j] + R[i]}{2}} \right] \tag{1}$$

Following the idea of Whiting et al. (2004), an approximation of their SMGM was implemented and evaluated as a third approach. Hereby, the spectrum area was not deduced from a fitted Gaussian curve, but directly from the convex hull generated from the normalized/scaled log-reflectance values.

The following steps were carried out when applying this method:

(4) Conversion of reflectance to natural log of reflectance

(5) Normalization of log reflectance by the maximum reflectance of the spectrum

(6) Determination of prominent local maximum reflectance indices and wavelengths with a convex hull

(7) Determination of the area from the hull points

The normalization in step 2 is intended to account for the different spectral shapes and especially the maximum reflectance values of the samples, which can vary significantly between soils.

By choosing appropriate hull points, i.e. a small number of points outside major absorption bands at wavelengths that are not affected by present covariates, the shape of the Gaussian curve could be approximated adequately. The first hull point was chosen at 1710 nm (average start of severe decline in reflectance) and the last hull point was set at 2400 nm for not being influenced by the low SNR in the longer wavelengths.

For the calculation of normalized difference features, following the successful methodology of established indices (e.g. NDVI), Eq. 2 was applied as the fourth spectral feature approach.

$$\frac{R[j]-R[i]}{R[j]+R[i]} \tag{2}$$

Parameter optimization

For each of the spectral features tested, not only a single band or set of bands was applied in the estimation models, but rather all possible band combinations from 350 to 2500 nm were investigated for their correlation with soil moisture under both prepared homogeneous and natural heterogeneous conditions. The resulting R^2-values for any wavelength or combination of two wavelengths were plotted in a diagram to visualize the typical correlation patterns in the vector space of wavelengths.

The estimation models were established applying linear regression based on the physical soil moisture measurements and spectral features. For testing the robustness of the models, the clayey samples were incorporated into the natural field samples for validation. The originality of the proposed methodology in this paper is that no a priori knowledge is used to determine the best soil moisture estimator.

4 Results

4.1 Soil characteristics

Physical and chemical characteristics

Some relevant physical and chemical properties of the samples measured for the first set are shown in Table II-2. The classification of the samples relied primarily on the location of the samples and the visual appraisal of crusts and organic layers.

The maximum gravimetric soil moisture reflects the amount that could be applied with the spraying bottle before water drains away through the sample. It therefore reflects the porosity of a sample. Differences between the substrates become visible, since tertiary samples generally show larger grain sizes and thus lower maximum soil moisture values compared to the quaternary sands. Table II-3 shows ranges for the grain size distribution and average carbon contents from a collection of representative samples in the tertiary and quaternary substrates.

Table II-2: Relevant physical and chemical properties of the prepared and wetted soil samples. Minerals have been determined by X-ray powder diffraction using a Philips PW2400.

Sample No.	Substrate	Max. gravimetric soil moisture [%]	Minerals					
			Albit [%]	Calcite [%]	Gypsum [%]	Illite [%]	Orthoclase [%]	Quartz [%]
1	Tertiary sand	18	-	-	-	2.28	5.30	92.42
2		18	-	-	-	2.30	4.91	92.79
3		18	-	-	-	2.24	4.50	93.27
4	Tertiary/Silica mixture	22	-	-	-	2.53	4.43	93.14
5	Silica sand	24	2.37	-	-	1.88	4.17	91.58
6	Quaternary sand	24	8.87	-	-	4.35	4.72	82.06
7	Quaternary sand + lichens	24	6.43	-	-	3.18	4.32	86.06
8	Quaternary sand + salt crust	22	4.82	-	0.62	2.55	4.31	87.64
9	Quaternary sand + iron crust	24	5.67	1.29	10.62	7.81	4.36	68.65
10	Quaternary sand	24	5.97	6.14	-	6.22	5.85	75.82
11		22	6.45	4.86	-	4.81	5.59	78.28

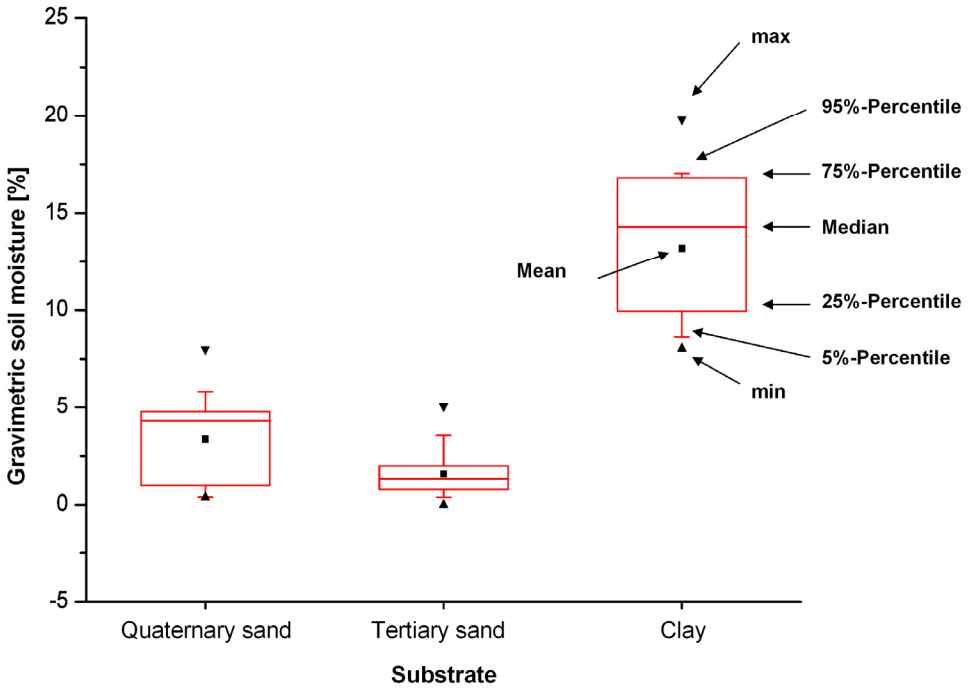

Figure II-2 Box-Whisker-Plot of soil moisture distributions from natural field samples.

Table II-3: Grain size ranges and carbon content (C) for representative soil samples from the field. Carbon content has been measured using an Elementar Vario EL.

	Grain size					Carbon
	>2 mm [%]	>630 µm-2 mm [%]	>200-630 µm [%]	>63-200 µm [%]	<63 µm [%]	C [%]
Tertiary sand	25.43-27.16	29.15-36.95	26.19-34.30	8.03-9.30	1.66-1.82	0.35
Quaternary sand	5.9-12.14	15.04-23.56	46.52-61.13	7.93-21.58	1.48-7.71	0.15

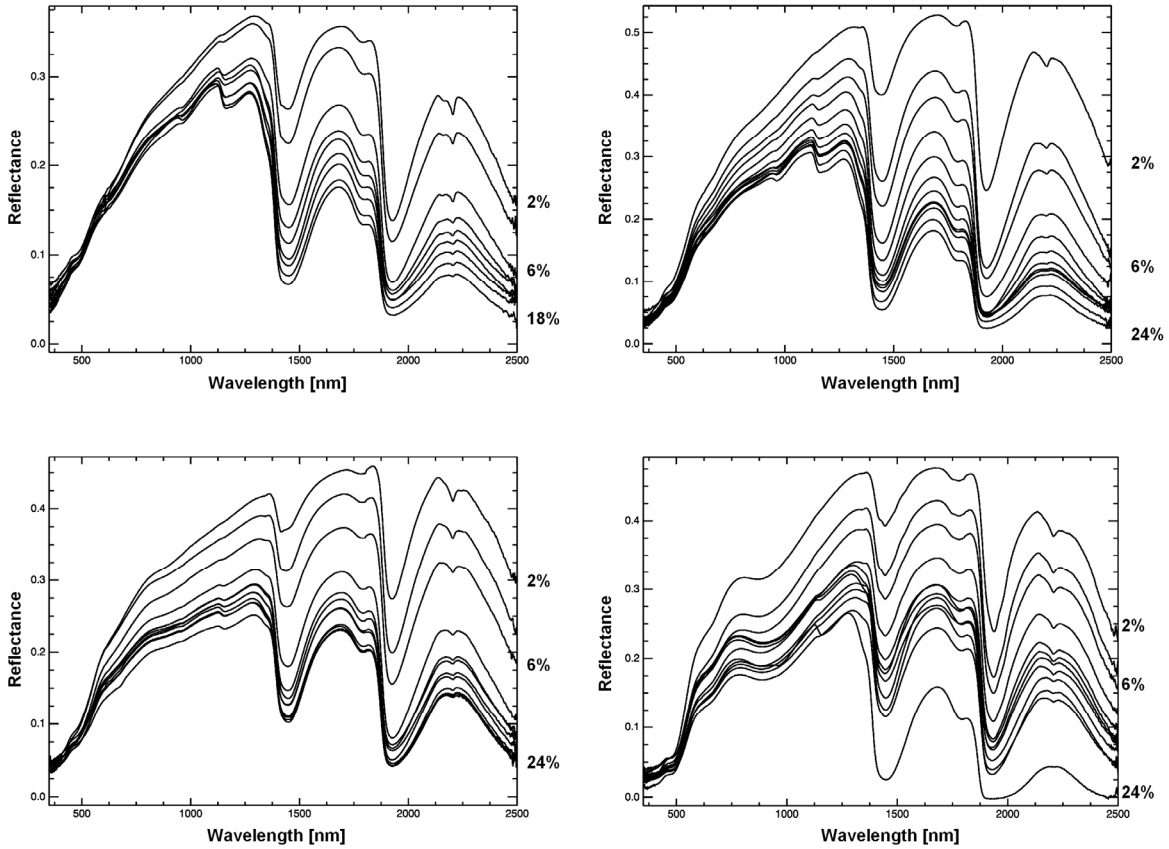

Figure II-3 Effect of artificially increased soil moisture on the spectra of four representative soil samples in the test area (a: tertiary sand from sample No.1, b: silica sand from sample No.5, c: quaternary sand from sample No.10, d: quaternary sand with iron from sample No.9. Numbers on the right of the graphs represent the minimum and maximum of gravimetric soil moisture that could be applied. In between, soil moisture values increase in steps of 2%. The 6% values are also shown for clearness.

Soil moisture distribution

The distribution of naturally occurring soil moisture values for the upper five centimeters shows that tertiary sands were relatively homogeneous in gravimetric soil moisture with typically low values (<5%) (Figure II-2). The quaternary sand samples ranged between 0 and 8 % in gravimetric moisture.The clayey samples that were additionally used for validation show a much wider range of observed soil moisture values from around 8 to 20 %.

4.2 Soil moisture effects on reflectance

Reflectance of artificially wetted samples

For each of the artificially prepared samples from the 11 locations at the site spectra were taken with varying soil moisture. A representative example of the resulting spectra is shown in Figure II-3 taken from four substrates. For three of the samples, the typical decrease in reflectance with increasing soil moisture is observed over the whole spectral range. For sample No. 1 (Figure II-3a), the ordering of the spectra from top (low moisture) to bottom (high moisture) is particularly visible in the range of 1150 to 2500 nm. However, between 350 and 500 nm, the typical order of the spectra is inverted, i.e. high reflectances are associated with high soil moisture values. Between 500 and 1150 nm, no systematic effect of soil moisture on reflectance can be identified for sample No.1. Also for the other samples, this region does not show very significant reflectance changes with varying soil moisture at higher levels (above 10%), while the reflectance changes are very pronounced at low moisture levels. Similar results were observed by Lobell and Asner (2002), who found that reflectance saturated at much lower moisture contents in the visible and near-infrared (VNIR) spectral region than in the shortwave-infrared spectral region, suggesting that longer wavelengths are better suited for measuring volumetric moisture contents above ~20% (volumetric soil moisture can be linearly transformed into gravimetric soil moisture by dividing through the dry bulk density). Our measurements show that this trend is valid for different soil classes, but with varying intensities.

Reflectance of natural field samples

In contrast to the artificially prepared samples, where increasing moisture causes very distinct patterns, samples taken from heterogeneous field substrates behave more individually. Figure II-4 shows an example of four different tertiary samples with either 1 or 4% gravimetric soil moisture, respectively. These soil moisture values were typical for this substrate in the field. While all samples consist of approximately the same constituents and were taken from adjacent spots, the spectra vary significantly. Obviously, single reflectance values as well as the overall albedo cannot be used as an indicator for soil moisture here, since covariates can affect the soil's brightness significantly, especially in the VNIR region.

4.3 Sensitivity of reflectances

In an a-priori-analysis, the sensitivity of reflectance values was analyzed for the 11 artificially wetted substrates. All samples in Figure II-5 show the effect that the visible part of the spectrum is much more stable with variable soil moisture.

For example, at 1700 nm, the reflectance with 18% gravimetric soil moisture ranges between 33 and 60% of the reflectance measured for the same sample when oven-dried.

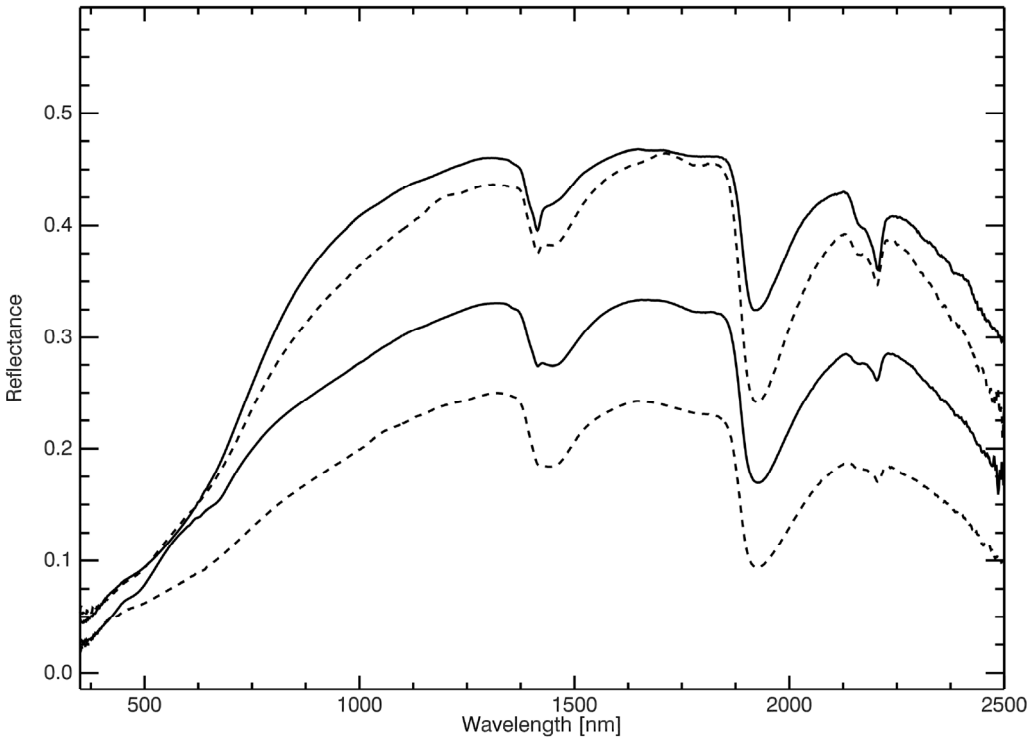

Figure II-4 Reflectance of tertiary samples with natural conditions. The solid line represents samples with 1% soil moisture, dashed lines stand for 4%.

At 1950 nm, the decreased reflectances reach relative values between 13 and 35%. In the visible range, however, the reflectance decrease is either less significant or even turns into an increase. It can also be seen that the four tertiary samples (solid lines) are relatively insensitive to soil moisture variability in the region of 600 to 900 nm since the dry-to-moist reflectance ratio is around one.

Thus, the distribution of relative reflectance values over the wavelengths shows three persistent trends with increasing soil moisture confirming and extending the findings of other authors: First, the reflectance decreases faster with increasing wavelength; secondly, it decreases particularly in the water absorption bands around 1400 and 1900 nm; thirdly, the soils behave differently in some wavelengths while preserving the overall trend.

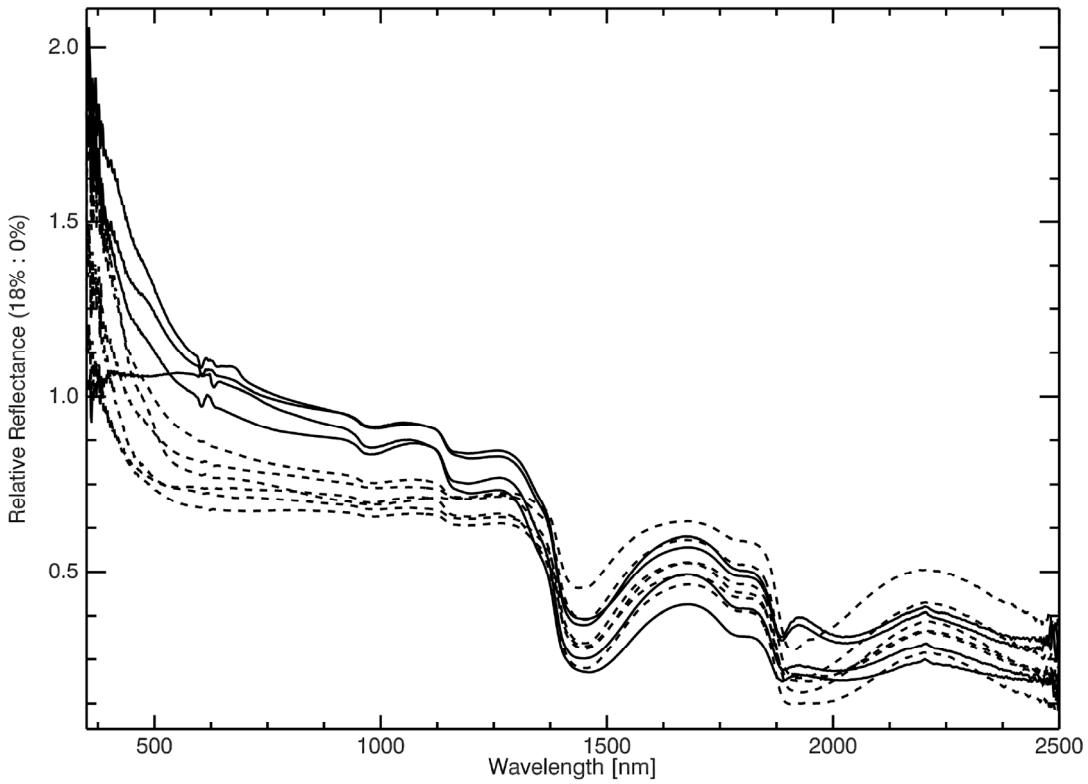

Figure II-5 Relative reflectance curves from oven-dry soils to 18% moisture (artificially wetted). Solid curves show tertiary sand samples, dashed lines represent quaternary substrates.

4.4 Soil moisture estimates

Absolute reflectance

In the first step, the absolute reflectance between 350 and 2500 nm as the most simple of all possible reflectance features was used as soil moisture estimator. The reflectance values were correlated with measured soil moisture for the artificially prepared and natural soil samples, respectively (Figure II-6). The soil moisture ranges varied between the samples as shown in Table II-2 and Figure II-3.

The relative insensitivity of reflectances in the VNIR leads to the fact that correlations are relatively poor. For the prepared soil samples, the best coefficient of determination is at 1392 nm (R^2=0.60; natural samples: R^2=0.50) while the optimum wavelength for this parameter with the natural soil samples is at 2274 nm (R^2=0.57; prepared samples: R^2=0.56).

Between 1300 and 1500 nm both spectra show a similar pattern with slightly better correlations for the prepared samples. On the contrary, the natural soil samples show better correlations in the VNIR. This effect can be explained by the composition of the natural

samples, containing not only the substrate, but also certain amounts of organic constituents. These impurities often lead to typical visual artifacts highly correlative with soil moisture (e.g. crusts, moss or lichens) and especially relevant for reflectance values in this part of the spectrum. When soil samples are measured in the laboratory after preparation, these side-effects are generally eliminated. For the estimation of surface soil moisture under field conditions, however, they are often present.

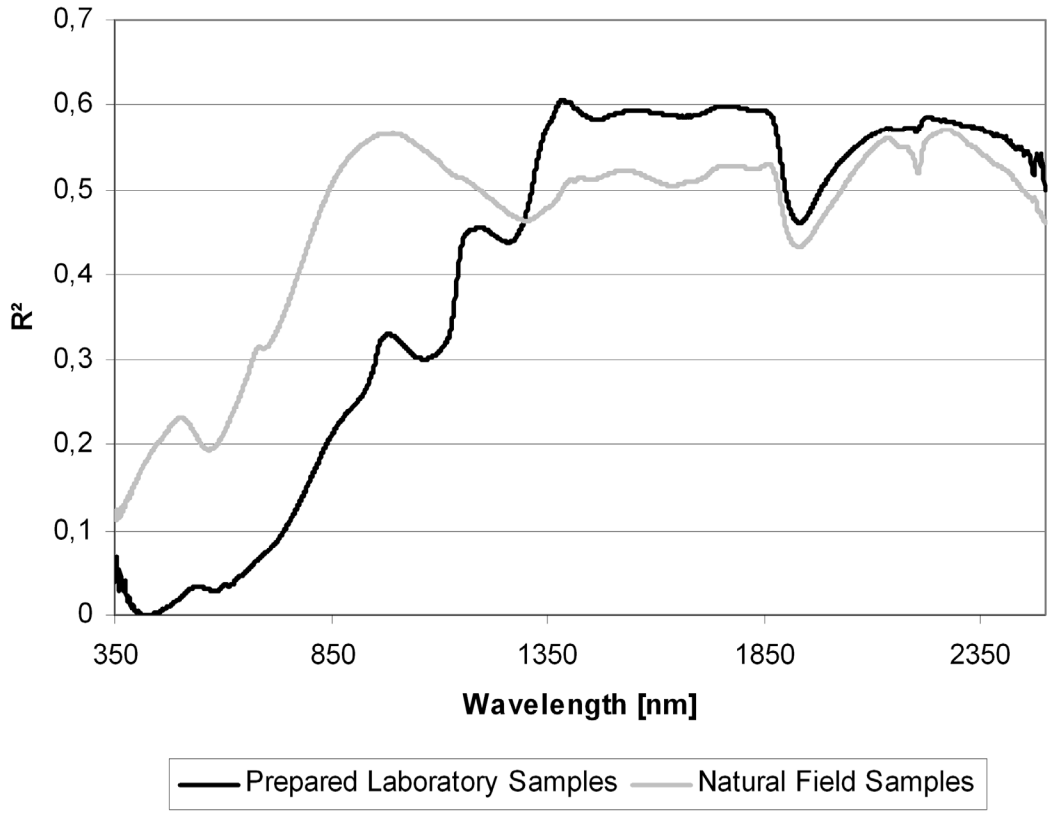

Figure II-6 Relative R²-values gained from linear correlation between soil moisture and absolute reflectance values in one wavelength for artificially wetted samples.

With a maximum coefficient of determination of R^2=0.57 for natural samples, the absolute reflectance cannot be considered as a sufficient estimator for surface soil moisture.

Absorption depths

Characteristic absorption bands can be appropriately quantified by their depths. The quantification of soil moisture with the aid of this spectral feature generated best results when being applied around the major water absorption bands. R^2-values between 0.57 (band centered at 1900 nm) and 0.61 (band centered at 1450 nm) were measured for the artificially prepared samples. However, although reflectances are particularly sensitive to varying soil moisture in these two overtone absorption bands, atmospheric absorption forms an obstacle for their use under field conditions.

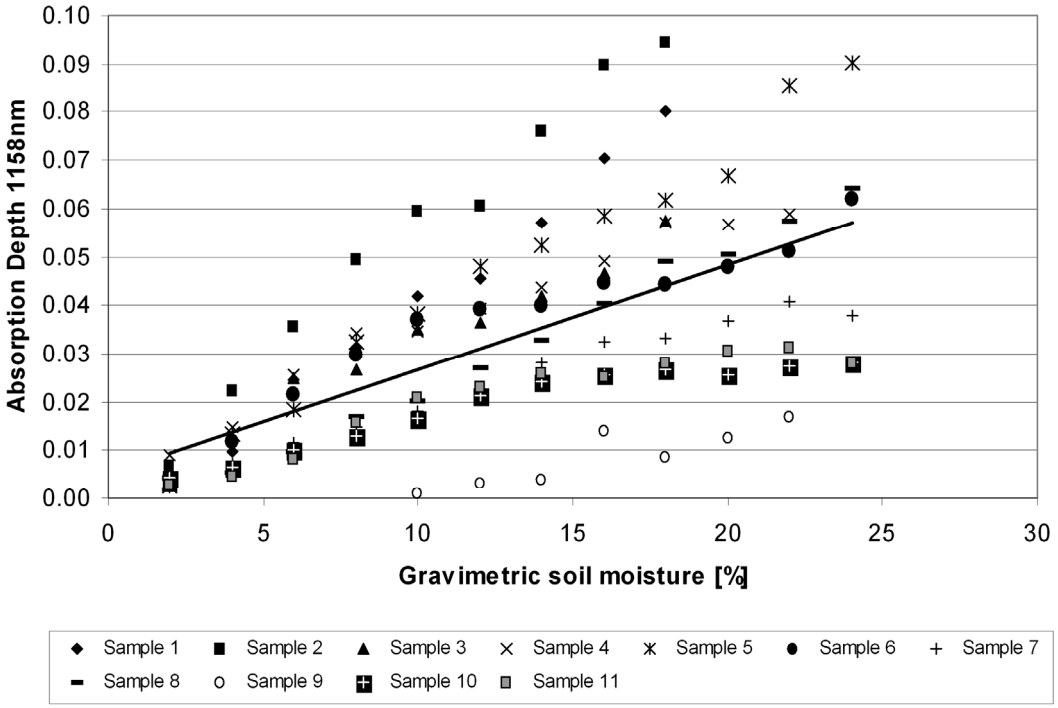

Figure II-7 Linear Regression curve between gravimetric soil moisture and depth of absorption band around 1158 nm for the 11 artificially wetted soil samples.

For being applicable when measuring outside the laboratory, other parts of the spectrum being less affected by atmospheric absorption were therefore exploited.

One of these bands being analyzed is centered at 1158 nm. Although caused by H_2O, it is much less affected by the atmosphere than the more pronounced bands at 1450 and 1900 nm.

Figure II-7 shows only tentatively a linear correlation between gravimetric soil moisture and the depth of this spectral feature with R^2=0.42. This relatively small value is due to the heterogeneity of the samples. While each data series would show a good linear correlation per sample, the slope of each line is different. Tertiary samples (samples 1 to 4) generally show a more pronounced increase in absorption depth with increasing soil moisture than quaternary sand samples.

When being applied to the natural field samples, the R^2-value declines to 0.27 (not shown here), reflecting the relatively weak moisture effect on this spectral band for the natural samples and the variability of the reflectance in this spectral region. Carbon, vegetation, crusts and other naturally occurring substances not filtered out here make the reflectance highly variable, in some cases resulting in the absence of any spectral features around 1158 nm.

Area under the spectrum

The area under the SWIR part of the spectrum between 1700 and 2400 nm, approximating the SMGM by (Whiting et al. 2004), was calculated for the prepared (Figure II-8a) and natural samples (Figure II-8b). The coefficient of determination was similar for both series with values of R^2=0.48 and 0.50, respectively.

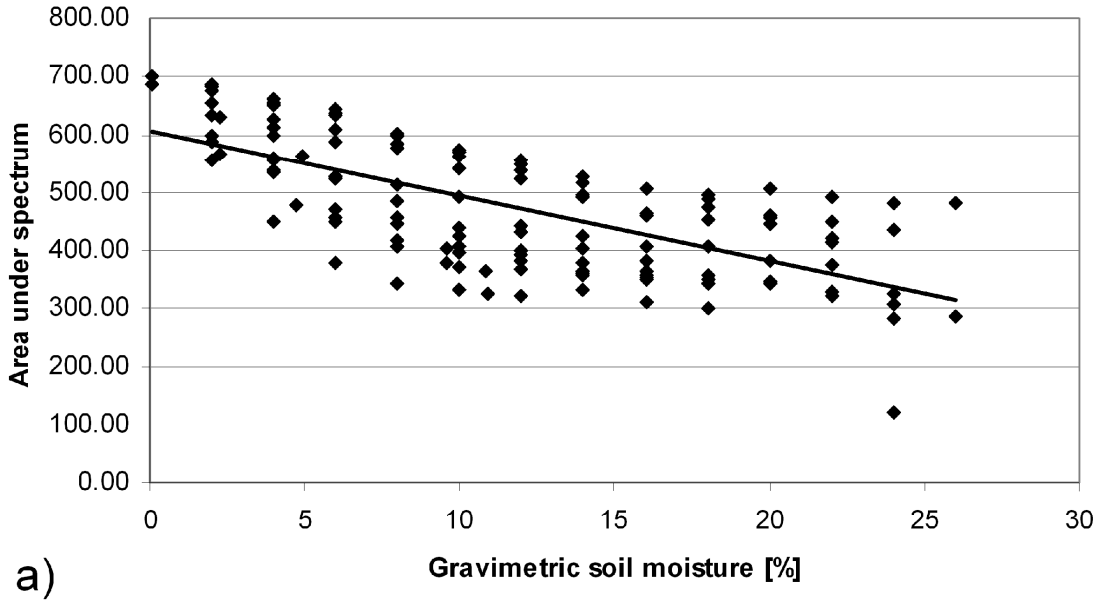

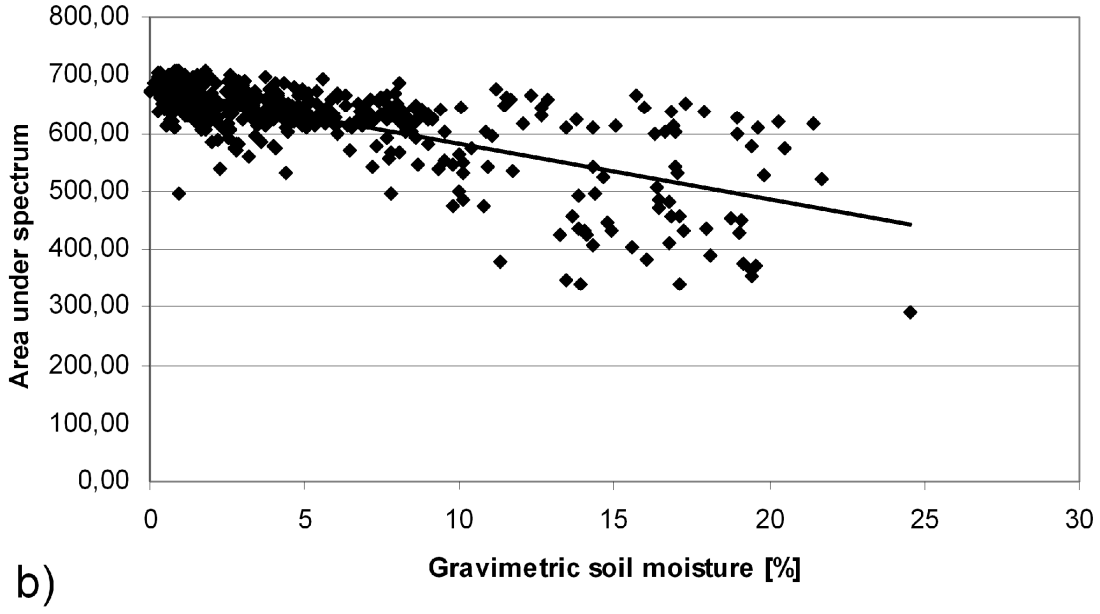

Figure II-8 Linear regression between soil moisture and approximated area under the convex hull of the log-spectrum between 1700 and 2400 nm for a) prepared and b) natural field soil samples (R^2=0.48 for artificially wetted samples, 0.50 for natural soil samples).

While a non-linear relationship between this spectral feature and gravimetric soil moisture seems to exist when regarding the whole spectrum of prepared samples, this cannot be confirmed by the second measurement series. In the plot of the natural samples, the area values show an increasing deviation around the estimated regression line at higher moisture values. These data points predominantly originate from the clay samples, which show moisture values of up to 24%, whereas moisture for tertiary and quaternary sands remained below 8% in the field samples. When regarding each type of soil separately, this spread in values can especially be stated for clay (R^2=0.28) and tertiary sand (R^2=0.35), whereas quaternary samples form a relatively stable linear fit (R^2=0.61) over a limited range.

Figure II-8 shows that the area feature, although a promising approach provides relatively low correlation values when being applied to the given heterogeneous sample set, and cannot be considered as adequate soil moisture estimator in this study when applying linear regression models.

Normalized difference

The coefficient of determination for the linear regression between gravimetric soil moisture and the normalized difference was plotted in a matrix where the first wavelength value is referred to by the x-axis and the second wavelength is referred to by the y-axis (Figure II-9). The grey-coded color scale from 0 to 0.8 represents the corresponding R^2-value. The atmospheric absorption regions, which cannot be exploited in the field or from remote sensors, have been masked out.

When comparing the value distribution between the artificially prepared (lower right) and the natural soil samples (upper left), similar patterns occur, although a better correlation can be generally observed for the prepared samples (darker shading). However, some major differences exist between these two sets of samples. While the normalized difference method seems inappropriate for the natural samples when at least one band is of a shorter wavelength then a certain threshold (around 1000 nm), high correlation values occur on the other hand for the artificially wetted samples in the case that one band is at about 600 nm and the other one around a major water absorption feature, i.e. near 1420, 1950 or 2450 nm. Although the correlation values are the best to be achieved for the artificially wetted samples, these band combinations cannot be applied in field studies, since the respective values for the natural samples are far below a reasonable value.

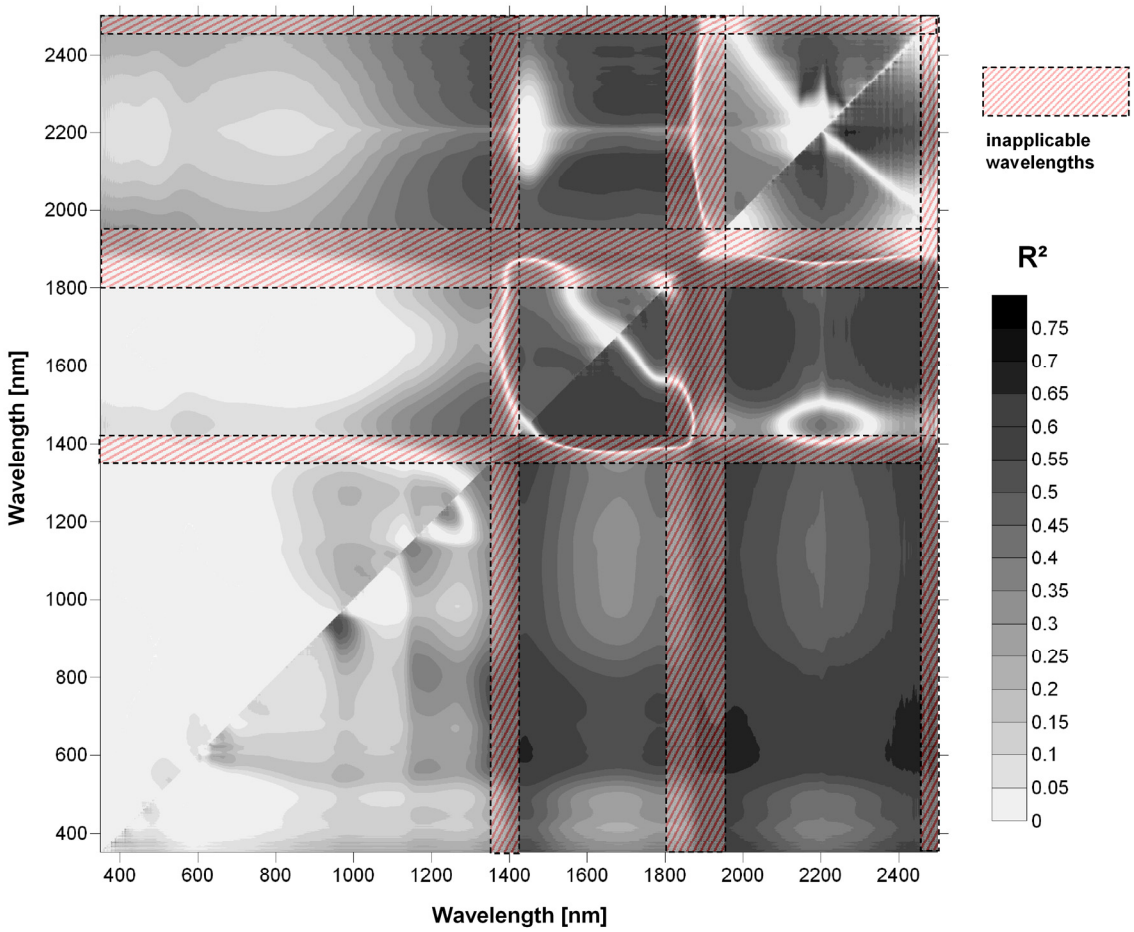

Figure II-9 R²-values gained from linear correlation between soil moisture and normalized difference of two bands. The lower right triangle represents R²-values for the artificially wetted soil samples, the upper left triangle for the natural soil samples.

For the prepared samples, the normalized difference value of bands 600 nm and a second band around 1450 or 1920 nm brings the best correlations (R^2 up to 0.72). For the natural samples, best R^2-values (up to 0.61) are obtained when one of the two reflectance values in the equation is on the lower edge of the two major overtone absorption features, i.e. around 1350 or 1700–1800 nm, whereas the other reflectance is around 2100 or 2300 nm.

Figure II-9 shows that the best soil moisture estimator for the natural samples can be achieved when using reflectances at 1800 and 2119 nm (R^2=0.61). A similar coefficient of determination (R^2=0.6) was observed at these wavelengths for artificially prepared samples.

Normalized soil moisture index

For a deeper investigation of this parameter, the normalized difference values of the wavelengths 1800 and 2119 nm were calculated and plotted for all analyzed samples.

Figure II-10 shows the correlation between gravimetric soil moisture and the calculated index values. Comparing Figure II-10 with Figure II-7, we can conclude that this new estimator is much more insensitive to soil type than e.g. absorption depth and gives good correlation results.

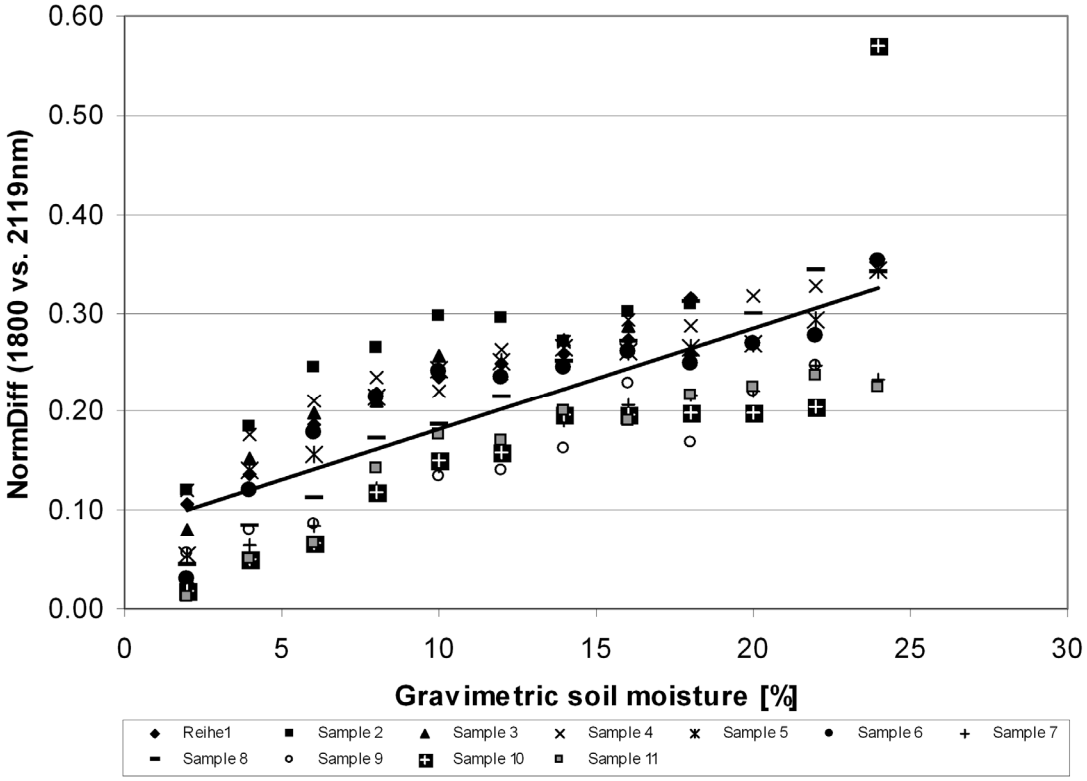

Figure II-10 Linear regression curve between gravimetric soil moisture and the normalized difference index between 1800 and 2119 nm for artificially wetted soil samples (R^2=0.60; n=121).

Based on the previous analyses, this parameter can be introduced as a new soil moisture index, named the normalized soil moisture index (NSMI):

$$NSMI = \frac{R[1800nm] - R[2119nm]}{R[1800nm] + R[2119nm]} \tag{3}$$

The NSMI represents a dimensionless parameter that can be used to quantify soil moisture using Eq. 4:

$$NSMI = a + b \times gravimetric\ soil\ moisture \tag{4}$$

In the case of this study, the values for a (0.032) and b (0.00897) led to reasonable correlations. However, the stability of the actual values of a and b needs to be analyzed.

5 Discussion

The aim of this paper is to find an estimation model deduced from a set of spectral reflectance features that should be a) straightforwardly applicable in the laboratory, field and from remote platforms, b) physically comprehensible and c) robust against changes in covariates (heterogeneity).

The NSMI feature fulfils the postulated criteria of easy applicability. It can be calculated with a simple arithmetic operation, based on two reflectance values. The actual gain and offset of the correlation equation based on the NSMI can be adapted easily for a distinct landscape class.

The sensitivity analysis showed that the SWIR and especially spectral regions around the major absorption bands are very strong in indicating soil moisture changes. The normalized difference approach already proved to be successful in the context of vegetation indices (e.g. NDVI), minimizing the effect of different albedo values and thus generalizing the vegetation characteristics over different species. In our analyses, ratio calculations without the normalization term generated slightly smaller R^2-values for the same wavelengths (0.58 and 0.57), indicating that normalization improves the correlation robustness.

In order to further evaluate the NSMI robustness, the effects of two important covariates were analyzed: soil crusts resulting from distinct surface processes and soil type. Since both variables have a major influence on the behavior of the surface, their specific impact on single reflectance values is of high interest.

The formation of soil crusts could not be quantified adequately due to missing standardized definitions and procedures. Thus only the presence or absence of structural soil crust was determined. Since the thickness of the soil crust layer is not crucial for reflectance measurements, this classification has been rated satisfactory. From the given 467 natural samples, every fifth originated from the very top, from which most samples showed a distinct physical or biochemical crust. These crusts often result in poor applicability of otherwise valid spectral quantification approaches. As can be seen in Figure II-7, absolute reflectances as well as spectral areas are not feasible when soil crusts affect the overall brightness of the spectrum.

Figure II-11a shows the linear regression function of the NSMI with differently symbolized deeper soil layers (1–5 cm deep) and top surface layers. The figure shows that soil moisture values are distributed over the whole range for both layer classes. When

applying the NSMI, the reflectance behavior of the top layers did not behave differently compared to the deeper layers, which were in most cases more homogeneous and therefore similar to the artificially prepared samples measured in the laboratory.

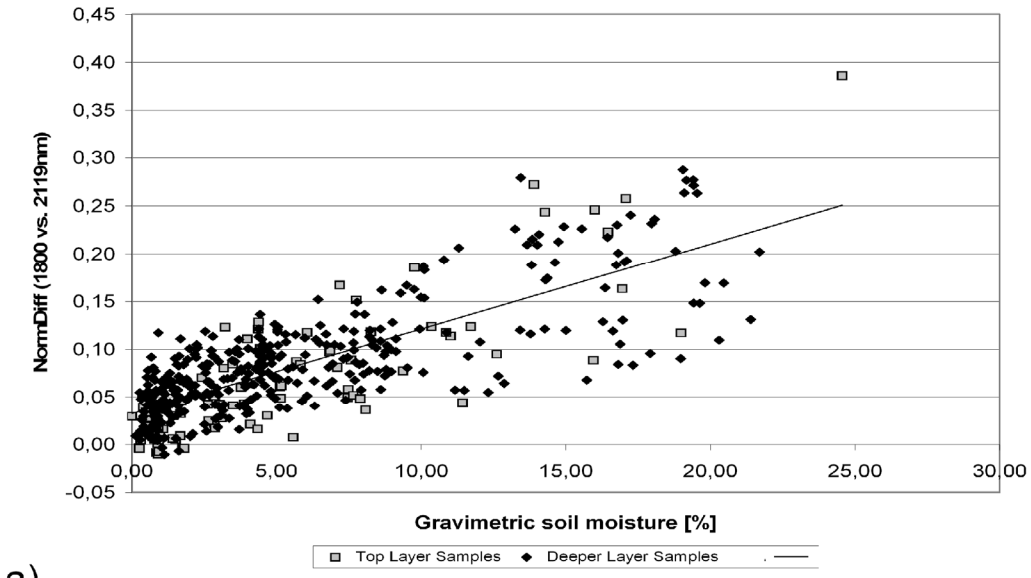

a)

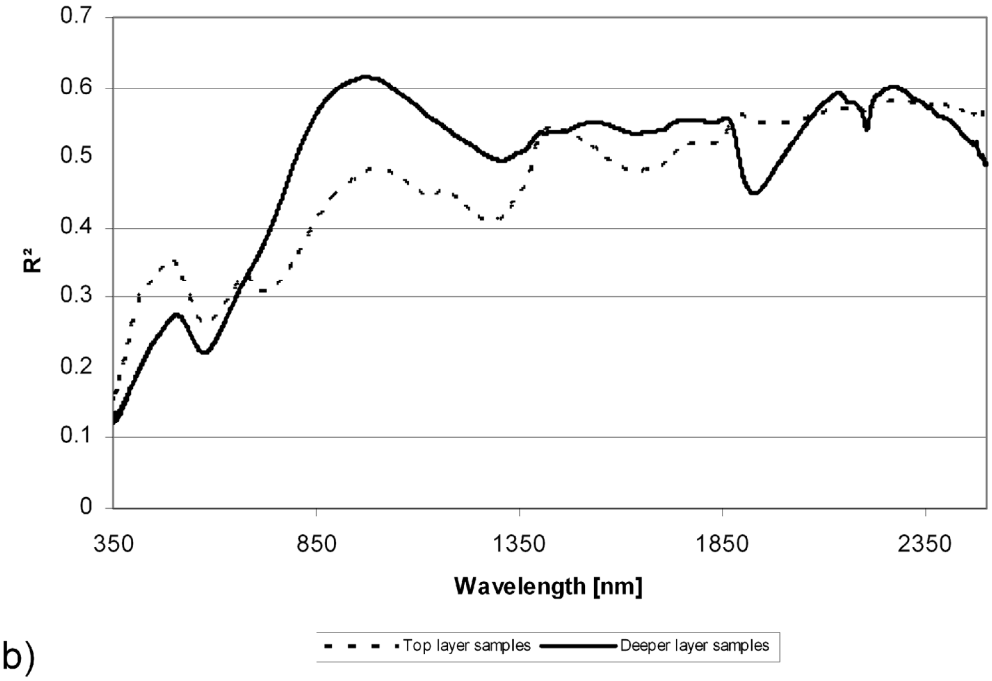

b)

Figure II-11 Linear regression a) Analysis of NSMI under natural field conditions with linear regression curve between gravimetric soil moisture and the NSMI between 1800 and 2119 nm for natural field samples (R^2=0.61, n=467). b) Comparison of squared correlation coefficients between soil moisture and absolute reflectance values for samples from top layer with potentially existing crust and lower soil layers.

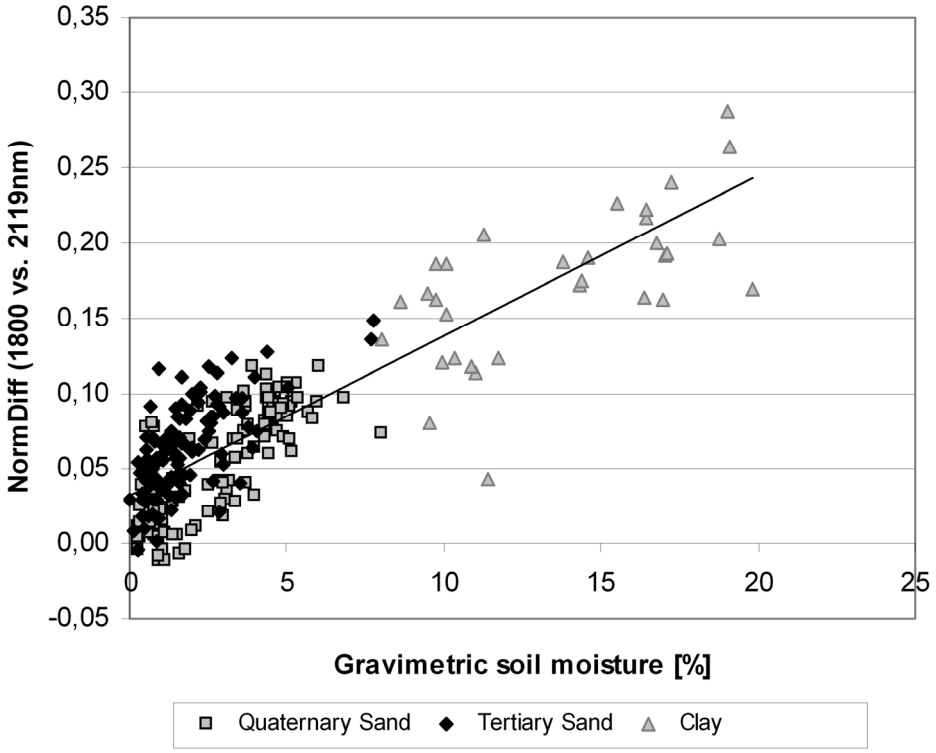

Figure II-12 Linear correlation between soil moisture and NSMI for homogeneous quaternary, tertiary and clay samples under natural field conditions (R^2=0.71, n=277).

When taking a look at single reflectance values over the range from 350 to 2500 nm, Figure II-11b emphasizes the generally slightly worse correlation of the single top-soil layer reflectances with soil moisture. Especially between the NIR and 1400 nm the top soil layers show the adverse effect of soil crusts on the regression goodness-of-fit.

The NSMI with its reflectances at 1800 and 2119 nm makes use of spectral regions where this effect is significantly smaller, while the correlation is maximized.

Figure II-12 points out the performance of the NSMI as function of soil type. It shows the regression plot for the NSMI vs. gravimetric soil moisture for those soil samples that could be unambiguously assigned to one single soil type. The two sands show relatively small soil moisture percentages under field conditions whereas clay samples are characterized by high percentages. The concentration of data values in the diagram for tertiary samples made a detailed analysis of the regression function over the whole range impossible. Visually, the tertiary samples seem to indicate a higher slope of the regression line for this substrate. However, when regarding the artificially wetted samples from the analysis before, the behavior of the regression function for higher soil moisture values could be analyzed and compared to the regression function from natural samples. The higher slope for tertiary samples for lower moisture rates has been detected in both experiment designs,

but the regression curves of all samples converged again beyond 10% in gravimetric soil moisture (Figure II-10). For the same reason, approximated linearity of the regression model can be preconditioned. In contrast to the NSMI, other approaches like the absorption depth at 1158 nm (Figure II-7) did not show the same effect.

The NSMI seems therefore especially suitable to quantify soil moisture differences among the whole soil moisture variability range occurring under the given field conditions, whereas the detection of subtle differences of less than a percent seems error-prone. However, this limitation applies for all established soil moisture estimation approaches.

Other approaches have been analyzed in this study as well, starting with single reflectance values, not leading to the same coefficients of determination. Since absolute reflectance does not take into account any soil specific properties (e.g. color) or illumination inconsistencies affecting the overall albedo, some authors proposed to apply the relative reflectances instead (Weidong et al. 2002). The basic idea of this approach is to calibrate each absolute reflectance value by relating it to the reflectance value of the appropriate dry reference sample and thus making the parameter more robust between different soils. As a consequence, relative reflectances can only be generated for those samples, which may be unambiguously classified as a certain substrate and which therefore could be assigned a distinct reference sample. While the relative reflectances could improve the coefficients of determination by 0.04 in average compared to the absolute values, the need for a strict classification of each substrate made this approach unfeasible in the case of this project. Many of the samples from the field were composites of different substrates, such that dry reference spectra could not be generated for class representatives.

The absorption depth approach generated acceptable correlations for laboratory measurements on prepared samples. When being applied for the natural samples, the correlation degraded significantly, as has been mentioned by other authors. In their research on soil mineralogy quantification of similar soils in a lignite dump, Krüger et al. (1998) found that the application of this feature is limited to those samples of similar composition and grain size distribution, to certain concentration ranges and to sample mixtures without interfering components. While the quantification of surface soil moisture is focusing on a broader spectral range than the detection of single minerals, similar limitations apply. In field studies, the named covariates are spatially heterogeneous and it is therefore not acceptable for a quantification method to be usable only for pure and well separated samples. Thus, while the approach seems feasible when being applied in the

laboratory after calibration for prepared samples, its applicability in the field seems limited.

The very good results that Whiting et al. (2004) found in their studies could not be reproduced here, which can be caused by several reasons. The most significant differences between this study and their work are the sample preparation strategy, varying classes of substrates (sands and clay in our studies, mainly loamy and clayey substrates in the other study) and the calculation of the spectral feature to correlate soil moisture with. The last criterion is able to cause only a minor difference in the quality of the results, since the approach applied here approximates the area under a Gaussian curve in the same spectral region adequately. The two other criteria make the application of the SMGM or its approximation critical for the study conducted here. The SMGM has been developed in the laboratory from prepared samples where crusts and other covariates are negligible. While the resulting homogeneous substrates lead to a better correlation with soil moisture, their transfer to the natural samples was not successful here. In contrast, the NSMI parameter set has been developed under consideration of soil crusts in this study. However, the difference in the substrates between this study and the work of Whiting et al. (2004) might have an influence on the choice of regression model and makes a direct comparison of the approaches difficult.

For finding the optimum wavelengths, the analyses showed that some spectrum regions are more sensitive to the covariates then others. Certain spectral features were able to take care of these covariates in order to set up a general model that is valid for all soils of a region rather than for a prepared set of samples in the laboratory. With the aid of the NSMI, the unprepared samples achieved similar coefficients of determination for the linear regression function, making its applicability under heterogeneous field conditions feasible. For the uppermost soil layer, which is prone to be affected by chemical and physical crusts, single reflectance values behave differently with increasing soil moisture compared to deeper layers. By analyzing the top and deeper layers of the field samples separately, it could be stated, that the NSMI as a combination of two wavelengths not only holds for all substrates, but also for different physico-chemical properties within each substrate.

The NSMI could however not achieve R^2-values as high as in other studies conducted in the laboratory (e.g. Weidong et al. 2002; Whiting et al. 2004). Although an increased coefficient of determination can be achieved with additional a priori knowledge of the surface substrate, its incorporation is not intended in this study in view of robustness and straightforward applicability.

Next to the soil heterogeneities observed here, the effect of vegetation needs to be further analyzed in order to make the NSMI more widely applicable, e.g. for agricultural areas. Hereby the maximum coverage with vegetation for which the model is valid is of special interest.

6 Conclusion and outlook

For the substrates originating from a lignite mining dump being under survey, it could be shown that laboratory spectral measurements generally achieve better correlations with soil moisture when the samples are cleaned, dried and sieved beforehand. Since this preparation, which can only be done in the laboratory, does not reflect the natural heterogeneity in the field, the measurements conducted here explicitly analyzed the different behavior of spectral estimation features when being applied with unprepared samples.

The findings emphasize an aspect already found by different authors: the SWIR spectral region is the most promising for deducing soil moisture quantities from a combination of surface reflectances. While the overtone water absorption bands cannot be utilized under field conditions, especially the spectral regions around them are the most sensitive for changes in soil moisture.

Different promising spectral soil moisture estimators from the literature did not show suitable results with our measurements. We introduced in this paper a new soil moisture index named the Normalized Soil Moisture Index (NSMI). From a systematic study over the whole spectral range from 350–2500 nm, the NSMI based on the reflectance at 1800 and 2119 nm was determined to be the best quantifier of water content for the surface of different substrates. The NSMI can therefore be seen as a generally applicable parameter, which can be used without any a priori knowledge about the surface substrates in a straightforward way. It was tested and developed with different types of substrates and considering soil depths from the upper surface to 5 cm.

Within the scope of this paper, the authors focused on analyzing linear relationships. In order to enhance the quality of the estimators under survey, non-linear regression analysis is likely to be an adequate approach. In future works, potential non-linear relationships need to be analyzed for finding appropriate regression functions, which might also improve the quality of the NSMI for each specific substrate.

Further studies are needed to test the robustness of the NSMI with other types of substrates under highly variable heterogeneous field conditions. In particular, research on the applicability of the model for regions with vegetation cover is of interest.

In future studies, the approach deduced from the laboratory work needs to be validated in field studies, with the sun as a light source. Hereby, the determination of soil moisture in the field provides a further challenge, since another set of measuring devices needs to be applied, bringing up additional issues to account for (inaccuracy, thickness of soil layer, etc.). The NSMI also needs to be tested for its applicability from remote sensing data, where the spectral and spatial resolution and the additional effect of the atmosphere complicate spectral measurements.

This study shows that the NSMI holds potential as being a widely applicable spectral soil moisture predictor. Its aim is to provide a new methodology for quick assessment of surface or near-to-surface water content directly in the field using spectral instruments or from adequate remote sensors e.g. in dry regions of the world having little vegetation cover.

Chapter III:
Surface soil moisture quantification and validation based on hyperspectral data and field measurements

Journal of Applied Remote Sensing 2 (023552), 1

Sören-Nils Haubrock, Sabine Chabrillat, Matthias Kuhnert, Patrick Hostert and Hermann Kaufmann

doi: 10.1117/1.3059191.

Received 3rd June 2008; revised 26th November 2008;
accepted 2nd December 2008.

.

Abstract

Surface soil moisture information is needed for monitoring and modeling surface processes at various spatial scales. While many reflectance based soil moisture quantification models have been developed and validated in laboratories, only few were applied from remote sensing platforms and thoroughly validated in the field. This paper addresses the issues of a) quantifying surface soil moisture with very high resolution spectral measurements from remote sensors in a landscape with sandy substrates and low vegetation cover as well as b) comprehensively validating these results in the field. For this purpose, the recently developed Normalized Soil Moisture Index (NSMI) has been analyzed for its applicability to airborne hyperspectral remote sensing data. Three HyMap scenes from 2004 and 2005 were collected from a lignite mining area in southern Brandenburg, Germany. An NSMI model was calibrated (R^2=0.92) and surface soil moisture maps were calculated based on this model. An in-situ surface soil moisture map based on a combination of Frequency Domain Reflectometry (FDR) and gravimetric data allowed for validating each image pixel (R^2=0.82). In addition, a qualitative multi-temporal comparison between two consecutive NSMI datasets from 2004 was performed and validated, showing an increase in estimated surface soil moisture corresponding with field measurements and precipitation data. The study shows that the NSMI is appropriate for modeling surface soil moisture from high spectral-resolution remote sensing data. The index leads to valid estimations of soil moisture values below field capacity in an area with sandy substrates and low vegetation cover (NDVI<0.3). Further studies will analyze the validity of the NSMI for surface soil moisture estimation from spaceborne hyperspectral sensors like the Environmental Mapping and Analysis Program (EnMap) in different landscapes.

1 Introduction

Soil moisture is one of the key variables in the hydrologic cycle controlling processes such as infiltration and discharge with consequences for surface water availability, plant growth, soil erosion and land degradation (Merritt et al. 2003). Today, it is evident that climate change has an impact not only on arid and semi-arid regions, but also on the environment of the temperate zone (Watson et al. 1998). Predicted changes in rainfall regime as a result of global warming may affect soil moisture, surface water balance, and deteriorate ecosystem functioning (Porporato et al. 2004). Knapp et al. (2002) discovered in their experiments that more extreme rainfall patterns, without concurrent changes in total rainfall quantity, increase temporal variability in soil moisture and plant species diversity. Under these conditions information about soil moisture becomes increasingly important for monitoring and predicting soil erosion, land degradation and land cover changes in general.

Remote sensing offers the potential to efficiently estimate this variable at different spatial scales. Many approaches quantifying surface soil moisture from airborne or spaceborne platforms exist, but few of them are based on optical reflectance data. While in the microwave range soil moisture measurements are strongly affected by surface roughness and vegetation cover, optical remote sensing approaches have to take into account several covariates affecting reflectance values, among others soil color, soil texture, organic material and crusts (Baumgardner 1985; Ben-Dor and Banin 1994; Goldshleger et al. 2002; Goldshleger et al. 2004b). For hydrological applications, the most important difference between optical and microwave approaches is the penetration depth and consequently the depth of the soil layer for which the water content is being quantified. Penetration depth with optical remote sensing is significantly lower, so soil moisture is quantified for the uppermost layer in a soil column. Capehart and Carlson (1997) analyzed the correlation of surface radiant temperature as a proxy for surface soil moisture derived from Advanced Very High Resolution Radiometer (AVHRR) data and soil moisture in deeper layers. Comparing these results, they found poor correlations and concluded that horizontal, vertical and temporal variability of soil moisture make a prediction based on top-layer remote sensing approaches very complex. However, they also found out that relationships between upper and deeper soil water content are mainly affected by soil hydraulic properties, surface variables (e.g. roughness) and spatiotemporal drying patterns, which in turn depend on initial soil moisture and potential evaporation. In the case that

corresponding information is given, stronger relationships between upper and deeper soil water content are likely to exist locally, but have yet to be confirmed. In combination with data quantifying soil moisture for the upper few centimeters (like microwave or in-situ datasets), optical data could make an indispensable contribution to describe the vertical profile of soil water content and also serve as a spatial index for surface hydraulic properties of the soil.

Radiative transfer models like GeoSAIL (Huemmrich 2001) or SLC (Verhoef and Bach 2007) are suitable means to analyze reflectance sensitivity in a theoretical framework. The influence of surface soil moisture on reflectance is considered in a submodel of GeoSAIL. Bach and Verhoef (2003) found out in their studies with GeoSAIL that the soil moisture effect is spectrally different from changes caused by variable plant water content and they concluded that hyperspectral sensors provide a means to distinguish between these two effects.

Many practical studies on soil moisture reflectance were performed in the artificial environment of a laboratory (Planet 1970; Lobell and Asner 2002; Weidong et al. 2002; Weidong et al. 2003; Whiting et al. 2004). In these studies it has been confirmed that the shortwave infrared (SWIR) part of the electromagnetic spectrum is especially sensitive to soil moisture heterogeneities in different substrates. Resulting models are therefore based on the fact that increasing soil moisture up to a certain level entails a decrease in reflectance values over the visible (VIS) to SWIR range.

In most laboratory studies soil samples are prepared (i.e. cleaned, sieved and oven-dried) before being spectrally analyzed, which facilitates the derivation of successful quantification models. In contrast, results from field and remote sensing studies are more affected by natural heterogeneities and covariates. Haubrock et al. (2008b) addressed the challenge of providing a quantification model from heterogeneous field samples, resulting in the Normalized Soil Moisture Index (NSMI). The NSMI is based on a normalized difference of reflectance values at 1800 nm and 2119 nm. It has been developed in laboratory studies measuring soil samples not modified by preparation. This approach has been determined to be the optimum quantifier of surface soil moisture in a heterogeneous field with quaternary and tertiary sands as well as clay soils in comparison with other published soil moisture quantifiers.

Besides studies based on laboratory results, approaches exist to quantify surface soil moisture from broadband optical sensors such as Landsat Thematic Mapper (Landsat

ETM+), Advanced Very High Resolution Radiometer (AVHRR), Moderate Resolution Imaging Spectroradiometer (MODIS) (Capehart and Carlson 1997; Profeti and Macintosh 1997; Vincente-Serrano et al. 2004; Zhang and Wegehenkel 2006; Khanna et al. 2007) or simulated Satellite Pour l'Observation de la Terre (SPOT) channels (Muller and Décamps 2000).

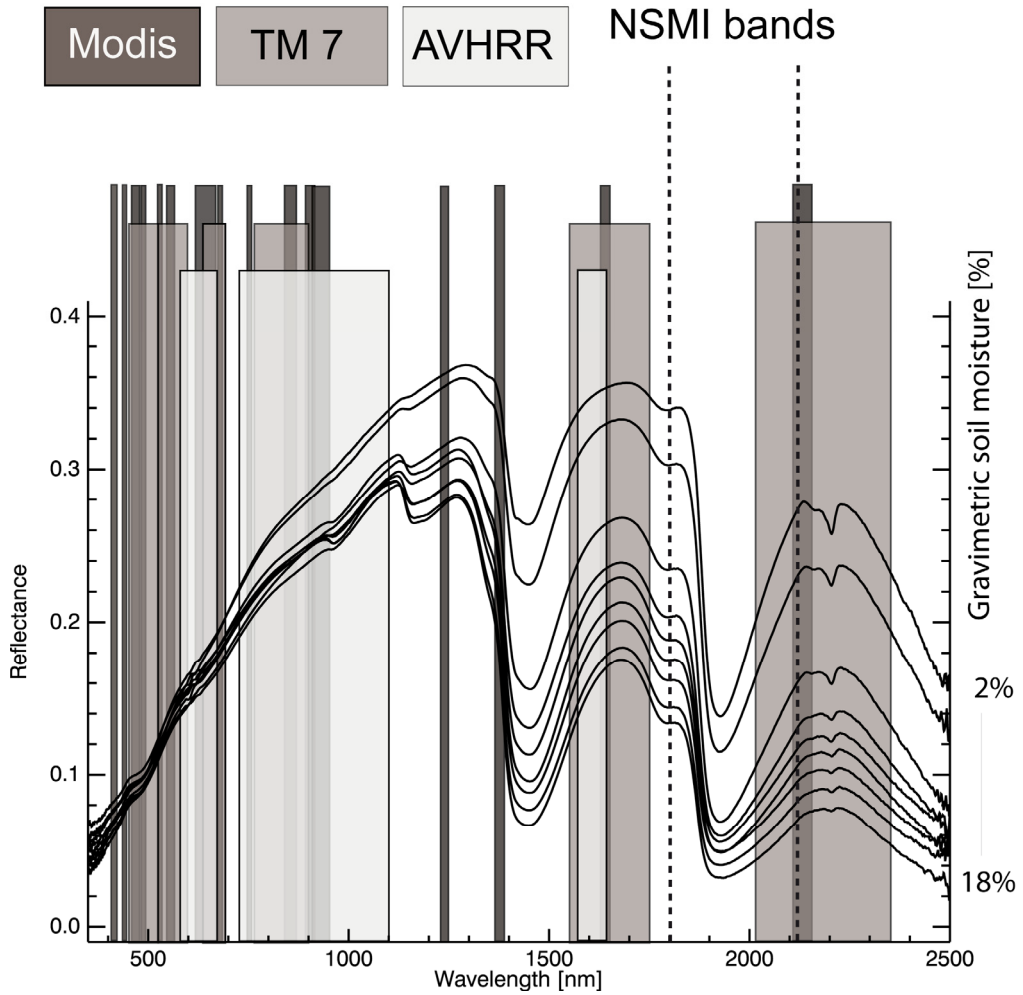

Figure III-1 Effect of increasing soil moisture on reflectance between 400 and 2500 nm compared to spectral resolution of MODIS, Landsat TM-7, AVHRR sensors. The spectra are taken from an artificially wetted sample of sandy substrates. Soil moisture is measured as percentage of weight (gravimetric soil moisture).

Due to the relatively broad spectral resolution of these sensors, none of the models developed under laboratory conditions can be applied here without restrictions. Figure III-1 shows the typical behavior of a reflectance spectrum derived from high-resolution spectral measurements of a soil sample with increasing gravimetric soil moisture (GSM). The wavelength band positions of the sensors Landsat ETM+, AVHRR or MODIS are provided for comparison, as are the wavelengths used by the NSMI.

Table III-1 gives an overview of common reflectance-based soil surface moisture quantification models applied in laboratory and from spaceborne platforms.

Research on soil moisture quantification from reflectance data has shown that existing models reveal reasonable accuracies in laboratory studies but have a) rarely been validated in the field and are b) hardly ever transferable to multispectral sensors without loss. The effect of covariates and natural heterogeneity requires a more detailed investigation of

Table III-1: Overview of common reflectance-based surface soil moisture quantification models, grouped by their application environment.

Quantification model	Reference	Wavelengths/ Sensor bands	Validation method
Laboratory studies			
Exponential model	(Lobell and Asner 2002)	350-2500 nm	gravimetric
Relative reflectance	(Weidong et al. 2002)	1998 nm	gravimetric
First derivative	(Weidong et al. 2003)	1834-1836 nm	gravimetric
Reflectance difference	(Weidong et al. 2003)	2250 and 2062 nm	gravimetric
Ratio	(Bryant et al. 2003)	1450 and 1300 nm	
Moisture Determination Ratio (MDR)	(Bogrekci and Lee 2004)	1340, 1290 and 1940 nm	gravimetric
Soil Moisture Gaussian Model (SMGM)	(Whiting et al. 2004)	1200-2500 nm	gravimetric
Normalized Soil Moisture Index (NSMI) (unprepared/natural field samples)	(Haubrock et al. 2008b)	1800 and 2119 nm	gravimetric
Remote Sensing studies			
Reflectance	(Muller and Décamps 2000)	SPOT	gravimetric
Triangle method	(Capehart and Carlson 1997)	AVHRR	hydrological model
Broadband ratio	(Profeti and Macintosh 1997)	TM 1/2/5	hydrological model
Hybrid triangle method	(Vincente-Serrano et al. 2004)	ETM+ and AVHRR	climate indices
Vegetation index proxies	(Zhang and Wegehenkel 2006)	MODIS LAI/NDVI	gravimetric and TDR
Angle indices	(Khanna et al. 2007)	MODIS NIR/SWIR	field crop data

valid relationships between reflectance values and surface soil moisture in the field. For this purpose, a spectrally more detailed analysis on the basis of hyperspectral imagery promises better results due to the comparability with spectral resolutions available in laboratory studies.

In this paper, we study the potential of the NSMI method for being applied to airborne remote sensing data. Multi-temporal surface soil moisture quantifications based on the NSMI derived from Hyperspectral Mapper (HyMap) data are presented from a test site within the lignite mine Welzow-Süd (Germany). In contrast to Haubrock et al. (2008b), the analyses are focused on sandy substrates, which are mostly free of vegetation cover in the field and show more homogeneous physical and chemical properties, which is necessary

for the generation of an appropriate in-situ validation dataset. A new validation method is introduced based on a total of 223 field soil moisture measurements collected at overflight time, which were interpolated between point locations. With this approach we were able to assess surface soil moisture estimations based on a pixelwise comparison with concurrently measured in-situ data. With this study, we take an important step to fill the gap between two application domains: high-precision laboratory measurements with accurate results based on synthetic surrounding conditions and broadband sensor systems with their limitations in accurately estimating and validating surface soil moisture in a natural environment.

2 Study site

2.1 General description

A small catchment being part of a bio-monitoring reclamation zone in the lignite mine Welzow-Süd near Cottbus, Germany, was selected as study site (Figure III-2). Elevations nowadays range between 129.4 and 135.6 m (AMSL). Slope gradients exhibit up to 25%. Low mean annual rainfall and a high evaporation characterize the study site (mean for the period 1961-1990 according to Wendling et al. (1999): precipitation 563 mm/year and potential evapotranspiration 600 to 650 mm/year). During the study period the amount of precipitation measured at a local weather station was lower than average (2004: 432.7 mm; 2005: 483.9 mm), while the potential evaporation was lower than average in 2004 (582 mm), but higher in 2005 (735 mm). Due to access restrictions, the area is undisturbed from anthropogenic influences. Low vegetation cover makes it suitable for remote sensing based research on soil parameters. Episodic surface runoff has formed a network of erosion rills in particular in the upper (northern-eastern) part of the test site.

2.2 Substrates

After the mining activities had finished in 2001, different substrates were dumped at the test site. An aquiclude (clay layer) is located at a depth of about two meters below the surface. The dumped substrates form a shallow aquifer above the clay layer, with groundwater levels located about 0.5 to 1.5 m below the terrain surface. The dumped substrates are quaternary and tertiary sands, which are coarsely textured and contain less than 4% clay. Both substrates were mapped as Technosol according to the World Reference Base (WRB) classification in (WRB 2006).

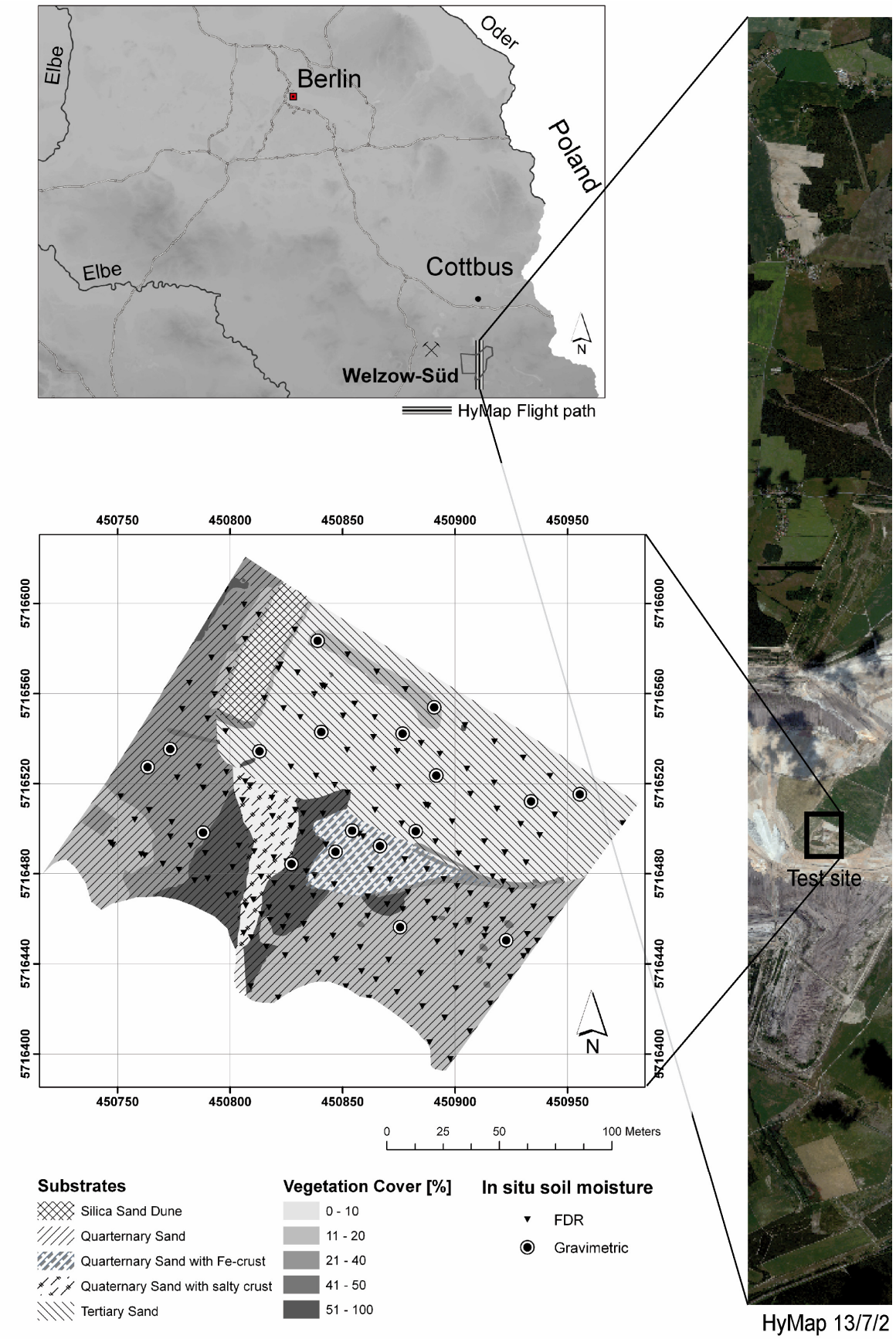

Figure III-2 Test site with soil types and vegetation cover (as from June 2005). Vegetation cover has been estimated in the field and by digital photography. (Spatial reference system: Universal Transverse Mercator (UTM 33N), World Geodetic System (WGS 1984))

The tertiary substrate in the northern part of the test site is characterized by very coarse grain sizes (44.7% > 630 µm) resulting in a poor water storage capability (field capacity) (Lemmnitz et al. 2007). Surface soil moisture values are therefore highly dynamic in time. The area is nearly free of any vegetation cover due to the high soil acidity (pH-value about 3.1). This part of the test site has the highest elevation with a slope facing southward.

In the adjacent area quaternary sand is predominating. A slightly acid character (pH-value about 5.6) and low to moderate field capacity is characteristic for this substrate (Lemmnitz et al. 2007). Surface processes have formed a more differentiated spatial substrate distribution after 2001 (see Figure III-2). Soil erosion patterns show a discharge of material from the upper part (tertiary substrate) and an accumulation of substrates with smaller grain sizes and very distinct chemical properties further south. Especially in the northern part of the quaternary sands, eroded substrates have accumulated and developed a specific formation that can be clearly distinguished from the surrounding substrates by their color, constituents and vegetation cover. Typical for this accumulation area is its high content in Fe_2O_3, which originates from chemical processes typical for lignite mines (Wisotzky and Obermann 2001). As a consequence, vegetation is absent here. In contrast, the surrounding areas show a relatively high vegetation cover. A naturally developed discharge and erosion channel further west transports water and sediments in a southerly direction and exhibits specific mineral crusts on top of the mainly quaternary substrates.

2.3 Data

Datasets for NSMI model setup

In the scope of this study, three HyMap scenes covering the test site were recorded during the HyEurope 2004 and 2005 campaigns organized by the German Aerospace Center. HyMap measures radiance in 126 bands covering the 440 to 2470 nm wavelength region with a spectral resolution between 13 and 17 nm (Cocks et al. 1998). Calculating reflectances from original radiance values was necessary to comply with field and laboratory based measurements. All scenes (Table III-2) cover the entire test site under cloud-free conditions. The images were acquired with 4m ground resolution and a swath width of 2048 m.

Calibration of the NSMI regression function for HyMap application was performed with independent long-term datasets. Seven sampling campaigns were undertaken between 2004 and 2005 collecting 5 cm deep soil cores from nine different locations in the field covering all substrates under survey.

Table III-2: HyMap scene characteristics.

Scene No.	Acquisition date	Acquisition time [CEST]	Average flight height [m]	Average flight direction [°]	Illumination	
					Sun zenith [°]	Sun azimuth [°]
1	2004, July 7th	11:58am	2006	-2.2	31.92	149.38
2	2004, July 30th	10:34am	1997	0.47	45.09	122.87
3	2005, June 20th	1:50pm	2077	0.0	29.24	199.39

Within 24 hours the sealed samples were brought to the laboratory and subdivided into five layers (sub-samples) of 1 cm width with the aid of a trowel. 208 reflectance spectra were measured using an Analytical Spectral Devices (ASD) FieldSpecPro FR® spectroradiometer, covering the 350-2500 nm spectral region with 2151 bands resampled to 1 nm. Gravimetric soil moisture values were determined for each layer applying conventional oven-drying for 24 hours at 105 °C. These values range between 0 and 25% and as such cover the whole domain of soil moisture values for which the NSMI had been developed in the laboratory (Haubrock et al. 2008b).

For image pre-processing purposes, 377 reference spectra were taken in the field simultaneous with image recording in 2005. Additional spectra were taken from characteristic surfaces outside the test site to improve the radiometric correction of the image (e.g. dark asphalt from a parking lot). All spectra were acquired with nadir view from approximately 1m height, resulting in a field of view (FOV) of ~40 cm in diameter. To cover larger areas and for enhancing the signal-to-noise-ratio (SNR), spectra were taken while walking with the ASD device. For each of the 5 to 10 m long transects, 100 spectral measurements were averaged. The area of interest was completely covered by walking in parallel lines. Differential Global Positioning System (DGPS) data were collected to locate the transects.

In order to measure a distinct contrast in soil moisture within a single substrate an area of approximately 100 m^2 was artificially wetted shortly before the overflight in 2005 with 200 liters of water.

In-situ soil moisture data

Volumetric soil moisture values were measured in the field using Frequency Domain Reflectometry (FDR) devices on June 20th 2005. FDR devices can be used for estimating the volumetric soil moisture values for the upper five cm column based on soil electric properties (Nadler et al. 1991; Heimovaara 1994).

205 FDR values were collected within three hours around overflight time. Measurements were acquired every 5 m on transects that were 10m apart resulting in a mesh of point measurements of 5x10 m ground resolution, which was interpolated to a 4x4 m raster image to facilitate comparisons with the HyMap scene. For geocoding the in-situ data, DGPS values were recorded for each FDR measurement.

3 Methodology

For the purpose of surface soil moisture quantification and validation at the micro-catchment scale a comprehensive methodological concept has been developed. Figure III-3 shows the components of this approach, which are described in more detail in the following.

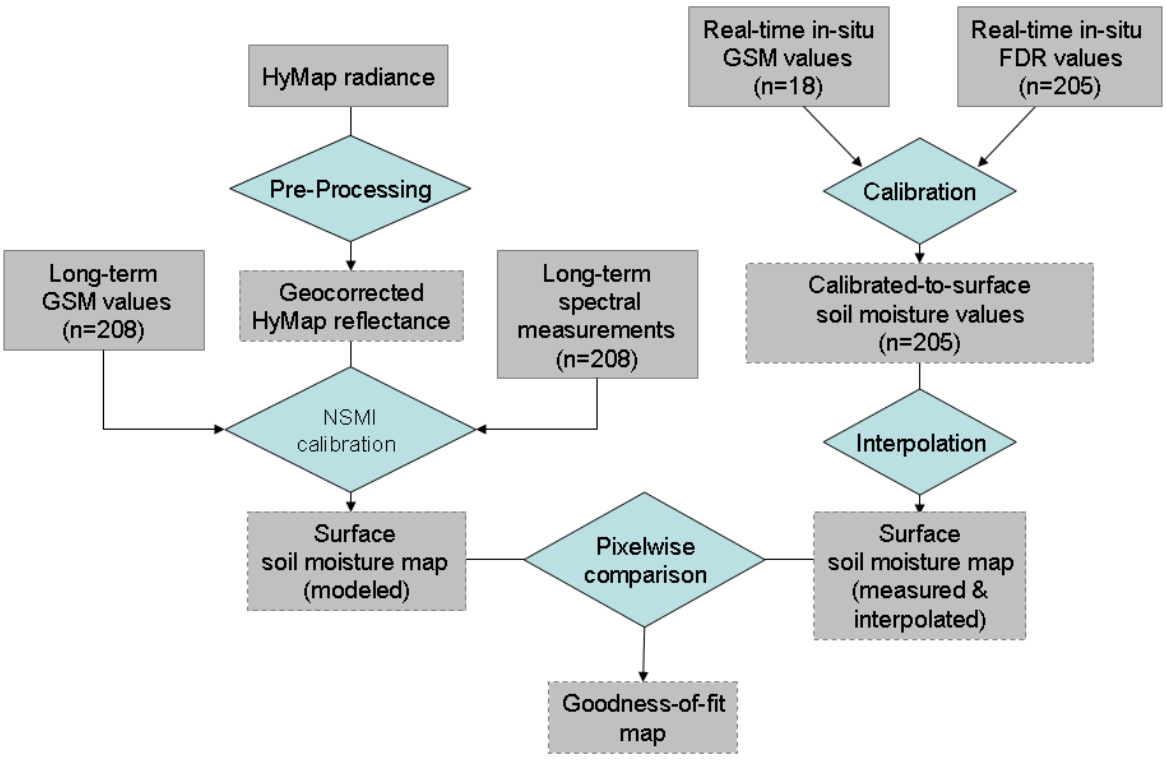

Figure III-3 Methodological concept for surface soil moisture estimation and validation.

Applying and evaluating a model on surface soil moisture quantification at the field scale involves two sequences of processing and analysis steps: a) quantifying soil moisture based on reflectance data and b) generating a validation map based on in-situ and laboratory measurements. The data sets collected in the scope of the HyMap 2005 campaign were

used for setting up the quantification model and validation maps. The resulting model was then applied to the other two images and compared to meteorological and in-situ soil moisture data.

3.1 Pre-processing of HyMap images

The HyMap scenes were atmospherically corrected using an in-house developed hybrid method (ACUM algorithm). It employs MODTRAN 4 (Berk et al. 2003) to calculate at-surface reflectance. The algorithm includes a scan angle dependent correction accounting for the large field of view of 61.3 ° and an adjacency effect correction. The resulting spectra were adjusted via empirical line calibration based on field spectra to minimize the residual artifacts around major water absorption bands. The field spectra were acquired at overflight time over homogeneous bare surfaces (bright soils, dark soils, asphalt). They were resampled to the spectral resolution of the HyMap sensor and geometrically mapped based on DGPS measurements before performing the empirical line calibration.

Parametric georectification removed scanline artifacts caused by aircraft movements. It was based on the DGPS coordinates measured for each scanline position on board of the aircraft in addition to the sensor calibration information and the flight parameters pitch, roll and heading. Additional reference points (n=12) from digital topographic maps (1:50,000) were used to account for remaining pixel shifts and to reconstruct the exact scanline of the aircraft, finally resulting in a root mean square error (RMSE) of 1.66 m.

After atmospheric modeling and empirical line calibration, the resulting image spectra consisting of 126 wavelength channels showed good accordance with independent field spectra resampled to HyMap spectral resolution. The highest discrepancies in reflectance (up to 0.04) occur for soil spectra near the water absorption bands at 1400 and 1900 nm. For the NSMI approach followed here, where reflectance values near 1800 and 2119 nm are considered, residual errors after calibration are within 2%.

Figure III-4 shows the resulting HyMap image of the test site (color composite with red-green-blue (RGB) channels at HyMap bands 13-7-2, centered around 615 nm-523 nm-449 nm) with representative image spectra taken at characteristic locations. Spectra T1 to T3 are taken from samples in the tertiary substrate. Most pixels in this area show soil reflectance characteristics similar to T1, with a typically high albedo and distinct absorption features in the SWIR diagnostic of clay fractions. Due to the absence of vegetation here, a red edge is not present.

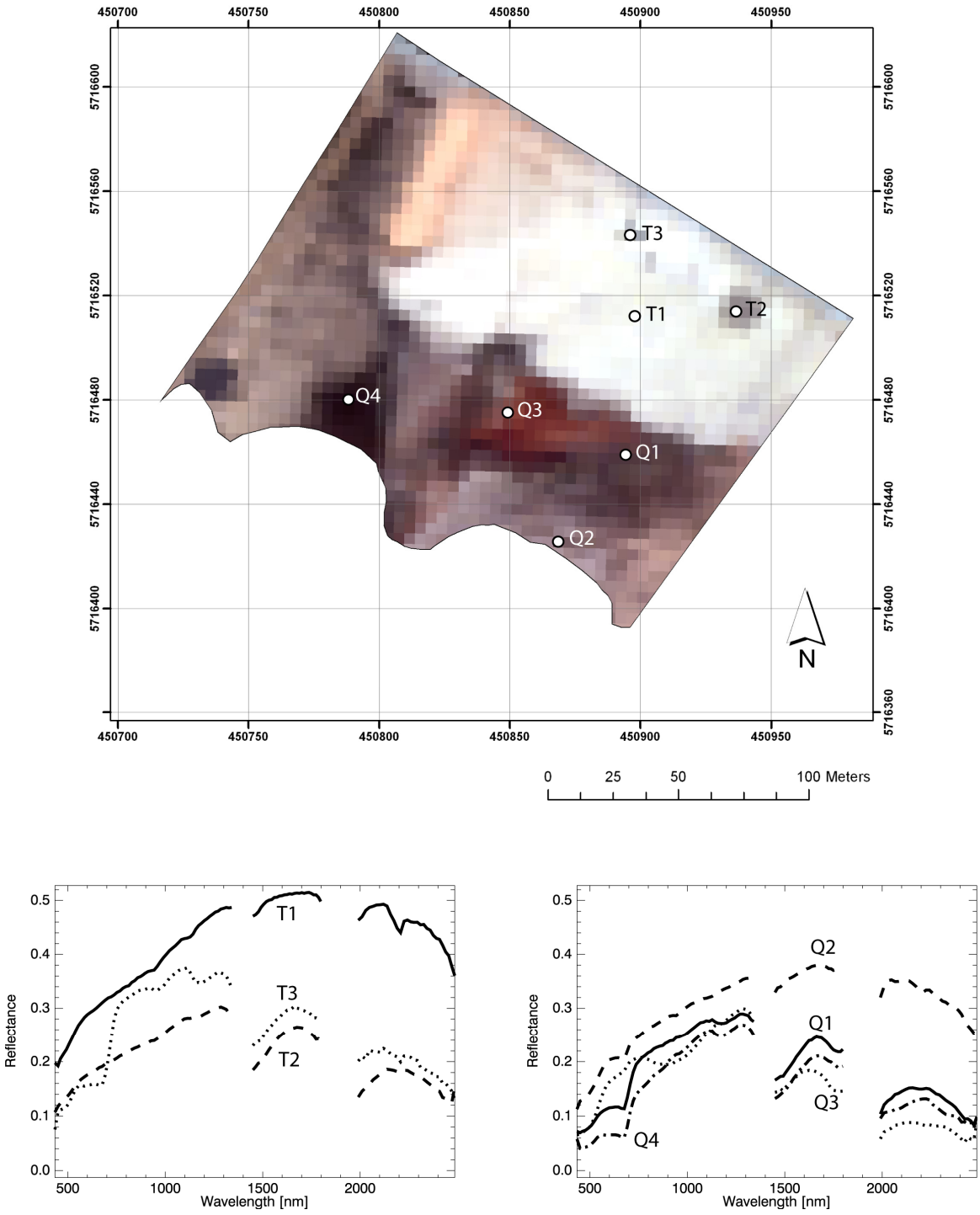

Figure III-4 True-color image in grey-coded scale of the pre-processed HyMap scene 2005 from the test site with representative image spectra from the tertiary (T1-T3) and quaternary (Q1-Q4) areas.

In contrast, T3 shows a spectrum associated with the only significantly vegetated part in the tertiary sand, where an area of around 3x3 m is covered with reed. An important effect of soil moisture on the spectrum of a HyMap pixel can be seen in spectrum T2. It has been collected from the 10x10 m area that had been artificially wetted just before image acquisition time. The substrate in this area is equivalent to the one resulting in spectrum T1, but the higher soil moisture value severely affects the shape of its spectrum. It can be

seen that not only the overall albedo is lower than in T1, but also the absorption band around 1900 nm is more pronounced and the clay diagnostic feature at 2200 nm has been drastically reduced. The difference in reflectance between the bands below and above the 1900 nm absorption band is higher. This well-known effect of increasing soil moisture is crucial for the NSMI quantification approach applied in this study. The pixels from the quaternary substrate are characterized by darker, grey-brownish color in the RGB image. Different subtypes within the quaternary soil can be reconstructed in this image. Increasingly reddish color tones can be observed in the regions of large iron content associated with diagnostic iron features in Q3. Additionally, higher density in vegetation can be identified by dark pixel values in the image.

The image spectra reflect the natural heterogeneity of the surface substrates in the area studied. Figure III-4 shows that soil moisture estimations based on the overall albedo decrease are of limited use here since they are partly caused by variable soil physical and chemical composition of substrates in the field.

3.2 Soil moisture estimates from reflectance data

To provide a model for surface soil moisture quantification based on reflectance data measured with the HyMap sensor, a calibration based on laboratory measurements was performed.

The NSMI was used to estimate surface soil moisture from HyMap data according to the normalized difference Eq. 1.

$$NSMI = \frac{R[1800nm] - R[2119nm]}{R[1800nm] + R[2119nm]} \quad (1)$$

R[x]: Reflectance at wavelength x

The NSMI represents a dimensionless parameter that can be used to quantify gravimetric soil moisture using the linear relationship

$$GSM = a + b \times NSMI \quad (2)$$

GSM: gravimetric soil moisture [g/g]

a,b: offsset and gain of linear regression function

Table III-3: Bands/center wavelengths chosen for application of NSMI with HyMap data.

Date	Wavelength 1 [nm]	FWHM [nm]	Wavelength 1 [nm]	FWHM [nm]
2004, July 7th and July 30th	1793.1	13.1	2116.5	20.1
2005, June 20th	1798	12.9	2120	20.2

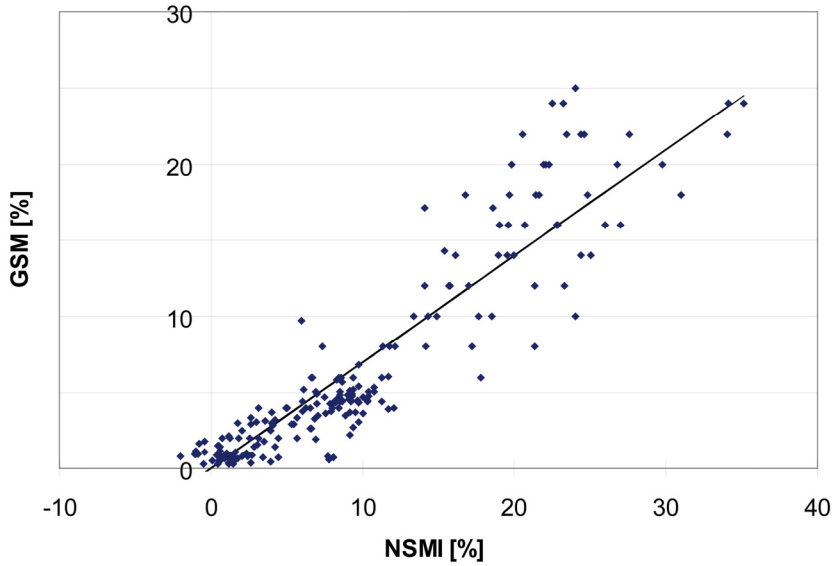

Figure III-5 Calibration function based on a long-term measurement series of gravimetric surface soil moisture and NSMI values generated from ASD spectra resampled to HyMap spectral resolution. Linear regression parameters: a=0, b=0.7; R^2=0.92; RMSE=2.55% GSM (n=208).

The full width at half maximum (FWHM) spectral resolution between 6 and 21nm required an adaptation of the NSMI for the HyMap sensor. Slight shifts in the index occurred in the datasets due to different band centre wavelengths in the sensor calibrations for the three datasets (Table III-3).

The 208 long-term ASD spectra described in 2.3 were resampled to HyMap spectral resolution. The bivariate dataset was used for a least-square linear regression analysis between HyMap-resampled NSMI and GSM. Gain and offset values according to Eq. 2 were determined (Figure III-5) and applied to all images.

3.3 Determination of surface soil moisture from in-situ data

The 205 FDR samples measuring average soil moisture values of the upper five centimeters allow for an appropriate spatial coverage to generate validation points for each pixel of the HyMap images. Since soil moisture in the upper five centimeters is in most cases not identical with the soil moisture at the surface, the FDR values needed to be calibrated-to-surface to allow a comparison with optical remote sensing data. The

additionally collected soil cores provided information on the vertical soil moisture distribution via separate measurements within five layers (one layer per cm). Soil specific vertical soil moisture distribution information could be gained from these datasets for each substrate. Preliminary analyses showed that soil moisture profiles were relatively homogeneous within each substrate in the field, so a relatively small number of samples was considered sufficient for representing substrate typical proxies for a total of 18 cores.

A graphical representation of the vertical soil moisture distribution measured in the field is given in (Figure III-6). The vertical distribution shows typical patterns for each of the substrates. In the case of the tertiary sand, the tendency of increasing soil moisture with increasing depth would lead to an overestimation of surface soil moisture when averaging over the upper five centimeters.

Linear relationships between volumetric soil moisture values based on 5 cm average FDR measurements and gravimetric soil moisture values of the uppermost layer based on core samples were established and applied as correction factors to account for the deviation between five-centimeter mean and top layer values. Specific values were calculated for the tertiary and quaternary substrate as well as for those quaternary samples that were affected by crust formation or significant Fe_2O_3 amounts. Conversion to gravimetric soil moisture was based on the average bulk density of 1.68 g/cm^3.

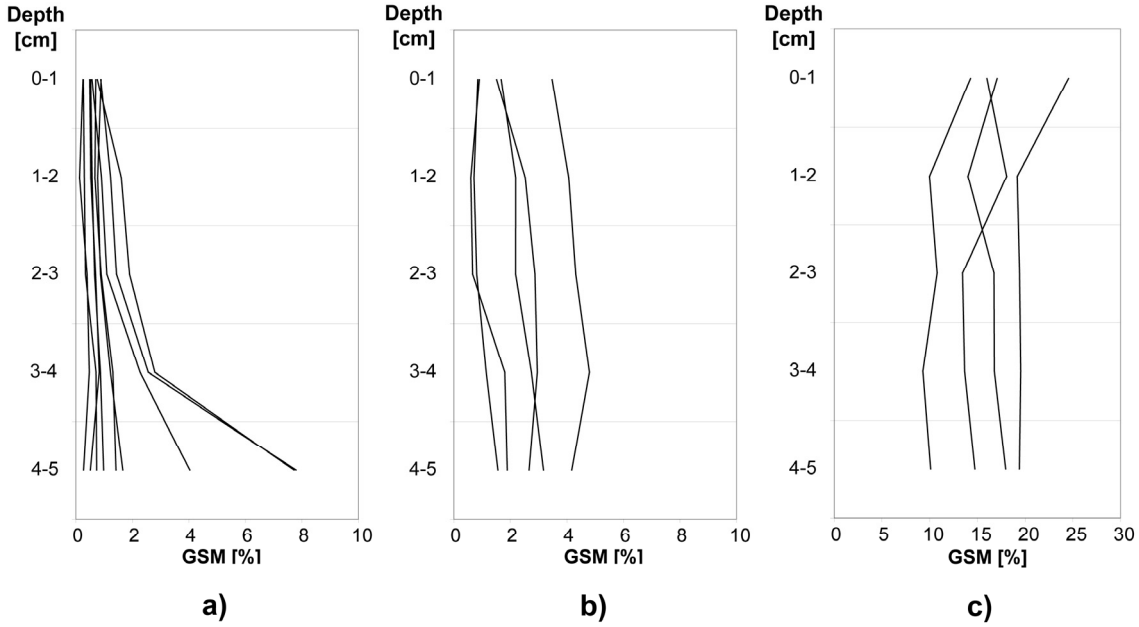

Figure III-6 Calibration function Vertical soil moisture distribution from 18 soil cores on 2005, June 20th: a) tertiary sand, b) quaternary sand, c) impure quaternary sand (affected by Fe_2O_3, crusts, lichens etc.).

The resulting calibration-to-surface factors for the three soil classes have been applied as follows:

$$GSM = a \times VSM / BD \quad (3)$$

GSM: gravimetric soil moisture [g/g]

$$a: \begin{cases} 0.59, & \text{for tertiary substrates} \\ 0.76, & \text{for quaternary substrates} \\ 1.21, & \text{for affected quaternary substrates} \end{cases}$$

BD: bulk density, here 1.68 [g/cm³]

VSM: volumetric soil moisture [cm³/cm³]

FDR values were adapted based on these calibration factors resulting in RMSE values of 1.94% GSM for the difference between FDR and gravimetric measurements.

Finally, a mesh of surface soil moisture data points was generated at the spatial resolution and coverage of the FDR measurements. For each of the substrates differentiated in the field (Figure III-2), the calibrated-to-surface FDR measurements were interpolated between all points using an Inverse Distance Weighting (IDW) algorithm (inverse quadratic distance to three reference points) (Shepard 1968). A separate interpolation for each soil type was necessary due to very sharp variations of surface soil moisture with substrate changes. The resulting raster maps were combined for all soil types and resulted in a 4 m resolution surface soil moisture validation dataset.

The accuracy of the interpolated pixel values was validated against a subset of 20 FDR point measurements based on regular sampling. For validation purposes, these measurements were not considered in the interpolation, but compared to interpolated values applying a leave-one-out strategy. Validation led to an RMSE of 2.07% GSM (median 0.38%, max 5.2%), which is below common uncertainties caused by the measuring device. The resulting uncertainty for the final in-situ dataset is therefore in an acceptable range for validation purposes in this study. Interpolation was particularly successful in the tertiary sand, where more homogeneous soil moisture distributions were observed. More critical was the part in the quaternary substrate with high spatial heterogeneities. Here, an increase in the number of FDR measurements certainly would

have improved the interpolation results with deviations of up to 5.2%. The resulting dataset is nevertheless invaluable for a pixelwise comparison with remote sensing data, although the given restrictions need to be taken into account for interpretation.

3.4 Validation of soil moisture model

A difference map was calculated between in-situ surface soil moisture estimates and HyMap-based NSMI for the scene from June 2005. Specific spatial patterns of conformance and deviation were discussed and the influence of vegetation cover and mixed substrates was further analyzed. To verify that the chosen HyMap channels (see Table III-3) provide optimum results for soil moisture quantification in this analysis, local variations in the choice of bands for NSMI calculation were evaluated.

The NSMI model was finally applied to the HyMap scenes from 2004. The two resulting maps quantifying surface soil moisture for the beginning and end of July 2004 were compared to each other by generating a moisture difference map. Precipitation data and soil moisture values from a time series over two months were qualitatively compared to the variation in the NSMI-based soil moisture estimation

4 Results and discussion

The goal of this paper is to analyze the potential of the NSMI index resampled to hyperspectral sensor resolutions for quantifying surface soil moisture. For this purpose the outcome of the quantification model is described and compared to the in-situ dataset derived from FDR and gravimetric samples in the field by calibration and interpolation. In the following, each resulting dataset is shortly described according to its spatial distribution pattern, before they are compared to each other by difference maps and statistical measures. The applied methods are discussed with respect to their success and limitations.

4.1 Estimation of surface soil moisture from reflectance data

Resulting gravimetric soil moisture estimations are in the range of 0 to 18.9% with a mean of 3.8%, and standard deviation of 5.2% (Figure III-7a). The overall surface soil moisture pattern deduced from the NSMI model can be depicted as follows: the tertiary sand shows mainly spatially homogeneous values below 4%.

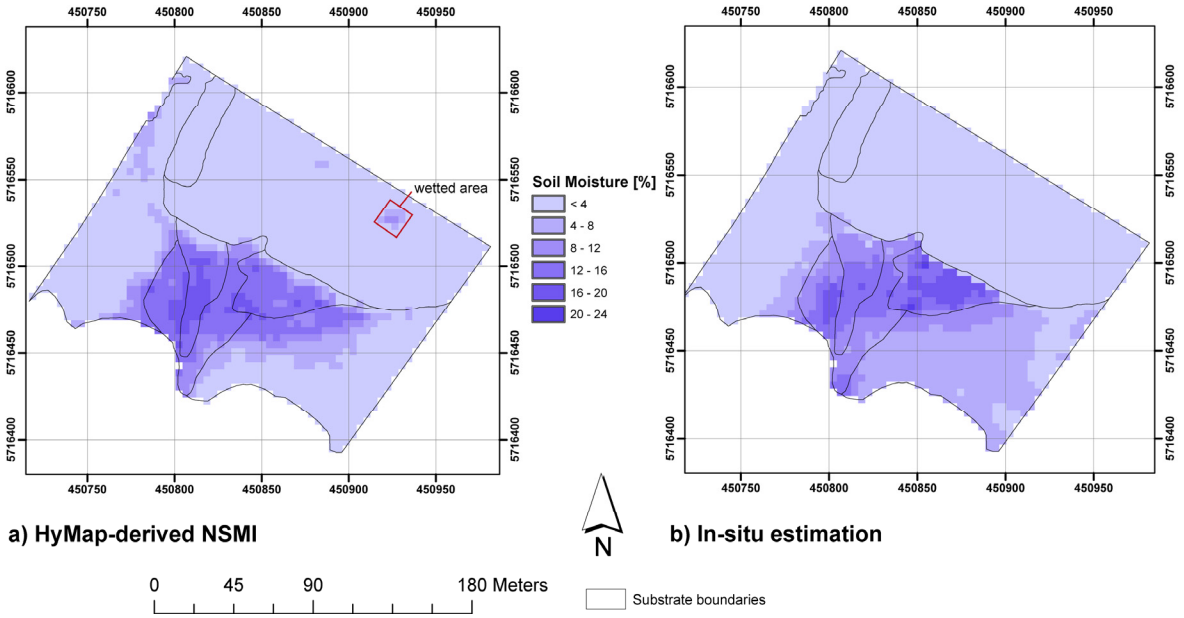

Figure III-7 a) Surface soil moisture derived from HyMap applying the NSMI. b) Surface soil moisture map derived from in-situ measurements on 2005, June 20th.

Two small areas stand out against this homogeneous pattern. An area of two adjacent pixels in the center of the tertiary substrate shows higher values than the surrounding parts. Reeds covering a few square meters affect the reflectance values in the HyMap image and lead to an overestimation by the NSMI model. The second outstanding soil moisture pattern further east is caused by the artificial wetting of an area of 10x10 m^2 shortly before the time of the HyMap overflight. Values range here between 8 and 18% at the surface, which reasonably reflects the resulting moisture caused by wetting and subsequent infiltration.

The values estimated for the quaternary substrates in the southern part of the image show a much more heterogeneous structure. In the center where elevation is lowest and erosion processes have formed a discharge channel, soil moisture is estimated highest with values around 18%. With increasing spatial distance from this accumulation zone, the values drop towards 0 in easterly and westerly directions. An elongated area of a few square meters in the north-western part of the quaternary substrate shows relatively high estimated surface soil water content between 4 and 8%. The sand dune area and the adjacent parts of the tertiary sand east of it represent the driest region in the map, with 0 to slightly negative GSM predictions. The latter are caused by the fact that reflectance at 2119 nm is equal to or slightly higher than reflectance at 1800 nm in these pixels. The sand dune with its different color and physico-chemical properties not taken into account in the NSMI model calibration is therefore subject to underestimations of up to 2% GSM. The mainly westerly wind direction additionally led to a deposition of dune sands on top of the tertiary sands.

4.2 Determination of surface soil moisture from in-situ data

FDR measurement values in the field range between 0.7 and 35.1% volumetric soil moisture, which corresponds to 0.4 to 20.7% gravimetric soil moisture applying the calibration-to-surface procedure. This range corresponds with long-term gravimetric measurement values (max. 25.7% GSM). However, the RMSE value for the calibration-to-surface of 1.94% GSM would have been higher if no strong relationships between soil moisture in the different layers were present. As discussed in (Capehart and Carlson 1997), stable relationships can be found either in the first phase of a typical drying scenario, i.e. directly after precipitation events and before a significant drying process has started, as well as in the third phase after drying processes in the upper centimeters of the soil column have finished, finally resulting in homogeneously dry compartments. On June 20th 2005, the drying process was in this third phase after five days without precipitation.

The subsequent interpolation procedure of the calibrated-to-surface FDR values led to a HyMap resolution pixel-by-pixel map, which is shown in Figure III-7b. The range of values derived from the spatial interpolation of calibrated FDR measurements (0.3 to 20.5%, mean: 4.2%) corresponds with the calibrated-to-surface FDR point measurements.

Figure III-8 shows the effect of the two-step correction of in-situ data by calibrating to surface values and interpolation. Both steps increase the linear correlations between field data and NSMI estimated. While the improvement caused by surface calibration accounts for the vertical differences in an appropriate way, the interpolation obviously reduces the effect of local inconsistencies within an area of one pixel (4x4 m). FDR point measurements can vary within centimeters and exact sampling locations can thus be critical. The smoothing effect of the interpolation is therefore beneficial for a pixelwise comparison of the two datasets.

The general pattern of soil moisture distribution is well reflected by the data. For the tertiary sand, a nearly homogeneous area of low surface soil moisture (<4%) is obvious in the in-situ map. It can be observed that, due to the early acquisition of FDR measurements before the wetting process, the 10x10 m wetted area is not visible in this FDR-based dataset. Also the reed area does not show higher soil moisture values than the surrounding area. In the quaternary substrate, the eastern part (east of the accumulation zone) shows relatively homogeneous values in the range of 4-8%, while the western part is similarly homogeneous, but slightly dryer (<4%). Due to the interpolation method applied here, the sharp transition of values between substrate boundaries could be reproduced, while more quasi-continuous gradients are present within a substrate.

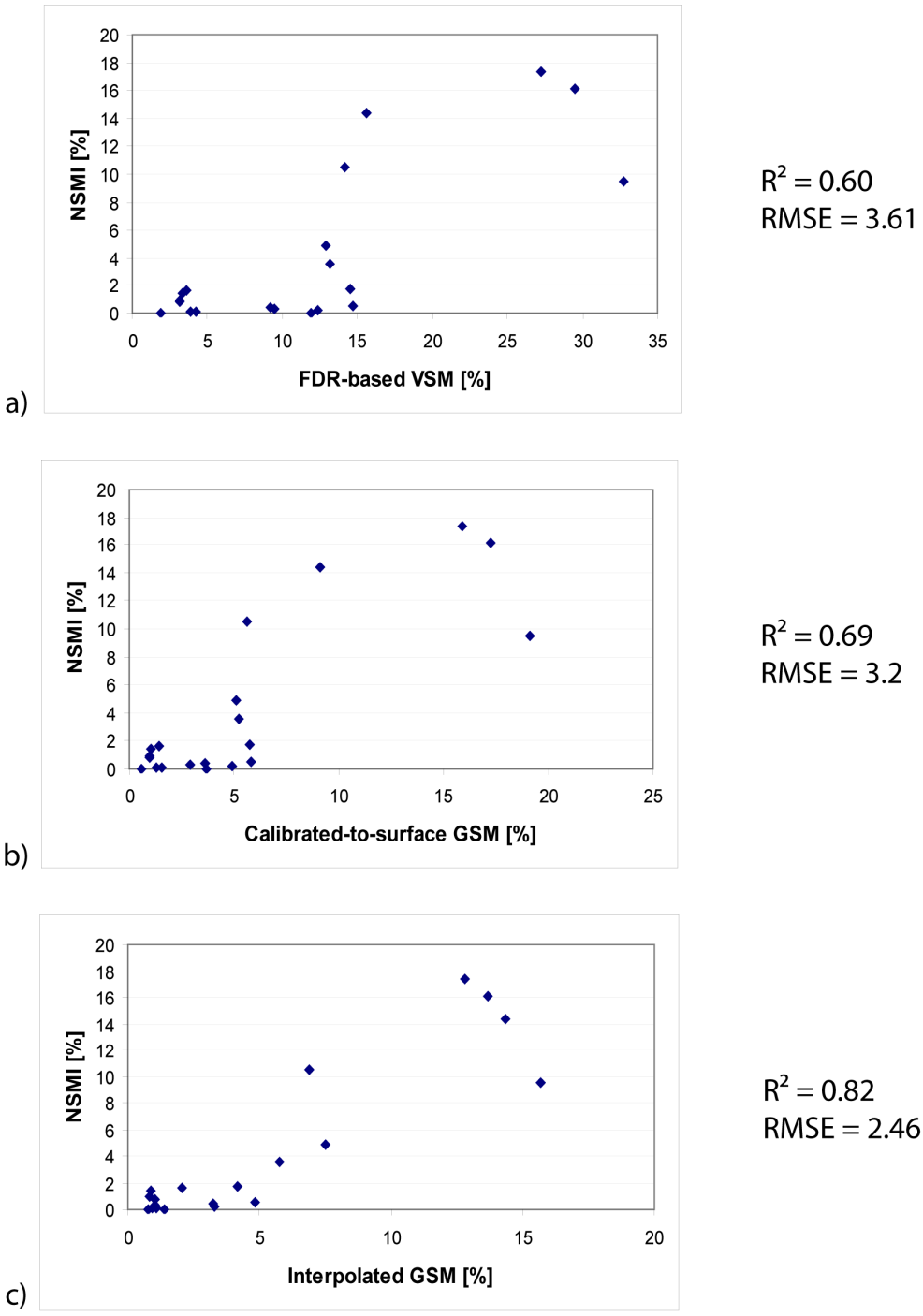

Figure III-8 Correlations between NSMI values and intermediate results of validation dataset based on a validation subsample (n=20, regular sampling): a) FDR values of upper 5 cm soil column, b) calibrated-to-surface GSM values and c) interpolated GSM values from the field.

4.3 Validation of the soil moisture model

A good conformance between remote sensing prediction and corresponding field interpolation GSM values has been shown in Figure III-7. In order to analyze the differences between the two datasets in more detail, a deviation map was generated (Figure III-9). Several patterns can be identified, giving indications of the locations and

consequently of the circumstances under which the soil moisture estimations show corresponding or differing results. In the following, all values are given as absolute GSM percentages.

Differences of the approaches amounted to -0.30% in average with an RMSE of 2.3%. In the tertiary substrate, higher soil moisture values based on reflectance data within the artificially wetted area can be explained since they are correctly detected by the NSMI model, but not included in the interpolation of FDR measurements. The correct estimation of the NSMI approach has been approved here by analyzing four soil core measurements conducted within the artificially wetted area, resulting in an averaged field value of ~12%, which corresponds with the NSMI values for this location. The second area showing differences between the two datasets is in the upper middle of the tertiary sand. The Normalized Difference Vegetation Index (NDVI) value (Figure III-9b) reflects the density of the reed scrub, leading to an overestimation of surface soil moisture in two pixels. Apart from these two spots where NSMI-deduced quantities are higher than field-based quantities, also a slightly increasing deviation can be observed from the middle of the tertiary area towards the sand dune in the north-west of the test site. NSMI-based values are marginally smaller than field-based measurements here. This underestimation of the NSMI is caused by the presence of the dune substrate introducing a minor inaccuracy in the soil moisture prediction as discussed earlier. The NSMI model therefore appears to be adequate for quantifying surface soil moisture in the case of the tertiary sand under the premises that vegetation cover is sparse and no additional substrates are present in significant amounts.

In the quaternary substrate, the deviation map shows more pronounced spatial heterogeneities. The highest deviation is located at the border between tertiary and quaternary substrates and is caused by two different factors. Firstly, the raster cells generated from the HyMap image represent mixed pixel values along the borderline, while the in-situ map shows a very sharp gradient caused by the substrate-specific interpolation. As a consequence, some pixels directly south of the borderline represent mixed values averaged over both substrates in the NSMI map and therefore show inconsistencies with the interpolated in-situ dataset. Secondly, the specifically high soil moisture values measured by the FDR device are not reproduced by the NSMI model. It has been noted in the field that surface soil moisture was partly above field capacity here, i.e. the surface was covered with water, which additionally contained iron compounds and other chemical constituents affecting its color.

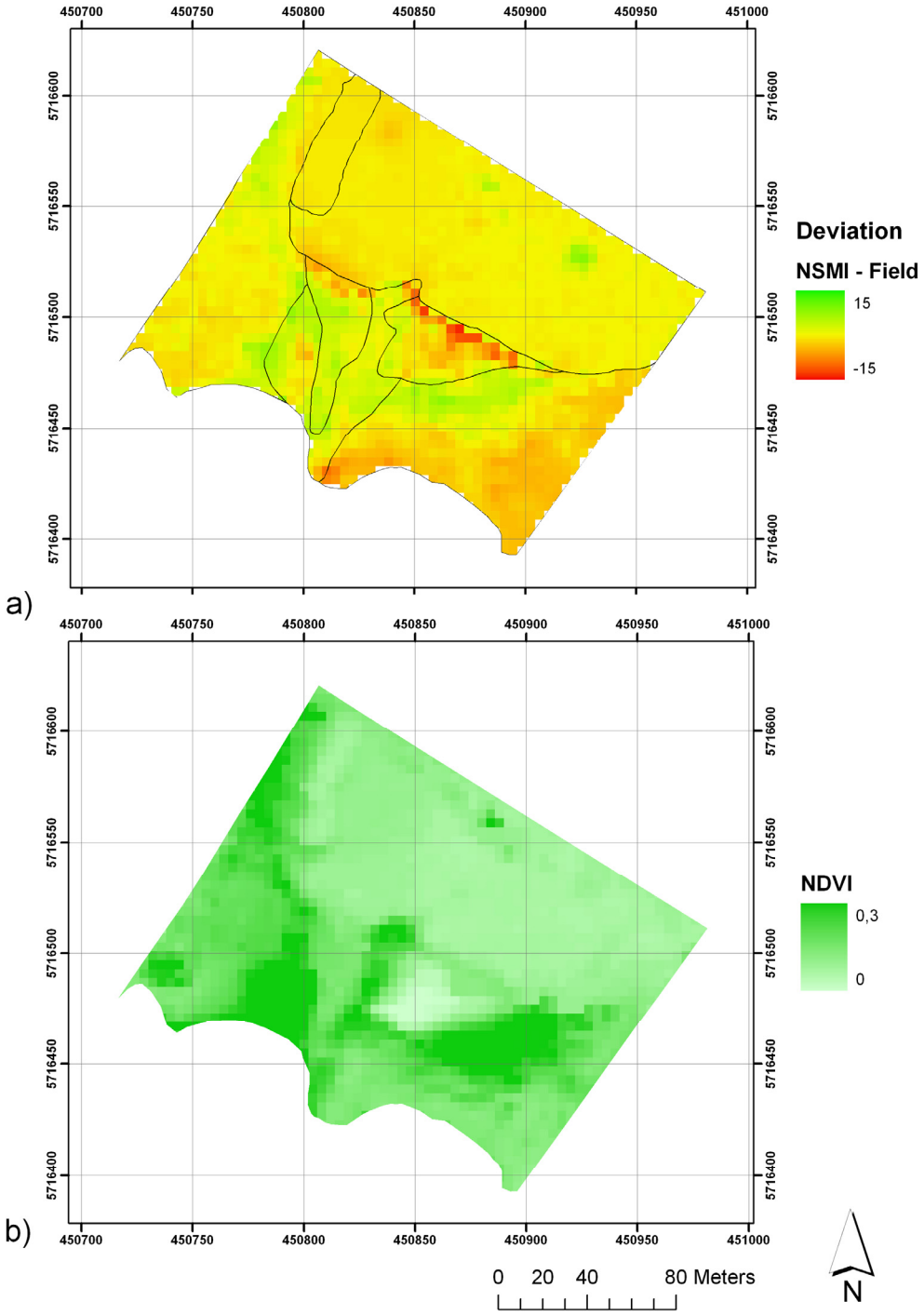

Figure III-9 a) Map of deviation between HyMap-deduced surface soil moisture and calibrated FDR-based interpolation map. b) NDVI calculation of the test site based on HyMap image.

Surface soil moisture above field capacity is inaccurately reproduced by the NSMI model as expected. Considering the NDVI map in Figure III-9b, an additional effect to note is the influence of the vegetation cover on the deviation map. Similar to the case in the tertiary sand, a high NDVI value corresponds with an overestimation of the NSMI value in the quaternary substrate. Vegetation water content is likely to affect the NSMI model outcome here, since a change in vegetation water content has a similar effect on reflectance in the

SWIR part of the spectrum. In the parts of the accumulation delta where vegetation is relatively low or absent, estimations by the NSMI model are consistently smaller compared to the field-based quantification. Since surface soil moisture values are particularly high at this location (partly above field capacity), a lower accuracy of the NSMI model is observed. Another factor affecting the remote sensing estimate is the presence of substrates that had undergone significant chemical reactions resulting in different reflectance properties. In the south-eastern part of the quaternary sand a consistently minor negative difference between NSMI and field values can be identified in an area with low vegetation cover. This effect is likely due to an overestimation of the in-situ dataset caused by an increasing amount of relatively moist clay particles below the surface here.

Figure III-10 shows pixelwise correlations between predicted soil moisture from remote sensing and estimated values from field data. Pixels representing the artificially wetted area as well as pixels showing artifacts at the substrate border were removed prior to the regression analysis. The linear regression function exhibits a high coefficient of determination (R^2=0.82), with an RMSE of 2.3%. Sources of deviation are caused by several factors, but can be explained by uncertainties in the measurements and influencing covariates.

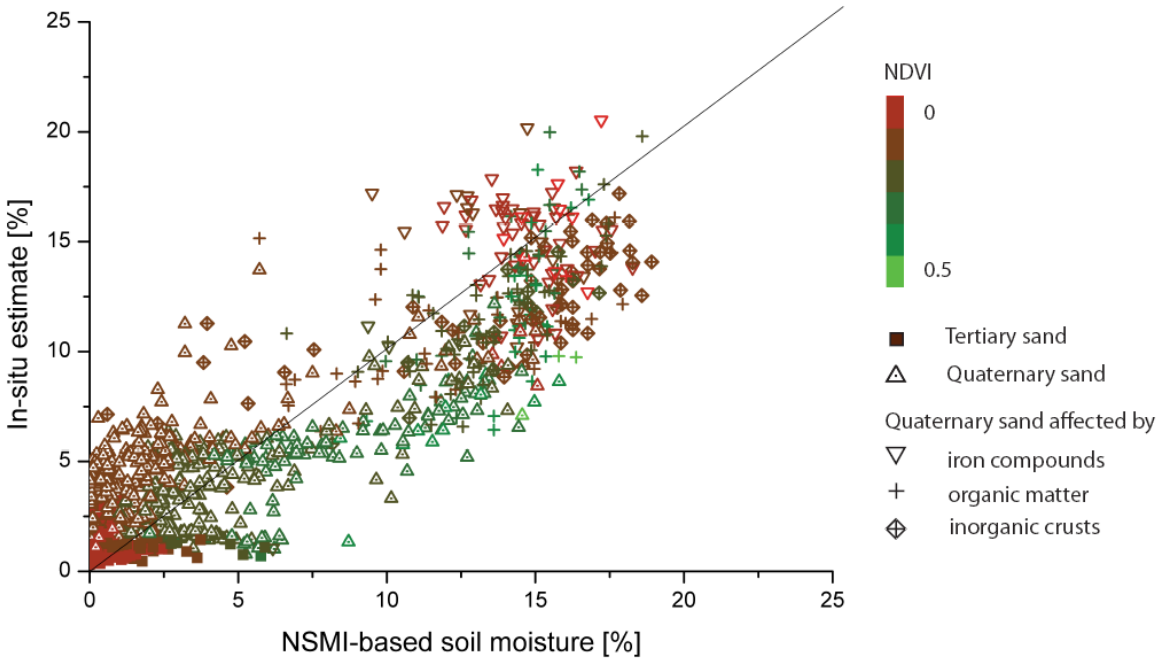

Figure III-10 Pixelwise correlation between in-situ soil moisture estimates and HyMap-based NSMI quantification (RMSE=2.3%; n=1806). NSMI pixel values biased by watering were removed beforehand. The 1:1-line represents equal values. Substrates are differentiated by symbology, the color represents the NDVI value of the pixel.

The graph confirms the assumption that vegetation cover severely influences the NSMI accuracy as discussed above. Pixels with high NDVI values (mainly quaternary substrates) deviate from the 1:1-line. Between 5 and 20%, NSMI values are generally higher than the in-situ estimates, as the data points in the diagram mainly occur below the 1:1-line. This results in a non-linearity visible in the scatter plot, which is mainly due to the vegetation cover in this range of values. For high NSMI estimations (with lower associated NDVI values) the discrepancy between the two estimations is increasingly replaced by a random deviation. However, the nonlinearity visible in the graph might also indicate a saturation of the NSMI for higher values, which corresponds with (Haubrock et al. 2008b).

Figure III-10 shows that for quaternary samples affected by iron compounds (Fe_2O_3), the data points spread significantly within the range between 9 and 20%, where NSMI values are in many cases smaller than in-situ estimates. This effect is likely to have two causes: an overestimation of the FDR device in the field due to different substrate compositions as well as specific soil properties at the surface that affect the NSMI value. Tertiary samples showing minor surface soil moisture values are clustered near the origin of the graph. Major deviations from the 1:1- line exist only for a few pixels showing increased NDVI values.

Table III-4: R^2-values of normalized difference quantifications with adjacent HyMap bands. For each model outcome a linear regression with the same generated in-situ dataset has been quantified. Wavelengths are shown as from the HyMap calibration in 2005. (*original NSMI bands)

Band 1	Band 2	R^2
HyMap 93 (1798 nm)*	HyMap 100 (2048 nm)	0.813
HyMap 93 (1798 nm)*	HyMap 101 (2066 nm)	0.816
HyMap 93 (1798 nm)*	HyMap 102 (2084 nm)	0.816
HyMap 93 (1798 nm)*	HyMap 103 (2102 nm)	0.817
HyMap 93 (1798 nm)*	HyMap 104 (2120 nm)	**0.819**
HyMap 93 (1798 nm)*	HyMap 105 (2138 nm)	0.819
HyMap 93 (1798 nm)*	HyMap 106 (2156 nm)	0.807
HyMap 93 (1798 nm)*	HyMap 107 (2173 nm)	0.797
HyMap 93 (1798 nm)*	HyMap 108 (2190 nm)	0.781
HyMap 89 (1750 nm)	HyMap 104 (2120 nm)*	0.808
HyMap 90 (1762 nm)	HyMap 104 (2120 nm)*	0.810
HyMap 91 (1774 nm)	HyMap 104 (2120 nm)*	0.813
HyMap 92 (1786 nm)	HyMap 104 (2120 nm)*	0.818
HyMap 93 (1798 nm)	HyMap 104 (2120 nm)*	**0.819**
HyMap 94 (1810 nm)	HyMap 104 (2120 nm)*	0.799

Pixels covering quaternary substrates with inorganic crusts, which were observable in the field, tend to cluster below the 1:1-line at high soil moisture values. The role of these crusts has not further been analyzed in this study, but obviously, they do affect NSMI model outcome to some degree. Studies on soil crusts confirm their implications on reflectance values (Goldshleger et al. 2002; Goldshleger et al. 2004b).

As can be seen from Figure III-10, a significant proportion of soil moisture values is scattered between 0 and 3%. While these values are characteristic for the test site, they also tend to artificially improve the coefficient of determination. An additional sub-dataset has therefore been generated consisting of n=808 observations, in which 75% of the measurements with NSMI-based values below 3% have been eliminated (regular sampling). As a consequence, the data points scatter more evenly in the range of values, while RMSE increases from 2.3 to 2.7% and can still be seen as acceptable.

In summary, a good conformance on a pixel-by-pixel basis can be observed between the remote sensing based NSMI and in-situ datasets. Spatial surface soil moisture patterns in the field are reproduced and gradients within each substrate as well as sharp transitions between substrates show up in both datasets. However, the given results have to be interpreted against the background of the different sources of uncertainties. With respect to the error margin, absolute values in the heterogeneous parts of the quaternary sand need to be interpreted with care.

Comparing the outcome of the applied NSMI model with normalized difference models using adjacent HyMap bands, the coefficient of determination has been calculated for each modified quantifier and can be seen in Table III-4.

The comparison confirms that the selected HyMap bands provided best results in this study. However, using adjacent bands would decrease the coefficient of determination only marginally. Corresponding with the results from Haubrock et al. (2008b), the wavelengths chosen for the NSMI are representing a local maximum for soil moisture quantifications within a range of similarly effective bands for the NSMI. The decline in R^2 is small near the chosen bands before increasing with distance in the spectrum.

Regarding the outcomes of Whiting et al. (2004) and previous works, these results can be explained by the typical effects in the SWIR. The overall decrease in reflectance with increasing soil moisture has been quantified in the Soil Moisture Gaussian Model by analyzing the convex hull of the log-spectrum over corresponding wavelengths. The NSMI channels at 1800 and 2119 nm represent local reflectance maxima and as such form anchor

points in the convex hull. Thus, the two channels combined as a normalized difference represent a simplified quantifier relying on the same effect as the SMGM quantification.

Since reflectance values above 2119 nm are increasingly affected by clay minerals like smectite and kaolinite in the given substrates, regression outputs fall off in this direction. On the other side, reflectance values are getting influenced by atmospheric noise towards the major water absorption band at 1900 nm, and regression coefficients decrease accordingly when corresponding channels are chosen for the generation of a normalized difference index.

Since vegetation (especially dry vegetation) was sparse in the test site of this study, the influence of cellulose and lignin on reflectance around 2100 nm could be neglected here (Daughtry et al. 2004). The Cellulose Absorption Index (CAI) is based on an absorption band at 2106 nm, which is compared to cellulose-invariant reflectance values at 2015 and 2195 nm. It might therefore be necessary to shift the chosen channels slightly in the case that crop residues or other types of organic matter affect the second band used in the NSMI calculation.

4.4 Multi-temporal NSMI analysis

A multi-temporal soil moisture analysis based on the NSMI model has been performed to show the potential of monitoring soil moisture from airborne sensors covering the hydrological mesoscale. Figure III-11 shows the results of applying the above calibrated NSMI model to the HyMap datasets from July 2004. Figures III-11a and b both clearly show a typical spatial surface soil moisture distribution over the test site, which is similar to the distribution of soil moisture in June 2005. The image from late July 2004 (Figure III-11b) indicates relatively high soil moisture values over the whole area. A difference image (Figure III-11c) shows an overall increase in soil moisture content within the 26 days (blue values). The actual increase rate forms a very distinct pattern. First it can be noted that surface soil moisture differences are much stronger in the quaternary substrate. This corresponds with the fact that the substrate generally exhibits higher soil moisture values (Lemmnitz et al. 2007; Haubrock et al. 2008b). Due to its physical properties it is able to store water longer than the tertiary sand. Also within this substrate differences in soil moisture increase can be observed: the highest values are located in the transition zone between the tertiary and quaternary substrates.

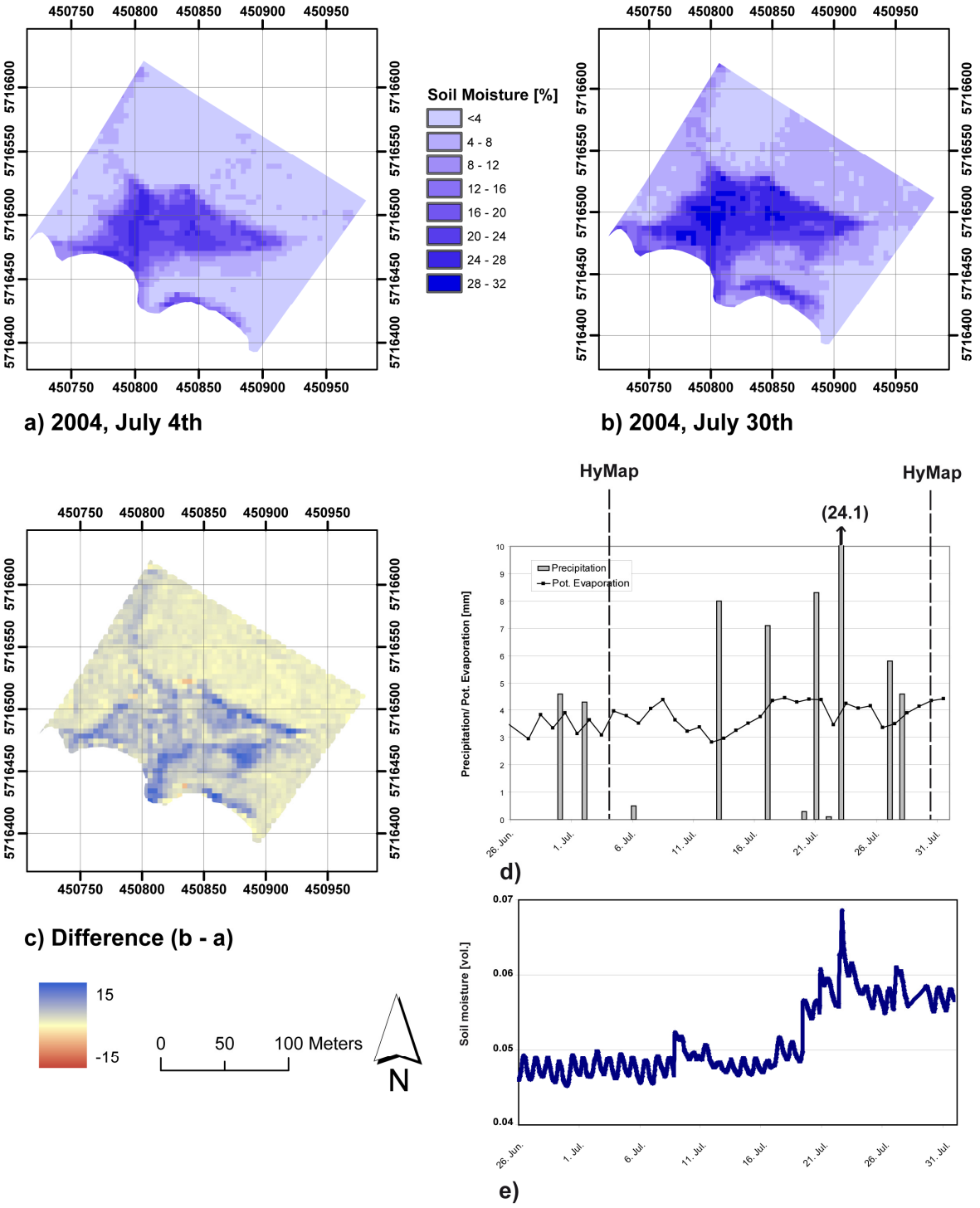

Figure III-11 Soil moisture determination from HyMap 2004 images based on NSMI model for a) scene from July 4th, b) scene from July 30th. c) Difference in soil moisture estimation (b-a), d) meteorological variables in June and July 2004, e) soil moisture measured by echo probe at a single reference point (tertiary sand).

This area is characterized by the accumulation of water that previously discharged from the tertiary part further north. The NSMI approach reflects these exceptionally high GSM values in the map. Additionally, in areas of relatively high vegetation cover, the NSMI increases significantly as well, which is also the consequence of increased plant growth due to higher soil water availability. Precipitation data as well as field soil moisture are

shown in Figures III-11d and e for June and July 2004. The higher soil moisture values in the later HyMap scene fit well with precipitation and moisture measurements in the field: the higher values indicated by Figure III-11b in the end of July are coherent with both, the much higher precipitation amounts in the second half of July and the in-situ soil moisture measured by the echo probe.

4.5 Assessment of the NSMI model

Most approaches focusing on soil moisture quantification from reflectance data are either based on laboratory measurements or have not been validated thoroughly in the field by surface soil moisture in-situ measurements on a pixel-by-pixel basis. In this study a small catchment of 4 ha size allowed for accurate geometrical and spectral analyses and especially for providing a comprehensive set of validation points in the field.

The correlation accuracies achieved are below the values from other studies (Weidong et al. 2002; Whiting et al. 2004) performed in the laboratory. However, the natural environment in the field has not caused the NSMI approach to fail here. Instead, strengths were found in quantifying wide ranges of soil moisture and in detecting spatial patterns. The NSMI allowed on the one hand for the detection of relative changes within as well as between substrates with different spectral properties. Quantification deviations with respect to the FDR-based map have been -0.3% GSM in average. Limitations of the NSMI are linked to the presence of vegetation (single deviation values can be and models.

The hyperspectral sensor used in this study provides very high spectral resolution images, which allowed to determine NSMI from narrow-band sensors and to analyze spectral differences in the area. The minor shift of the two used HyMap bands compared to the NSMI bands used for laboratory spectra did not affect the performance of the quantification here. The transferability of the NSMI to broadband sensors holds promises, but has yet to be confirmed.

4.6 Assessment of the validation approach

This paper presents the production of a pixel-by-pixel validation soil moisture map generated on the basis of real-time in-situ field measurements. Soil moisture pixel-by-pixel maps derived on the basis of FDR measurements and subsequent processing steps are independent validation datasets that reflect an optimum trade-off between sample number and timeliness at this scale. Such a study has not been published so far, as validation is often produced with a relatively small number of field measurements at real-time. When

higher numbers of field samples could be collected in other studies, they were mostly either not taken at overflight time or were analyzed in the laboratory hours or days after collection, since it is unfeasible to directly collect a sufficient number of surface soil moisture values in the short time frame associated with a remote sensing acquisition. In the approach presented here, the collection of a high number of soil moisture values was possible due to the combination of the quick measurement process of the FDR device and an additional smaller number of soil core samples, allowing for the generation of a dense mesh of validation data. The interpolation of these point measurements further improved correlation in a validation subset, since spatial variability caused by local inconsistencies has been smoothed by adjacent pixel values.

The approach followed here to generate the in-situ dataset is subject to a number of uncertainties and can only be applied when certain preconditions are met. The interpolation itself is only valid when the density of base points is high enough, which proved to be the case for most but not all parts of the study area. Additionally, spatial interpolation can be critical at this scale when no sharp boundaries between different substrates exist, since continuous transition zones cannot be taken into account appropriately. However, this source of error becomes less significant with an increasing size of the area covered. The deduction of gravimetric soil moisture values based on the volumetric values taken with the FDR device had to be simplified, since an average bulk density value was used here for the whole area. This is only valid in the case that substrates do not differ significantly in their physical properties. One critical assumption that had to be made when using FDR devices is related to the vertical soil moisture distribution. Since surface values are of interest and in fact average values over the upper five centimeters are measured, a correction factor had to be implemented based on substrate-typical patterns. Applying this factor postulates that vertical soil moisture profiles are relatively homogeneous and well-known, which is only the case in certain phases of the drying process after precipitation events (Capehart and Carlson 1997).

Considering all uncertainties and inaccuracies that are associated with field data and with the methodology developed here for in-situ map generation, an optimum validation data set combining information of spatial coverage and vertical soil moisture profile has been generated, allowing to determine an RMSE based on pixelwise comparisons between remote sensing estimation and field validation.

5 Conclusions

The studies described in this paper involve the first application of the recently established surface soil moisture quantification approach NSMI to a hyperspectral airborne sensor. The following main results can be concluded.

The NSMI has been applied successfully as an easy-to use, comprehensible model for surface soil moisture quantification in an area of quaternary and tertiary sands with absent to low vegetation cover. The high spectral resolution of the HyMap sensor made a quantification based on two bands in the SWIR possible.

- The strength of the NSMI in this study is particularly in detecting soil moisture variations over a wide range of values in sandy substrates. Naturally occurring soil moisture gradients within a substrate are detected by the NSMI. Additionally, a larger range of soil moisture values has been reproduced by the quantification model in an artificially wetted area. The accuracy of the NSMI is consistent within the range between 0 and 20% GSM with an average RMSE of 2.3%.
- Soil types affect the parameters of the regression function differently. Chemical composition and the presence of crusts need to be taken into account when calibrating the model for a specific area. Further research is therefore necessary to analyze the applicability of the NSMI in regions with other soil types.
- Vegetation density exceeding a certain threshold value leads to overestimation. The maximum threshold value for which the NSMI still delivers valid results was observed to be at 0.3 in our test site. For an application of the NSMI in agricultural areas, further analyses concerning the effect of crop residues are of specific interest.
- The validation of remote sensing estimates with in-situ soil moisture is afflicted with different types of uncertainties. Substrate information on vertical soil moisture profiles of proxy samples proved to be feasible for calibrating FDR measurements with an overall RMSE in the validation dataset of 1.94%. FDR-based point measurements density was adequate for the homogeneous tertiary substrate, but need a higher spatial resolution in environments with heterogeneous surface properties in order to be usable for validation purposes. With the interpolation method applied here (RMSE 2.07%), an overall appropriate in-situ validation dataset could be generated.

- While the HyMap bands chosen for the NSMI calculation provided best results in this study, the use of adjacent wavelengths turned out to result in only marginally lower coefficients of determination. The chosen NSMI bands can therefore be seen as representing a locally optimum choice for soil moisture quantification, while they may be substituted by adjacent or broader bands if necessary. As a consequence, applying the NSMI to other sensor types might be feasible, but yet needs to be analyzed in detail.

This study is a new attempt to link remote sensing prediction with hydrological in-situ measurements. It shows that a gap has to be filled between two research domains - optical remote sensing science that focuses on the uppermost part of the surface, and the hydrological research community studying processes within and between different soil layers. Especially in areas with low vegetation cover, rainfall events yield in runoff coefficients that are heavily depending on the antecedent soil moisture (Beven 2002). Besides major challenges in fully understanding soil surface processes, optical data could make an indispensable contribution to describe the vertical profile of soil water content and also serves as a spatial index of the soil surface hydraulic properties (Capehart and Carlson 1997). The use of reflectance measurements to quantify surface soil moisture is therefore invaluable for hydrological modeling approaches.

Soil erosion models covering areas at the mesoscale (10^1 to 10^3 km^2) are of specific interest for hydrologists (Merritt et al. 2003). Spaceborne hyperspectral sensors with their high spatial coverage and temporal resolution will allow for quickly generating datasets on surface soil moisture in the future based on methods such as the one presented in this paper. Consequently, datasets from remote regions will be available, making a significant contribution to monitor and improve the understanding of surface and near-to-surface soil processes, where surface soil moisture is a key variable.

Chapter IV:Spatiotemporal variations of soil surface roughness from in-situ laser scanning

Catena, in print (revised version)

Sören-Nils Haubrock, Sabine Chabrillat, Matthias Kuhnert,
Andreas Güntner and Hermann Kaufmann

DOI: 10.1016/j.catena.2009.06.005
Received 24th April 2009; revised 17th June 2009;
accepted 24th June 2009

Abstract

Microtopography and roughness are highly dynamic properties of the soil surface and important factors governing surface runoff and erosion processes. While various remote sensing technologies were successfully applied for topography measurements at different spatial scales, there is a lack of field studies that collected systematically microtopography data over long observation periods. In this paper an approach to measure and quantify surface roughness in the field based on laser scanning technologies is presented. Between June 2004 and November 2005 97 in-situ measurements were conducted in a test site with two different sandy substrates in vegetation-free conditions. Two-dimensional high-resolution (1 mm) datasets where generated for eight micro erosion plots of 0.25 to 2.9 m² in size. Dynamics and pattern formation were quantified for surface roughness and surface height changes. Roughness patterns at different scales were analyzed by local roughness indices using sliding windows of 3 to 55 mm in size. Results show strong spatial and temporal dynamics in surface roughness as well as substrate-specific variations. Temporal roughness variations could be detected and were linked to precipitation patterns. The methods presented in this paper are considered suitable to generate high-resolution datasets on spatiotemporal and multi-scale microtopography patterns and to advance the understanding of surface processes at small scales in natural environments.

1 Introduction

Soil surface roughness is a highly dynamic variable playing an important role for surface processes in natural environments (Kirkby 2001). Under the influence of precipitation, discharge and wind erosion, substrate movements affect the structure of the soil surface and form spatial heterogeneities in microtopography. At the same time, resulting roughness patterns have an effect on infiltration and runoff rates by forming physical barriers or providing discharge channels for water (Solé-Benet et al. 1997; Govers et al. 2000; Römkens et al. 2001; Huang et al. 2002). Bull and Kirkby (2002) developed a conceptual model describing dominant geomorphological processes and their impacts in dryland environments. According to this model, high erosion rates cause a segregation of fine and coarse textured materials finally resulting in typical spatial distribution patterns of microtopography among hillslopes and channel beds. While the general sequences and interactions resulting in such patterns are well understood on a conceptual level, underlying processes need to be quantified at the microscale in the field to better assess their role in the context of soil erosion.

1.1 Measurements of microtopography

For the purpose of a better process understanding, methodologies for monitoring topography and roughness dynamics at the microscale are necessary. Among the published field studies dealing with the quantification of soil surface properties, several describe data collection methods based on mechanical devices. van Wesemael et al. (1996) used pin meters in 50 cm transects along contour lines to study the effect of rainfall and soil properties on surface roughness in Spain. Desir and Marin (2007) used the same methodology in addition to erosion pins to analyze erosion rates for a different test site in Spain. Their studies showed that this data collection method is easily and efficiently applied in the field. However, while pin meters or erosion pins are able to reflect surface topography in one-dimensional transects of arbitrary length, they do not provide data necessary for the generation of two-dimensional topography models in millimeter or sub-millimeter resolution.

Remote sensing methods have the advantage of measuring coherent areas without physical contact. Several technologies exist to generate three-dimensional surface models using remote sensing devices. While photogrammetry (Carbonneau et al. 2004), laser altimetry

(De Vries et al. 2003) or Synthetic Aperture Radar (SAR) Interferometry (Massonnet and Feigl 1998) are the most important approaches used at the catchment scale and above, measurements at the plot or micro scale are predominantly performed with laser scanning technologies. Earlier works already approved the feasibility of laser scanner devices to detect elevation differences within a mm range (Huang et al. 1988; Römkens et al. 1988; Bertuluzzi et al. 1990; Huang and Bradford 1990). Jester et al. (2005) performed a thorough comparison of different data collection and processing methods quantifying soil surface roughness in the laboratory. One of their major results was that laser scanners providing millimeter resolutions in horizontal and vertical direction are particularly well suited for representing fine structured areas compared to other mechanical (pin meter, roller chain) and optical (photogrammetry) approaches. However, being designed for laboratory work, they concluded that such devices cannot be used efficiently in extensive field studies.

Laser scanners have in some cases been applied to quantify surface topography and roughness in field environments. Huang and Bradford (1992) analyzed the impact of different precipitation patterns and agricultural treatments on surface roughness measured with laser scanner devices. They found a strong scale-dependence of roughness and argued that its quantification depends on a chosen scale, which in turn is related to the process of interest. Flanagan et al. (1995) developed a scanning system for the microscale to quantify erosion processes. Beyond laboratory experiments, their device was successfully applied within a set of field experiments on a 3x10 m erosion plot measuring soil microtopography.

In most of these studies, laser scanner measurements were performed by using devices that collect point data in a specified grid. While the technology allows a flexible determination of the spatial resolution ranging from millimeter to centimeter scale, the setup and calibration of these devices is more complex compared to other approaches. Coherent three-dimensional datasets gained from a different type of terrestrial laser scanner allowed Schmid et al. (2004) to compare roughness and volume balances in great detail and with relatively low operating expense in a forest test site before and after severe logging activities. Their study, however, was restricted to the comparison of microtopography at a single location between two points in time.

1.2 Surface roughness indices

Surface roughness is reflected by the spatial heterogeneity of elevation values at a pre-defined scale and can thus be derived from microtopography data. Its quantification depends on the dimensionality and resolution of the data as well as the desired expressiveness of the index. The most common parameter applied in recent studies is the standard deviation in vertical direction from a single mean value (root-mean squared height RMSH) calculated for a regular raster dataset of n×m pixel values. van Wesemael et al. (1996) successfully derived RMSH values from a previously detrended surface in order to separate multi-scale effects from each other, with the remaining so-called random roughness representing spatial variations in the sub-millimeter range.

The root-mean squared height represents a single global value representing surface roughness for a two dimensional dataset of arbitrary size. However, variations in height at different scales interact in this index (Huang and Bradford 1992), making its interpretation difficult. While detrending can be applied to remove the effect of larger scale roughness patterns (i.e. slope or curvature), it is obvious that multiple interfering scale-dependent phenomena cannot be represented by single values. Consequently, a set of indices quantifying roughness on different scales needs to be collected to represent surface roughness comprehensively. Bertuluzzi et al. (1990) combined RMSH calculations with minimum, maximum, skewness and kurtosis criteria from their sample datasets for this purpose. Huang and Bradford (1992) followed a more complex approach based on semivariograms and statistical models representing multi-scale roughness by two parameters. However, information on the spatial distribution of roughness was not provided, although necessary for studying surface processes in greater detail.

1.3 Objective of this study

While several studies proved the general applicability of laser scanning methods to generate surface microtopography models, to derive roughness parameters and to quantify surface properties, their contribution for the understanding of surface processes has not yet been analyzed systematically. The aim of this study is to evaluate a laser scanning technology and a subsequent quantification method for the purpose of analyzing surface changes for long time periods in the field, where erosion can be linked to processes of the hydrological cycle. For the first time, long-term multi-temporal microtopography measurements were performed in the field based on a mobile laser scanning device. Novel

multi-scale roughness parameters were developed and derived from the generated microtopography models in form of spatial distributions. Based on the study design and methods applied, the analysis enters new territory by focusing on the detection of spatial surface roughness heterogeneities and the formation of distinct roughness patterns over time. Meteorological input data that has been measured concurrently in the field is related to the results. Finally, the feasibility of monitoring long-term microtopography changes with such a technology in the field to gain a deeper understanding of underlying surface processes is discussed.

2 Materials and methods

2.1 Site characteristics

Field studies were performed in a small micro-catchment located in a bio-monitoring reclamation zone of the lignite mine Welzow-Süd near Cottbus, Germany (Figure IV-1). Elevations range between 129.4 and 135.6 m (AMSL) with slope gradients reaching up to 25%. At a weather station located in the study area, annual precipitations of 432.7 mm in 2004 and 483.9 mm in 2005 were measured. Potential evaporation derived with the Penman-Monteith equation (Penman 1956; Monteith 1965) was 582 mm in 2004 and 735 mm in 2005.

Substrates

After the mining activities had finished in 2001, sandy substrates of quaternary and tertiary origin were dumped in the reclamation zone. Both substrates are coarsely textured, contain less than 4% clay and were mapped as Technosol according to the World Reference Base (WRB) classification (WRB 2006). The tertiary substrate in the northern part of the test site is characterized by coarser grain sizes (44.7% > 630 µm, compared to 11.4% > 630 µm for the quaternary substrate) resulting in low field capacity, while infiltration rates are highly dependent on varying hydrophobicity (Lemmnitz et al. 2007). In the south-west of the test site, quaternary substrates predominate. On the south-facing slopes of the tertiary substrate, soil erosion has formed a set of erosion rills and interrill areas (Figure IV-2b).

Micro-erosion plots

Six bounded micro erosion plots (microplots) (three in the tertiary, three in the quaternary substrate) and two unbounded plots covering parts of naturally formed erosion rills (both in the tertiary substrate) were monitored in this study between June 2004 and November 2005

(Figures IV-1 and IV-2). The size of the plots ranged between 0.5×0.5 m^2 (P3) and 1.7×1.7 m^2 (P5), the open plots were scanned within an area of up to 2×1.1 m^2 (R1) and 1×1 m^2 (R2). The confined plots are surrounded by shelves on three sides, but open in the major runoff direction, allowing for the discharge of material out of the confined area. The locations of the microplots represent the range of slopes present at the test site: the tertiary bounded microplots exhibited slopes between 4.9 and 14.1%, the quaternary microplot slopes between 5.3 and 9.3%.

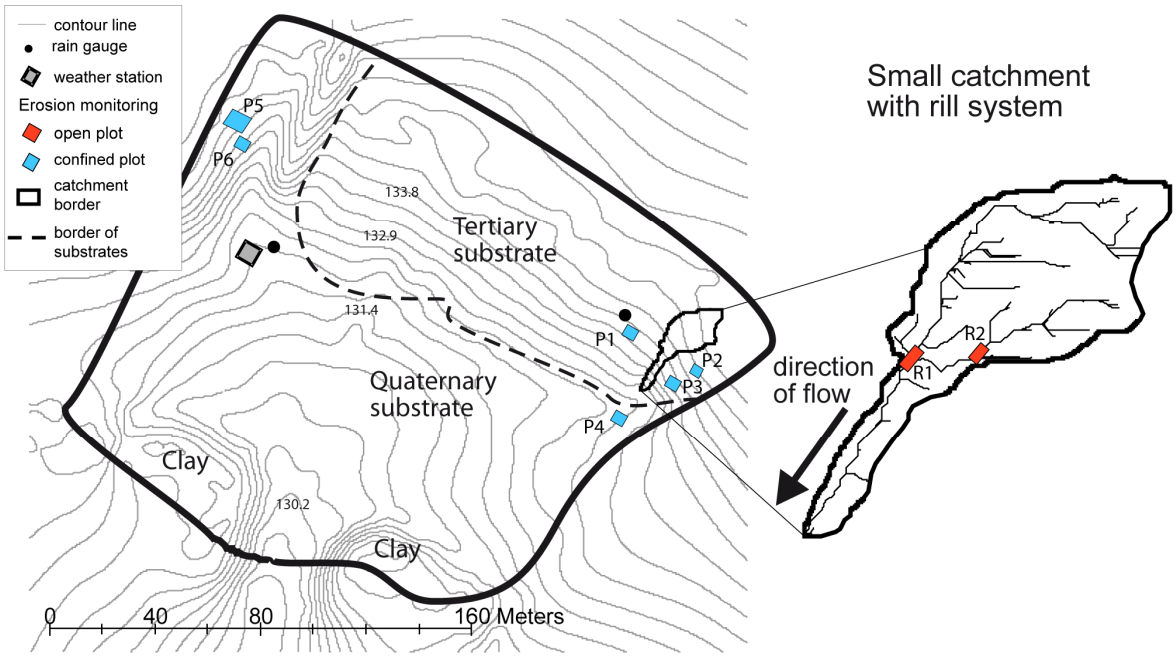

Figure IV-1 Test site in the reclamation zone of the lignite mine Welzow-Süd.

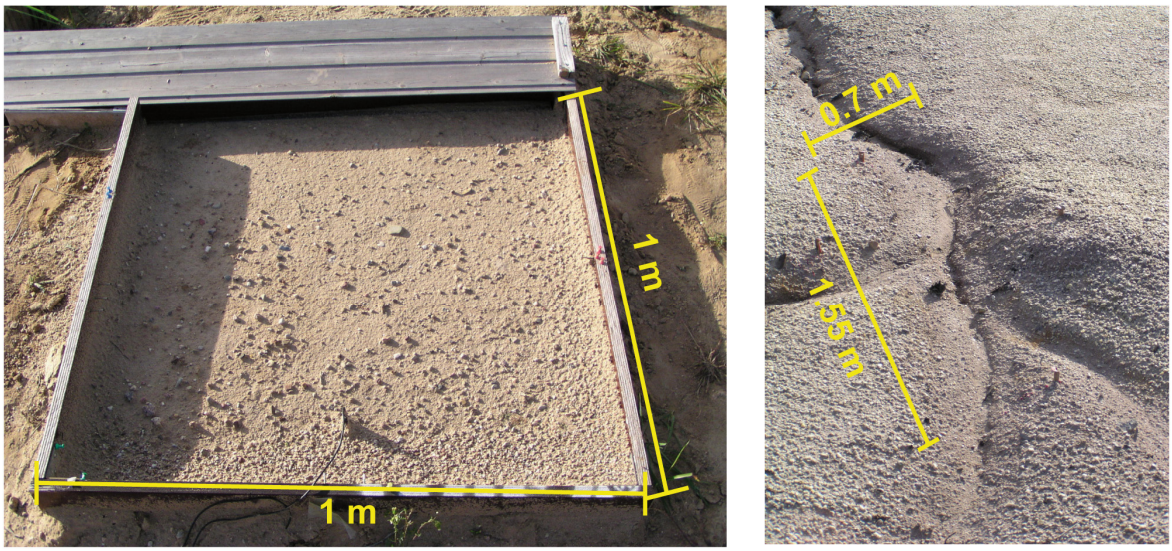

a) b)

Figure IV-2 (a) Confined erosion plot P3 and (b) open erosion plot R1 with tertiary substrate in the field. Substrates eroded from the confined plot were collected in the small channel in the upper part of picture a).

Table IV-1: Overview of plot microtopography measurements (n=97).

	Date	Tertiary substrate					Quaternary substrate		
		P1	P2	P3	R1	R2	P4	P5	P6
2004	June 24th	-	-	x	-	-	-	-	-
	July 7th	x	-	x	-	-	-	-	-
	July 28th	x	x	x	x	-	x	x	x
	August 11th	x	x	x	x	-	x	x	x
	September 1st	x	x	x	x	-	x	x	x
	October 4th	x	x	x	x	-	x	x	x
	October 20th	x	x	x	x	-	x	x	x
	December 8th	x	x	x	x	-	x	-	x
2005	March 31st	-	-	x	-	-	-	-	-
	April 13th	x	-	x	x	x	x	-	x
	May 10th	x	x	x	x	x	x	-	x
	May 26th	x	x	x	x	x	x	-	x
	July 13th	x	x	x	x	x	x	-	x
	August 8th	x	x	x	x	x	x	-	x
	August 31st	x	x	x	-	x	x	-	x
	October 12th	x	x	x	-	x	x	-	x
	November 2nd	x	x	x	-	x	x	-	x

The unbounded plots were located in a small hillslope catchment of 300 m² size (Figure IV-1), characterized by strong spatiotemporal variations in terms of surface shape and grain size distributions.

2.2 Data collection

Laser scanning was performed in the field using a Minolta Vivid 900 device, mounted on a tripod and positioned at a distance of 1.5 to 2.5 m from the scanned area. For each erosion plot, scans were performed from each side of the plot (every 90 ° of the azimuth) with vertical incidence angles between 45 and 65 °. Preliminary laboratory studies showed that a larger number of scans would only marginally improve the precision of the results, while less than four scans proved to be insufficient for the generation of three-dimensional microtopography models. Field measurements were performed in twilight conditions to avoid the distracting influence of the sunlight on laser reflectance. To achieve better scanning results, a dark sheet of 4 m² was additionally used to manually cover the scanned area from the sunlight.

In 2004, measurements started with a single open plot (R1) in the tertiary substrate. After preliminary analyses following the first season, relatively high dynamics in substrate processes have been detected in the network of rills and interrill areas.

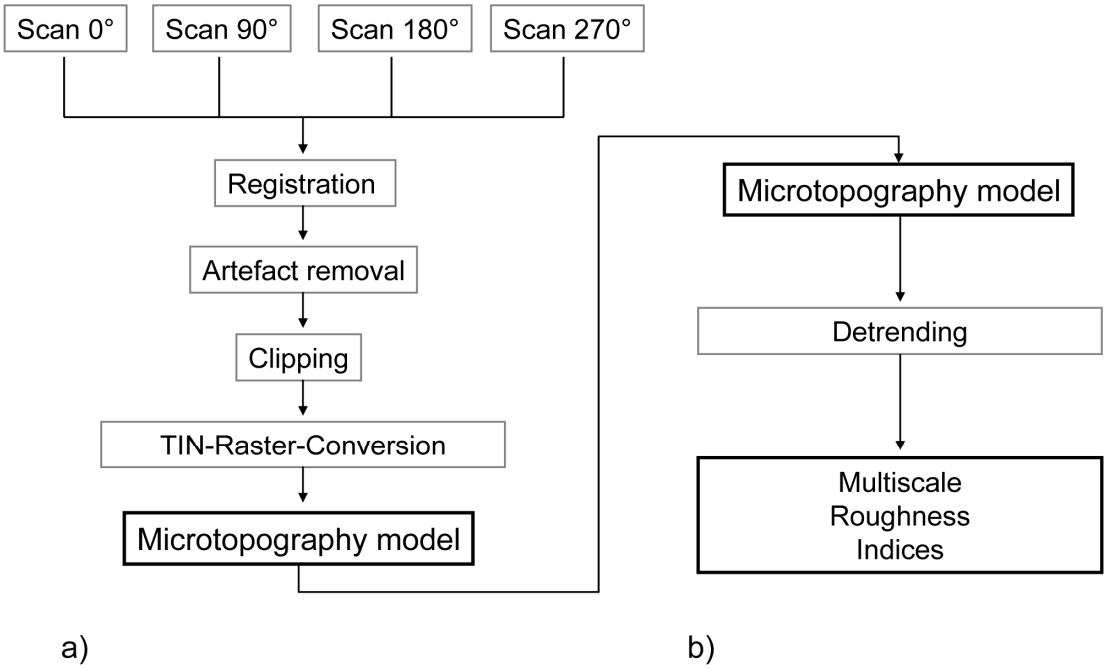

Figure IV-3 Data processing chain for generation and analysis of microtopography model comprising the steps a) microtopography model generation and b) roughness quantification.

Consequently, an additional open plot (R2) was monitored in 2005, while on the other hand further measurements of erosion plot P5 had to be abandoned instead for practical reasons. Table IV-1 gives an overview of the resulting microtopography models for each measurement cycle.

2.3 Data processing

After data collection, multiple post-processing steps were necessary in order to generate the final models and variables. Fundamentally, post-processing consisted of two different phases: 1) the generation of a three-dimensional microtopography model representing surface elevations in a 1 mm grid, and 2) the calculation of surface roughness parameters. Both phases are described in the following and summarized in Figure IV-3.

Microtopography model generation

For each plot, four single measurements were co-registered in a first step to generate a raw three-dimensional model of the area. Co-registration was done with the software RapidForm 2004 (INUS Technology). Distinct reference points (n=7-10) visible in each dataset were used for this process (e.g. small gravel, screws in the border of the plots, pegs next to the rills). Emphasis was taken on the even distribution of these reference points in order to minimize inaccuracies. After co-registration some artifacts caused by materials reflecting the laser beam while measuring needed to be removed. Resulting peaks in the

microtopgraphy model were erased and remaining holes filled by local interpolation. Depending on the light conditions during data collection, the area covered by these artifacts ranged between 0 and 5% of the surface. Finally, the dataset was clipped to a pre-defined extent, removing those parts that were not covered by each of the four scans. The resulting data model, represented as a Triangular Irregular Network (TIN) in RapidForm, was then converted to an ASCII raster format for further analyses with spatial resolutions of 1 mm in x and y direction and in the sub-millimeter range for the z-direction.

Roughness determination

Before applying surface roughness calculations from the microtopography models, linear detrending was performed to separate the effects of slopes and micro roughness on the indices. For this purpose, a planar raster dataset was generated for each measurement based on the least squares method. The resulting raster representing average two-dimensional slope in a plot was then substracted from the original microtopography model to systematically remove the slope effect. This detrending procedure was also carried out for the microtopography models covering the open plots with erosion rills, although planar detrending could not account for the highly curvaceous surfaces. For this reason, a focus was laid here on local roughness measures, which are only partly affected by slope effects at a larger scale. For comparison, each of the models was normalized to a minimum base elevation of 0 after detrending.

Within-plot elevation range (WPER)

Surface roughness has in the first step been quantified by the range of elevation values within a plot. It is calculated as the difference between maximum and minimum values within each detrended microtopography model. This global index represents roughness at the plot scale and reflects gross changes in microtopography.

Root-mean squared height (RMSH)

An apparent quantifier for surface roughness is the random roughness index. According to Eq. 1, this index was generated for all plots in the area, representing a single global value for the entire plot area.

Local root-mean squared height (locRMSH)

Since microtopography is highly heterogeneous in space, a local adaptation of the RMSH, the locRMSH (local RMSH) index, was applied to all plots according to Eq. 2). With this index, a sliding window of size $m_x \cdot n_y$ calculates the local variations in random roughness

and is therefore suitable for finding local inconsistencies within a microtopography model. The choice of an appropriate window size is crucial for capturing different surface patterns and has been varied in four steps between 3 and 55 mm (3, 7, 21, 55 mm), resulting in considered areas of 9 mm² to 3.25 cm² (Figure IV-4).

$$RMSH = \sqrt{\frac{1}{MN}\sum_{c=0}^{M-1}\sum_{r=0}^{N-1}\left[z(x_c y_r) - \mu\right]^2} \quad (1)$$

RMSH: Root-mean squared height

M: number of columns

N: number of rows

c: column index

r: row index

$z(x_c,y_r)$: z-value at position x_c, y_r

μ: average z-value

$$locRMSH = \sqrt{\frac{1}{(x_l - x\ ) \cdot (y_l - y\ )}} \cdot \sqrt{\sum_{c=x_f}^{x_l}\sum_{r=y_f}^{y_l}\left[z(x_c y_r) - \mu\right]^2} \quad (2)$$

locRMSH: Local root-mean squared height

x_f: index of first column

x_l: index of last column

y_f: index of first row

y_l: index of last row

c: column index

r: row index

$z(x_c,y_r)$: z-value at position x_c, y_r

μ: average z-value

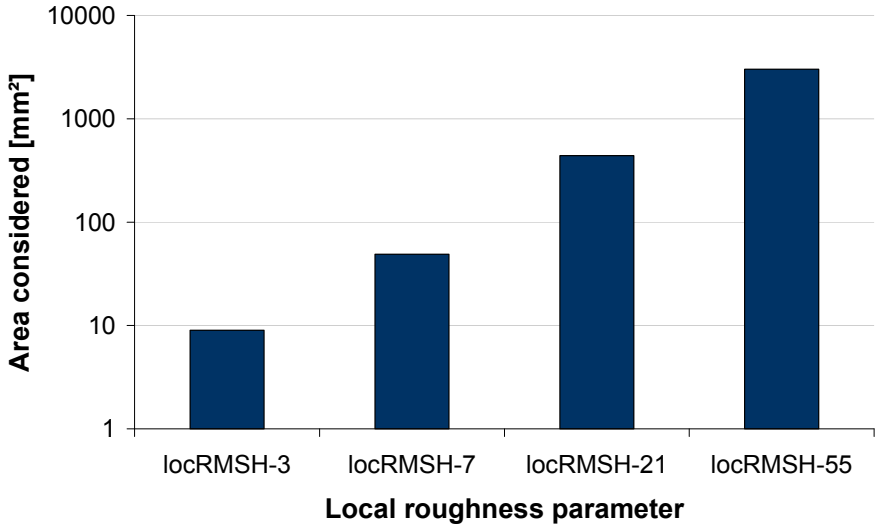

Figure IV-4 Localization of roughness parameter locRMSH.

For all indices at each plot, statistical parameters to summarize the temporal variability among the measurement dates were calculated. Two-dimensional raster datasets were additionally generated to represent the spatial roughness distributions spatially.

3 Results

Soil microtopography models were generated according to the processing chain shown in Figure IV-3a. The accuracy of the data collection and pre-processing method was estimated based on redundant measurements of plot P3, resulting in an average error of 0.19 mm (Standard Deviation (SD)=1.05 mm), while 80% of the pixels show accuracies in sub-millimeter resolution. Larger deviations mainly occur near the plot boundaries as well as around large particles within the plots.

3.1 Within-plot elevation ranges

The temporal variability of elevation ranges (WPER) of the linearly detrended microtopography models is summarized in Table IV-2. The minimum within-plot range is 13.13 mm (P3 on 2005, May 10th), while the maximum range of 204.56 mm can be found in the open plot R1 (2004, August 11th). The variations of WPER within the confined plots P1 to P6 are generally smaller compared to the variations found in the open plots R1 and R2. This corresponds to the fact that linear detrending achieves best results when surfaces are almost planar at the plot scale, i.e. when the slope is homogeneous in direction and

magnitude over the entire area, as is the case in the confined plots (Figure IV-5a). In contrast, R1 and R2 exhibit small interconnected and non-parallel erosion rills with relatively low elevations surrounded by interrill areas of convex surface shapes and relatively high elevations Figure IV-2a. While the overall slope in drainage direction is removed by linear detrending, remaining nondirectional surface height variations persist.

Smaller remaining non-linearities can also be observed in the confined plots (Figure IV-5a). These are partly caused by slightly higher elevation values detected near the plot borders facing the main wind direction. Detachment of soil particles by wind erosion and subsequent accumulation at the physical barrier are likely to be the processes that form this spatial pattern. A quantification of these processes was, however, not in the focus of this study and therefore not further considered.

P4 and P5 stand out relative to the other plots with very high and low variations of WPER values, respectively. While the low variation for P5 together with a relatively low standard deviation of 5.77 mm indicates a specifically stable surface structure, the high values at P4 are due to a combination of two features observed in the field: first, the formerly described accumulation of surface material near the plot borders, and secondly, small depression areas due to pawprints of >40 mm depth, which were accidentally formed by a dog between October and December 2004. Comparing P3 with the other confined plots on the same tertiary substrate, it can be observed that the plot size (P3: 0.25 m² compared to 1m² for the others) has an effect in terms of lower range of WPER.

Table IV-2: Elevation ranges per plot from 17 measurement series within 2004 and 2005 (after detrending). SD: Standard Deviation; CV: Coefficient of Variation.

	Plot	Min	Median	Mean	Max	SD	CV
T	P1	30.48	52.43	50.47	67.88	11.88	0.24
	P2	30.04	47.13	45.36	65.35	10.02	0.22
	P3	13.13	27.21	27.42	49.38	10.62	0.39
	R1	162.89	182.64	182.54	204.56	13.93	0.11
	R2	70.79	97.56	97	116.86	15.58	0.16
Q	P4	33.93	54.72	60.81	117.1	23.61	0.39
	P5	45.9	49.36	51.19	60.22	5.77	0.11
	P6	35.66	49.07	55.67	85.72	16.64	0.27

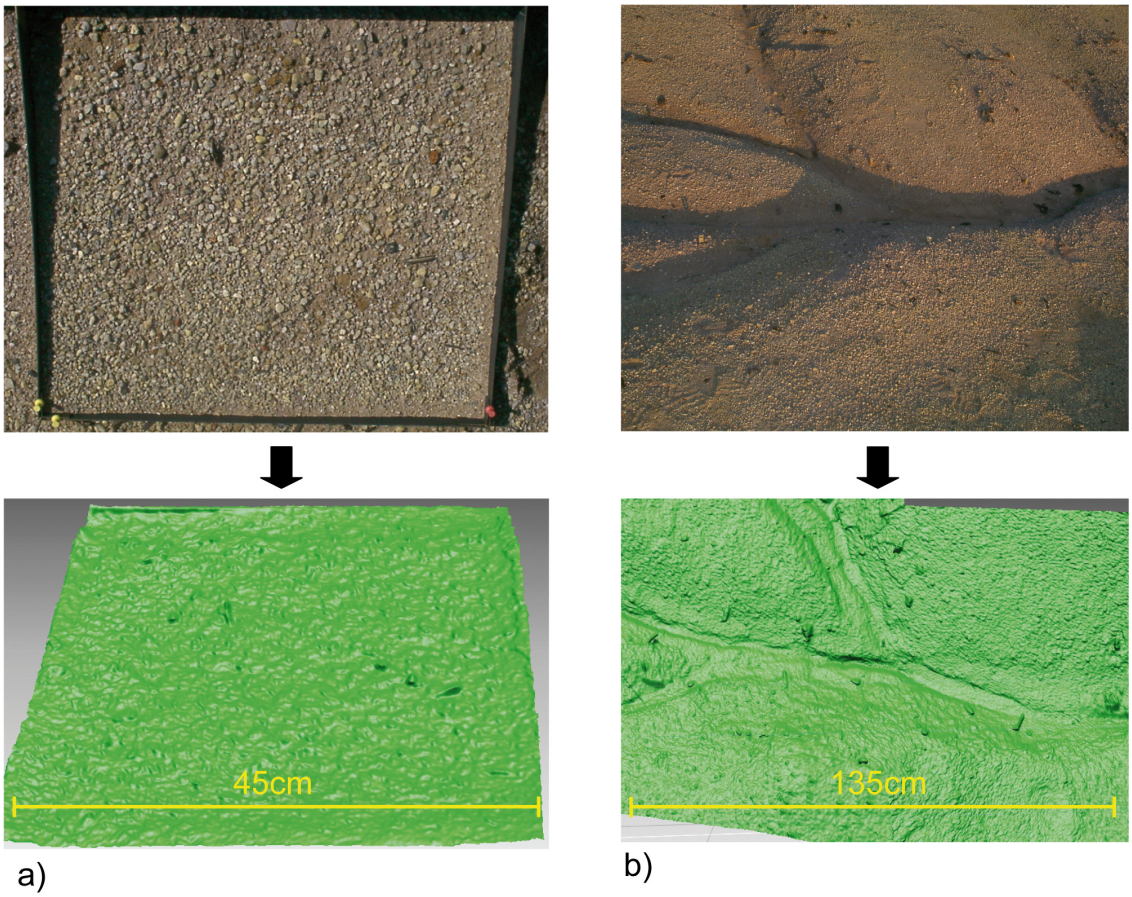

Figure IV-5 Results from microtopography model generation for a) open erosion plot (P3) and b) confined plot (R1) in the tertiary substrate (2004, September 1st).

3.2 Spatiotemporal roughness quantification

For each of the detrended microtopography models the global RMSH as well as four local roughness indices were calculated, with the later being localized to all pixels in the microtopography raster dataset. Table IV-3 summarizes these results in form of statistical distribution measures covering the multi-temporal data collection series. The values characterize the average temporal roughness variation in each plot as quantified by the different indices.

The size of the averaging window area has a direct effect on RMSH values. While global indices are highest, the locRMSH values decrease with the size of the window in all cases. This corresponds with the assumption of non-linear slopes within the plots: after linear detrending elevation trends remain in the microtopography models. Particularly in the open plots this is obvious, since the relative increase of the locRMSH index value with the window size of the analysis mask is highest. In contrast, locRMSH-3 median values of the measurements are similar in all plots. The relative large coefficient of variation (around 1) of this index within each time series of the confined plots is caused by high standard

deviations, while the mean values are consistently low. This indicates high temporal roughness dynamics at this scale. Roughness variability within the 3 mm neighborhood can be linked to either grain size variations or elevation differences that remain after detrending. In order to find the actual cause of roughness variations, analyses were performed locally in a later step.

For plot P5, the lower SD value of locRMSH-3 can be explained with a higher stability in terms of roughness within the 3 mm window. In case of the open plots R1 and R2, the range of median values per plot measurement is generally smaller (above a higher minimum threshold of 0.25 mm and 0.28 mm, respectively), indicating the influence of the elevation curvature also on aggregated roughness indices at this scale.

In terms of multi-temporal variability, locRMSH-7 indices are most stable for six of the eight plots (lowest SD and CV values). For the open rill R1 the relative large roughness values at all scales lead to relatively low CV values, while SD is lowest for the locRMSH-7 index similar to the other plots. In P5 roughness dynamics are similar for the local indices with 7 and 21 mm windows size. A comparison of the locRMSH-55 indices shows that highest dynamics at the larger scale are to be found in the open plot R1. This corresponds with the field observations of rill formation with time.

The local indices also show a different behavior for the two sandy substrates. While for the confined plots locRMSH-3 and locRMSH-7 values are similar in tertiary and quaternary sands, the roughness is generally higher in the quaternary plots with the larger window sizes. This corresponds with distinct surface structures that were noted in these plots. One potential explanation for this phenomenon is the relatively high soil moisture in average as reported by Haubrock et al. (2008b), which resulted in more stable soil aggregates and higher plasticity, and consequently in relatively large spatial elevation heterogeneities at the scale of few centimeters.

Spatial variability

The aggregated statistical values in Table IV-3 give an overview of the average dynamics of local and global roughness indices for each plot. In contrast to these global descriptors, the presence of spatial roughness patterns within a dataset becomes detectable applying local indices.

Table IV-3:Surface roughness ranges of single erosion plots from 17 measurement series within 2004 and 2005. The parameters representing local RMSH indices are based on median values calculated for each plot measurement.

	Plot	Index	Min	Median	Mean	Max	SD	CV
		RMSH	3.91	7.3	7.42	11.51	2.69	0.36
		locRMSH-3	0.001	0.23	0.18	0.42	0.17	0.98
	P1	locRMSH-7	0.43	0.53	0.52	0.65	0.07	0.14
		locRMSH-21	0.69	0.94	0.91	1.19	0.17	0.19
		locRMSH-55	0.99	1.25	1.29	1.87	0.27	0.21
		RMSH	3.4	5.7	5.61	9.9	1.98	0.35
		locRMSH-3	0.001	0.29	0.2	0.43	0.18	0.9
	P2	locRMSH-7	0.43	0.5	0.5	0.65	0.06	0.12
		locRMSH-21	0.67	0.86	0.83	0.98	0.11	0.13
		locRMSH-55	0.91	1.15	1.13	1.39	0.18	0.15
		RMSH	1.69	3.53	3.52	6.14	1.57	0.45
		locRMSH-3	0.001	0.16	0.16	0.34	0.15	0.97
T	P3	locRMSH-7	0.46	0.53	0.55	0.70	0.07	0.13
		locRMSH-21	0.73	0.93	0.96	1.36	0.18	0.19
		locRMSH-55	0.96	1.25	1.33	2.18	0.32	0.24
		RMSH	30.73	35.85	35.4	38.92	2.6	0.07
		locRMSH-3	0.25	0.35	0.34	0.45	0.07	0.2
	R1	locRMSH-7	0.69	0.77	0.81	1.05	0.12	0.15
		locRMSH-21	1.83	2.13	2.13	2.56	0.23	0.11
		locRMSH-55	4.48	5.19	5.21	6	0.54	0.1
		RMSH	15.9	18.95	19.17	22.71	2.7	0.14
		locRMSH-3	0.28	0.36	0.35	0.4	0.05	0.13
	R2	locRMSH-7	0.57	0.6	0.6	0.63	0.02	0.03
		locRMSH-21	1.2	1.29	1.29	1.36	0.06	0.04
		locRMSH-55	2.51	2.84	2.80	3.05	0.25	0.09
		RMSH	3.94	7.46	8.06	17.32	3.7	0.46
		locRMSH-3	0.001	0.16	0.18	0.43	0.19	1.04
	P4	locRMSH-7	0.46	0.49	0.51	0.67	0.06	0.12
		locRMSH-21	0.82	0.95	1	1.49	0.19	0.19
		locRMSH-55	1.25	1.68	1.73	2.55	0.38	0.22
		RMSH	6.44	7.3	7.62	8.78	1.05	0.14
		locRMSH-3	0.34	0.36	0.38	0.43	0.04	0.11
Q	P5	locRMSH-7	0.56	0.63	0.62	0.66	0.04	0.06
		locRMSH-21	1.18	1.23	1.24	1.32	0.06	0.05
		locRMSH-55	1.79	1.98	1.97	2.22	0.17	0.08
		RMSH	5.31	7.29	7.94	10.59	2.14	0.27
		locRMSH-3	0.001	0.29	0.2	0.43	0.2	0.98
	P6	locRMSH-7	0.49	0.62	0.61	0.81	0.1	0.16
		locRMSH-21	1.05	1.29	1.36	1.9	0.24	0.17
		locRMSH-55	1.8	2.14	2.4	3.22	0.45	0.19

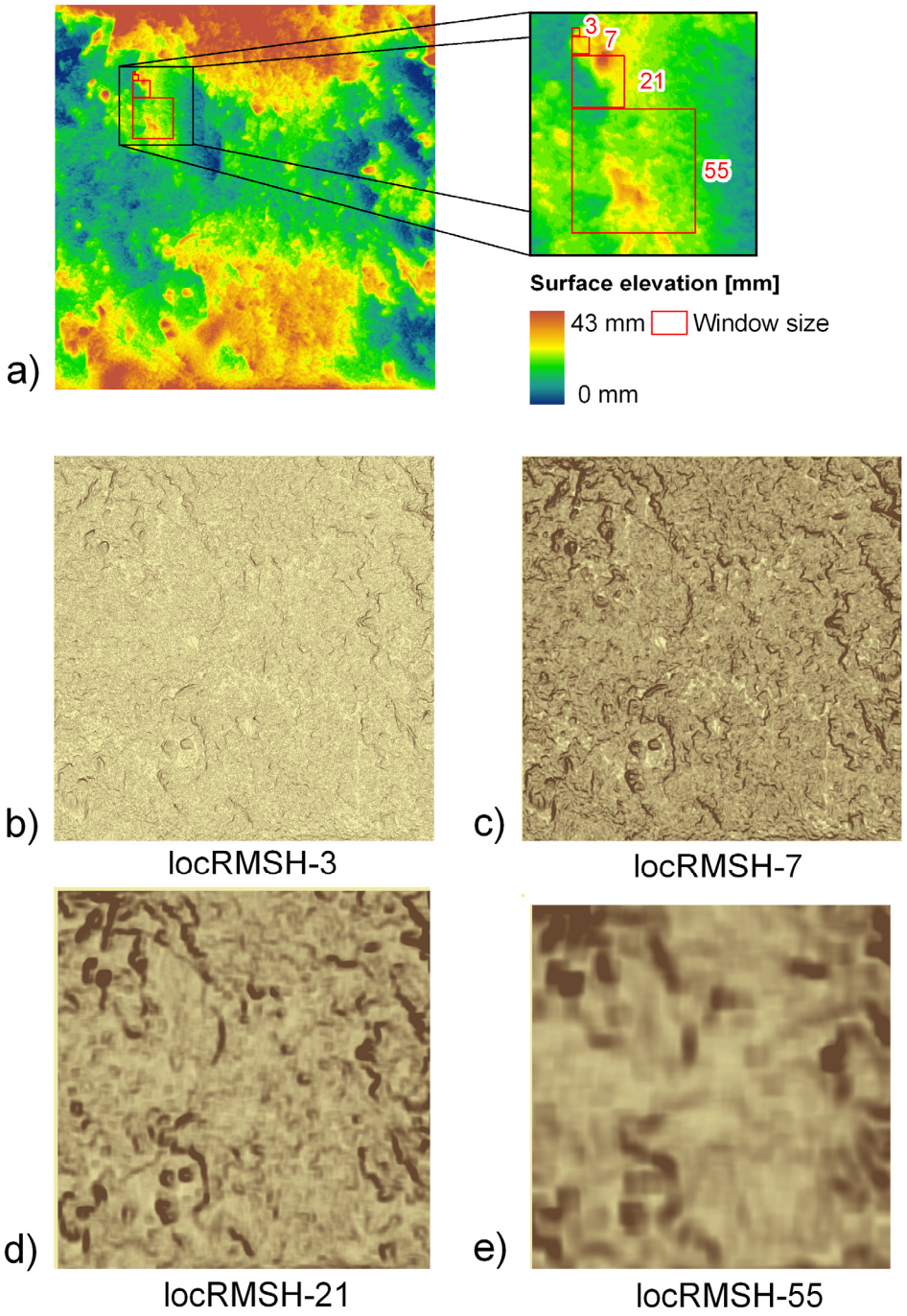

Figure IV-6 Window size effect for local RMS calculation: a) microtopography model, b) to e) local roughness maps with window sizes ranging between 3 and 55 mm (dataset from plot P6, 2005, October 12th).

Figure IV-6 shows the results of local RMSH calculations for a subset of plot P6 (2005, October 12th). In the microtopography model generated from the laser scanner data (Figure IV-6a) elevations range between 0 and 43 mm. Elevations are particularly high near the plot borders at the top and bottom of the image, whereas the central part shows significantly lower values. Between these three regions, relatively sharp transition zones exist.

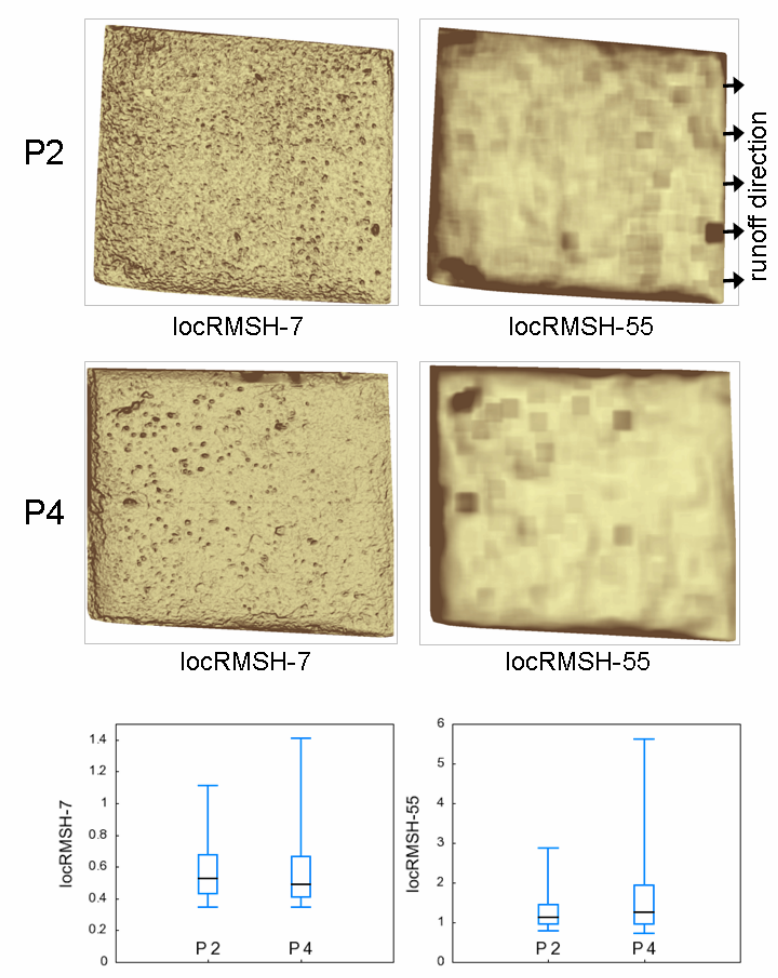

Figure IV-7 Local roughness indices for confined plots of tertiary (P2 from 2004, October 4th) and quaternary substrate (P4 from 2004, July 28th). Global roughness indices RMSH for comparison: P2: 5.86 mm, P4: 8.97 mm)

The locRMSH-3 indices visualized in Figure IV-6b show a typical salt-and-pepper effect. Microtopography roughness as represented by this index is highly heterogeneous within a small range of pixels, while this local variability is stable all over the plot. In contrast, distinct spatial roughness patterns become apparent in the locRMSH indices of larger window sizes. With a window size of 7 mm, larger particles, local depressions and ridges can be detected within the dataset (Figure IV-6c).

With further increase in size, the local spatial heterogeneity of the index is reduced, while single high roughness values form a strong contrast to the low roughness background. Finally, with a window size of 55mm the remaining high roughness values represent only sharp gradients from the original dataset. Due to the smoothing effect of the large window, the visualization is highly blurred and makes the exact location of the gradient in the original dataset difficult.

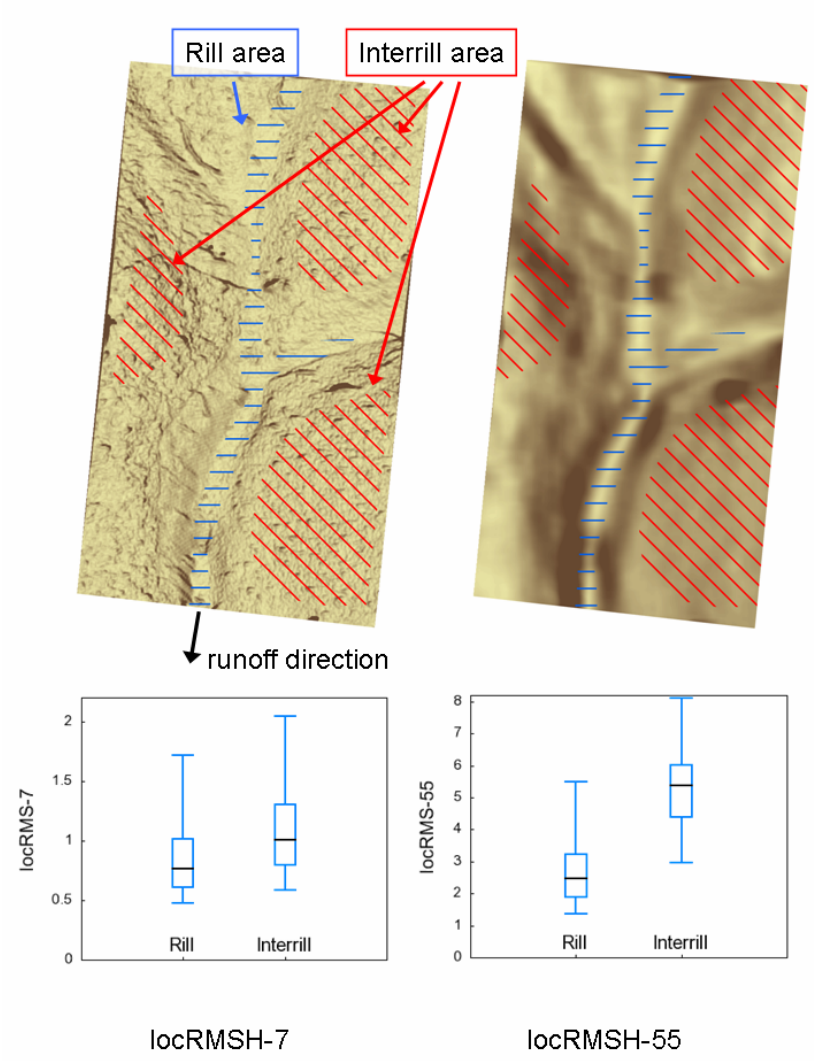

Figure IV-8 Local roughness quantifications of rill and interrill areas in plot R1.

Figure IV-6 shows that roughness index performance is highly dependent on the size of the local window. While local heterogeneities can be represented and localized using small windows sizes, larger windows enhance the separation of gradients that cover a corresponding number of image pixels. For the purpose of a more detailed analysis of these patterns, Figure IV-7 shows an example of within-plot surface roughness distribution (locRMSH-7 and -55) in the two confined plots P2 and P4 covering different substrates. In both models, heterogeneous surface roughness distributions can be observed, which are characterized by two patterns. First, single grains, particles and depressions form local roughness maxima within each plot. These local maxima are detectable mainly in the center of the plots, where slope effects are absent in the confined plots and therefore do not affect microtopography roughness values. Secondly, the plot borders show a different local

roughness distribution, with mainly lower values on the right side and higher values on the others.

Both patterns reflect the segregation processes taking place in the plots. While single soil particles above 2 mm size can be detected in the entire plot area, the right part of each plot is covered with material of smaller grain size. Since the general slopes are oriented towards this direction, this can be explained with the accumulation of fine grained material in front of the gutter that collects the plot runoff.

Roughness values near the other plot boundaries that form higher obstacles for substrate movements in P2 and P4 are different from those of the centric plot area. Consequently, soil particles of different sizes pile up near the borders. Thus, higher values in these parts represent slope effects rather than roughness at the microscale. This assumption is underpinned by the local maximum of locRMSH-55 values near the three plot borders.

While roughness values are locally very heterogeneous within the tertiary substrates in P2, a more distinct spatial pattern can be observed in P4: the overall roughness in the middle of the plot is almost homogeneous, while a relatively low number of particles account for locally increased roughness values. This difference between the plots corresponds to the fact that quaternary substrates are characterized by a much smoother surface, lower average grain sizes and a small number of large particles. Comparing the local roughness indices with global RMSH values for the two confined plots, a significant difference between these two approaches depending on roughness type becomes obvious: the global RMSH index of P4 is 8.97 mm, while the same index for P2 is only 5.86 mm. In contrast, the statistical parameters of the locRMSH-7 distribution show a smaller median value for plot P4, while the 95%-percentile greatly exceeds the one of plot P2, i.e. global and local roughness indices come to different estimations for the plot.

In the open plots, erosion processes have formed a highly heterogeneous elevation and roughness distribution at all scales considered. Figure IV-8 represents the spatial heterogeneities of R1 in terms of the indices locRMSH-7 and locRMSH-55. The larger window size is appropriate for a separation of rill and interrill areas within the plot, where smaller index values tend to indicate rill areas (Figure IV-8b).

This effect can partly be explained by the comparatively flat surface of the rill bottom, but also by the detrending procedure, which almost completely removed the linear slope in the rill while the strong curvature of the interrill area remained. Consequently, roughness values of different scales interact in local roughness indices with large window sizes and

the latter need to be interpreted with care. For the quantification of grain sizes or micro-patterns, smaller window sizes as used by the indices locRMSH-3 and locRMSH-7 are to be preferred.

Temporal variability

The temporal development of surface roughness for the year 2004 has been analyzed in four plots based on the locRMSH-21 index (Figure IV-9). The index showed to be most dynamic in the upper percentiles per plot (95%-percentiles), with ranges between 2.3 and 3.1 mm for plot P1 and between 6 and 10.7 mm for plot R1. Plot P6 showed lowest roughness dynamics (3.7 to 4.2 mm), while substrate movements in the rill were responsible for high roughness dynamics in plot R1, as could be derived from roughness location maps.

Corresponding precipitation events were quantified in terms of duration and intensity (Table IV-4). Highest roughness values in the confined plots were measured in September (P1) and December (P4 and P6) of the year. Rainfall patterns before these two dates are characterized by the highest precipitation intensity per hour (9.1 mm) and a moderate volume (40.7 mm) for the period before September, and a maximum volume (95.6 mm) and moderate intensity per hour (4.8 mm/h) prior to the period before December. In open plot R1, rainfall conversely affected the surface roughness parameter, with low values appearing after both periods.

The number of datasets does not allow for a detailed statistical analysis, so no quantitative relationship with precipitation amounts can be derived from the data. While the analysis of the causes that lead to the observed temporal roughness distributions are beyond the scope of this paper, the observations, however, demonstrate that they are useful to set up relationships between dynamics of the surface roughness and other environmental factors.

Table IV-4: Precipitation data from local field measurements. I_{10}: maximum rainfall intensity in 10 minutes; I_{60}: maximum rainfall intensity in 60 minutes; -: no data available.

	Date	Sum [mm]	I_{10} [mm/10min]	I_{60} [mm/h]
2004	June 24th - July 7th	-	-	-
	July 7th - July 28th	50.2	3.4	7.8
	July 28th - August 11th	-	-	-
	August 11th - September 1st	40.7	3.1	9.1
	September 1st - October 4th	30.7	4.2	7.7
	October 4th - October 20th	45.9	0.9	2.1
	October 20th - December 8th	95.6	2.3	4.8

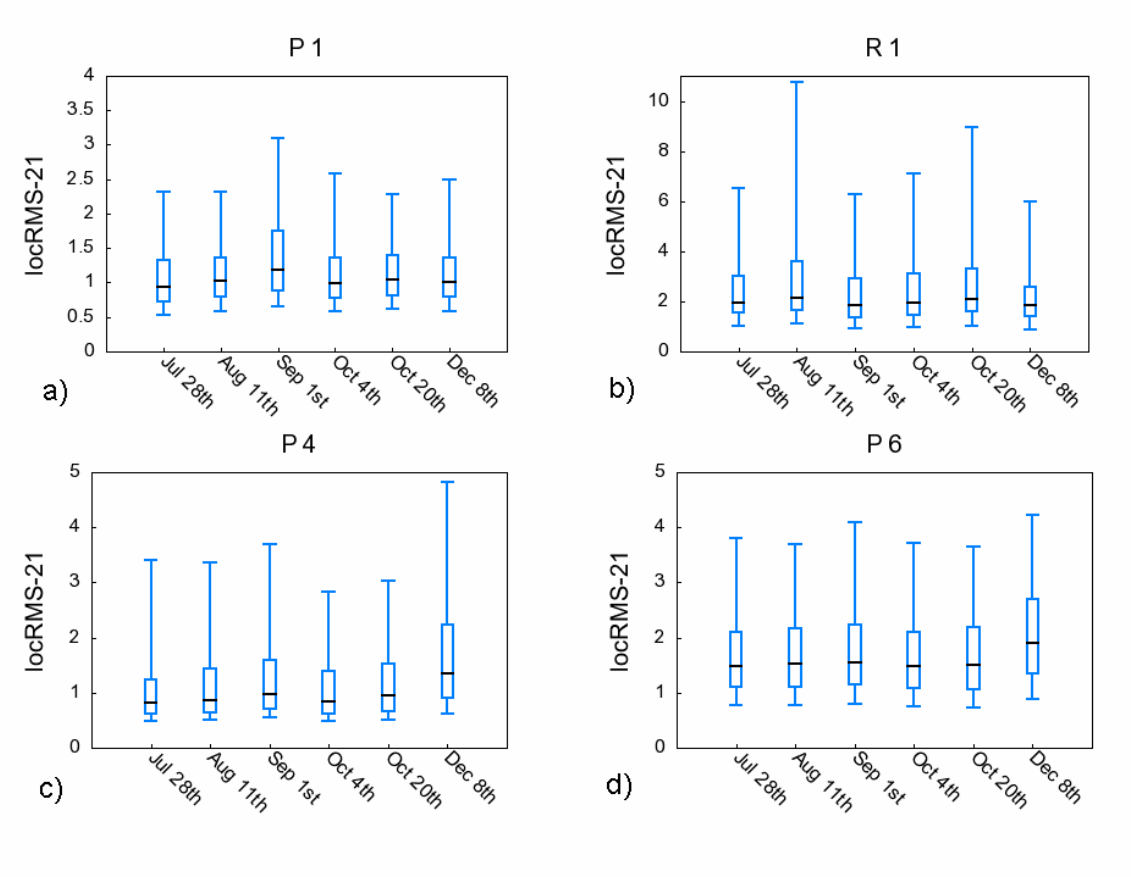

Figure IV-9 Roughness dynamics of four erosion plots in 2004 quantified with locRMSH-21: a) P1, b) R1, c) P4 and d) P6.

4 Discussion

4.1 Field laser scanning

This paper presents for the first time the field application of a laser scanner technology that has originally been developed for use in laboratory environments. The analyses performed in this study demonstrate its applicability also in natural environments in the case that appropriate illumination conditions and careful measurement setups are ensured.

While remote sensing methods are in most cases more efficient than mechanical in-situ measurements, the technology applied shows additional advantages. Compared to point lasers that have been comprehensively used in laboratory and field studies, this technology generates continuous results with higher spatial resolution by four measurements covering an area of a square meter. In former studies data collection was often performed by transportation of samples to the laboratory with subsequent laser scanner measurements (e.g. Solé-Benet et al. 1997). The possibility of direct in-situ measurements in the field

presents major advantages such as avoiding a potential bias due to material transport and the opportunity to observe surface processes under natural conditions in terms of e.g. wind and water erosion.

The effect of rainfall on roughness has been demonstrated in many studies before, but only few related roughness variations to natural precipitation events, which are much more heterogeneous in terms of intensity, duration and incident angle of raindrops. For a better understanding of surface processes in the field, natural heterogeneities, however, need to be taken into account. Huang and Bradford (1992) calculated roughness indices at different scales ranging from 1 to 400 mm using a point laser scanning technology in the laboratory and field. These indices were related in a few use cases to soil structure modifications caused by agricultural management and rainfall simulations, while natural precipitation events were not considered. For a better understanding of surface processes in the field, these rainfall effects, however, need to be taken into account. Indeed, studies with measurements of roughness parameters performed directly in the field have seldom been published with a corresponding spatial and temporal coverage, potentially due to the practical difficulty of such measurements. This paper demonstrates that the technology is appropriate for such studies under consideration of the discussed requirements.

4.2 Quantification of surface roughness

Data processing is critical for roughness quantifications, as co-registration is sensitive to accurate locations of ground control points, while artifact removal can affect roughness directly. Absolute quantification should therefore be related to the preprocessing accuracy, while relative spatial roughness distributions within a plot are invariant towards the preprocessing methods applied.

Quantification of surface roughness is highly scale-dependent as has been discussed by several authors (Huang and Bradford 1992; van Wesemael et al. 1996). The methods applied in this study account for this fact and additionally allow for the quantification of spatial heterogeneities.

Linear detrending is necessary for removing the effects of uniform and unidirectional slopes at the larger scale. Nonlinear slopes remain after detrending and affect roughness indices increasingly with larger window sizes. Some authors propose more heuristic procedures to improve the detrending effectiveness. Bryant et al. (2007) concluded from their studies that combining several transects of one-dimensional laser scanner measurements was useful to derive representative surface roughness datasets for a larger

area. A more sophisticated detrending procedure based on the combination of directional transects as well as higher-order regressions might have improved the removal of large scale elevations from the data, but was beyond the scope of this study. Instead, the generation of multi-scale indices allowed for determining and locating these effects visually.

Only in few studies before, the performances of various roughness indices was compared to each other (Govers et al. 2000), while most authors applied global indices for representing roughness in their study areas. This study shows that the choice of scales as well as local heterogeneities are significant and allow for interpreting surface processes in more detail.

Figure IV-10 shows the effect of varying locRMSH window sizes on correlations with grain size as represented by homogeneous tertiary substrate samples after sieving in the laboratory. It corroborates the assumption that the choice of indices for roughness quantification is highly dependent on the subject of interest. While grain size variations are best reflected by a window size of 7 mm, locRMSH-55 allowed for the detection of accumulation zones near the plot borders. An evaluation of multiple indices is therefore suggested for separating the effect of different surface processes.

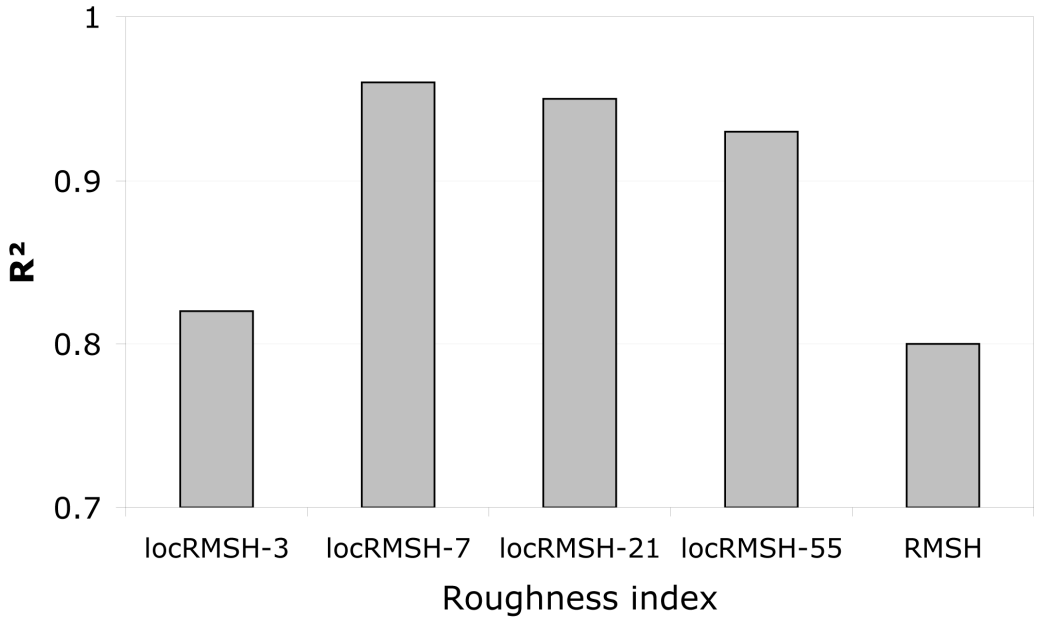

Figure IV-10 Correlation between grain size and RMSH roughness index values as a function of windows sizes for mixed tertiary substrate sample from the study area (RMSH and locRMSH median values). median values).

Other commonly used roughness indices include the dimensionless relations between measured and planar profiles in one (profile index) or two dimensions (Jester et al. 2005). A similar approach of multi-scale adaptation has not been published for these indices, but would certainly be interesting in comparison with the locRMSH index.

In the method proposed by Huang and Bradford (1992), surface roughness was quantified at different spatial scales using a combination of fractal and Markov-Gaussian processes. While these indices provide a means to represent scale-dependent roughness indices, information on their spatial distribution within an area cannot easily be represented. However, based on the findings of this study the visualization of spatial heterogeneities is strongly suggested in order to comprehend surface patterns which can be linked to relevant soil processes at the microscale.

As can be expected, the datasets show a higher variation in surface topography as the area under survey (the window size) is increased. Scale dependence is therefore an essential characteristic of roughness indices and should be explicitly accounted for. Linear detrending can only remove parts of the elevation effect on random roughness. While higher-order detrending might be an option for the confined plot areas, complex surface elevation structures as in the open plots will not be accounted for appropriately. For this reason, the determination of local roughness indices seems necessary. However, this is only possible when spatial resolution is high enough, which is the case for the laser scanner method presented here.

4.3 Understanding spatiotemporal patterns of surface roughness

Although a full analysis of spatiotemporal variations of surface roughness in relation with substrate type, scale of plots, precipitation events and other factors is beyond the scope of this paper, we demonstrated that the laser scanner method can be appropriate for this analysis based on some representative example analyses.

Processes that govern different soil surface morphologies are mostly assumed to be related to rainfall events by a) rain drop impact and subsequent soil aggregate collapse and b) shear stresses induced by runoff. In combination with other factors such as soil and solute physico-chemical properties (Römkens et al. 1990) and the spatial heterogeneity of slope and aspect, highly heterogeneous micro-relief patterns develop. In our study, the effect of raindrop impact has been noted in the quaternary plots and was represented by local roughness indices (locRMSH-7). The results in this study show different roughness characteristics for interrill and rill areas, which corresponds with the results from other

studies (Abrahams et al. 1996; Govers et al. 2000). While the data indicate relations between precipitation intensity and surface roughness, they were not further quantified in the scope of this paper. Further studies are therefore needed to enhance the understanding of processes taking place and their interrelationships at the microscale under consideration of substrate characteristics.

The increased knowledge about inter-relationships between variations in precipitation and infiltration characteristics provide an essential conceptual basis for scaling up the results from plot-scale measurements to catchment scales. Inter-relationships between precipitation, infiltration, runoff and erosion are beginning to be understood well enough to be quantified in effective erosion and landscape development models (Kirkby 2001). More knowledge needs to be gathered to perform this upscaling with manageable uncertainties, e.g. concerning the choice and number of representative proxy erosion plots.

5 Conclusion

In this study, multi-temporal monitoring of soil microtopography changes in the field was performed for the first time based on two-dimensional high-resolution laser scanning. This study suggests both, a method to collect microtopography data in the field at very high resolution and a set of roughness indices that can be used to account for different scales and local heterogeneities. Only the combination of three factors allowed for performing an analysis of surface processes: the technology used with its high spatial resolution in the mm scale, the development of local roughness indices at multiple scales as well as the multi-temporal study design facilitating the monitoring of roughness changes in detail.

The feasibility of the method has been demonstrated by the successful generation of microtopography models over 17 measurement series in eight bounded and unbounded erosion plots over two years. Based on a set of newly developed local roughness indices, the applicability of this method to detect spatiotemporal roughness patterns has been illustrated. Changes in surface height are detected down to the scale of single (larger) grains. Local variations in surface height as quantified by the locRMSH-7 index can be linked to elevation edges, small particles and rainfall impact. With the locRMSH-55 index slopes in the cm scale can be quantified, allowing for the evaluation of the detrending performance and thus the interpretation of global roughness indices.

It has been shown that roughness variations are due to heterogeneities in substrate composition, allocation to rill and interrill zones as well as boundary effects caused by physical obstacles. The methods applied based on high-resolution microtopography datasets provide an efficient means to quantify these spatial patterns adequately and thus allow a more detailed analysis of surface processes over time.

Interactions between soil surface properties, water runoff and erosion occur at many temporal and spatial scales (Kirkby 2001). For future soil erosion modeling, the effect of soil microtopography needs to be analyzed in greater detail. More experimental work is needed in order to better understand pattern formation and process interdependencies..

So far, data limitation was a crucial bottleneck in advancing the understanding of roughness effects on infiltration (Govers et al. 2000). With the technology presented and methods developed in this paper, it becomes feasible to generate invaluable datasets representing spatiotemporal microtopography patterns in the field. The application of the technology allows for the derivation of advanced roughness indices from remote sensing data to be linked with hydrological variables. It enables the determination of grain size distributions and mass movement quantifications and as such bares a high potential for delivering data that can advance the understanding of surface processes taking place at the plot-scale.

Chapter V:Synthesis

1 Summary and main conclusions

The overarching goal of this thesis was to develop and evaluate the feasibility of new remote sensing methodologies for the quantification of soil surface properties and to assess the potential and limitation of these methods to contribute to an improved understanding of surface processes in the context of soil erosion. For this purpose, data was collected from of 4 ha study area sensitive to erosion processes that similarly occur in dryland environments suffering from land degradation.

The unique setting of the test site in sandy substrates allowed for a thorough analysis of surface properties and their changes related to surface and near-surface processes taking place. Remote sensing measurements performed in the laboratory, field, and from airborne platforms resulted in quantification models that were linked to the data collected in-situ. Based on the facilities at the test site, soil moisture and roughness patterns as dominant factors for surface processes were monitored in adequate spatial and temporal resolution. Due to the interdisciplinary study approach, validation of the remote sensing results was ensured.

<u>Research question I:</u> *What is the potential of reflectance-based soil moisture quantification models in natural environments and how are they affected in comparison with laboratory set-ups?*

Chapter II developed and compared different surface soil moisture quantification models based on reflectance datasets of high spectral resolution. The study design focussed on a comparison of model outcomes for two types of samples. Correlations between reflectance-based quantification models and validation data were generally better when soil samples had been cleaned, sieved and stratified by their substrate composition (sample type 1). For unprepared and impure samples, representing natural field conditions (sample type 2), most of the established methods failed due to the influence of covariates like variable organic matter, physical crusts, particle size, and impurities. Based on the systematic combination of reflectance values from multiple bands, the analyses discovered an optimum surface soil moisture quantifier named the *Normalised Soil Moisture Index (NSMI)* based on reflectance values at 1800 and 2119 nm. While the correlation of the NSMI estimations with validation data was insufficient for allowing prediction of soil moisture in the field with very high precision (R^2=0.61), removing the effect of organic matter could significantly improve the model outcome (R^2=0.71). The effect of substrate

composition and physical crusts did not affect the estimation accuracy essentially, indicating a great potential of the NSMI as surface soil moisture quantifier in field studies for different sandy soil types provided that organic matter abundance is marginal.

Research question II: Are soil moisture quantification models applicable to airborne hyperspectral sensors (imaging spectroscopy) and under which terms can the resulting data sets be integrated into surface processes analysis?

Chapter III analysed the potential of the NSMI quantifier when being adjusted to airborne spectral imaging datasets recorded with the HyMap hyperspectral sensor. Important differences to the first study were associated with the recording system, spatial resolution, surface cover heterogeneities in the field as well as validation methods applied. The second study focused on the sandy substrates resulting in an improved correlation (R^2=0.82), since clay areas were not considered as in the first study due to high vegetation cover in the field. The pixelwise soil moisture quantification model allowed for the identification of spatial patterns in surface soil moisture distribution as well as sources of quantification uncertainties. The spatial resolution of 4x4 m² pixels allowed for the detection of soil moisture gradients over a large range of values among and between different substrates, which were congruent with datasets derived from physical in-situ measurements. Vegetation cover in the field was identified to be the main source of uncertainty, resulting in significant overestimations when NDVI values were around 0.3. The effect of substrate composition on validation accuracy was marginal compared to common uncertainties associated with data collection and the effect of vegetation cover. The broader spectral resolution of the HyMap sensor proved to be sufficient for an acceptable quantification accuracy. In addition, local shifts in bands used by the NSMI affected the correlation only marginally, while the original wavelengths detected in the first study were confirmed to represent the optimum choice. The resulting soil moisture maps represented well the surface properties, while in-situ measurements identified a distinct substrate-specific vertical soil moisture profile. Consequently, only the combination of these datasets has the potential to reflect infiltration and runoff processes adequately in the field.

Research question III: Are in-situ laser scanner measurements suitable for deriving soil microtopography models to be used for the quantification of surface roughness and the monitoring of substrate movements?

Spatiotemporal surface roughness heterogeneities at the test site were quantified and analysed in Chapter III. The application of a high-precision laser scanning technology

allowed for collecting multi-temporal microtopography datasets of eight micro-erosion plots directly in the field. Novel roughness parameters could be defined based on the availability of high precision microtopography models. Roughness was quantified based on a multi-scale parameter set, which accounted for various spatiotemporal patterns that could be related to grain size distribution, particle movements, the separation of rill and interrill areas, substrate classification and slopes. The effect of precipitation patterns on roughness development as well as associated substrate movement processes was indicated and undermines the relevance of the methods applied for a better understanding of surface processes related to soil erosion.

What can be learned from the research in this thesis about the role of the applied remote sensing methods for understanding surface processes?

Soil erosion processes are manifold phenomena occurring in complex systems composed of various interrelated variables. The spatial heterogeneities and temporal changes of soil surface properties are paramount for underlying processes like infiltration and runoff. For a more comprehensive monitoring of surface properties as well as for a better understanding of the causes and consequences of surface processes such as soil erosion, studying surface properties at the plot to microcatchment scale at high spatial and temporal resolution proved to be useful. Laboratory experiments provide an adequate starting point for soil studies by analyzing the isolated effects of single parameters individually. The thesis has explicitly shown that only experiments in the field reflect natural conditions sufficiently, with an abundance of factors interacting in a complex environmental system.

The findings of this study underpin the potential of state-of-the-art remote sensing technologies to provide unprecedented datasets on soil properties. The technologies form in the first place a basis for the development of new quantification indices to be used with complementary information bringing further insights into the complex system of soil erosion. Reflectance spectroscopy can be applied at all relevant spatial scales, either in laboratory or field environments as well as from remote sensors. While different challenges arise with changes in scale (Ben-Dor et al. 2008), the potential of quantifying soil properties is generally given, allowing for the generation of datasets that are much-needed in studies aiming at a better understanding of surface processes. Surface soil moisture maps can be readily supplied based on the NSMI index provided that the quantification model has been calibrated to a specific environment and dataset. High spectral resolution is hereby essential to make best use of the effect of increasing soil moisture on reflectance in

the SWIR spectral range. This thesis further demonstrated the great potential of high-precision in-situ laser scanning for generating surface roughness maps at the micro-plot scale. Roughness patterns that are undetectable or can not be quantified when using other technologies are now comprehensible. The laser scanning method is associated with an elaborate data collection and processing procedure, making the coverage of larger areas by repeated measurements in the field infeasible. However, it bares the potential to provide invaluable information exceeding the plot scale. The results indicate the formation of spatiotemporal patterns that primarily depend on substrate types and boundary conditions, which can both be determined in the field by applying other methods if needed. Consequently, the total coverage of a larger area may be unnecessary in the case that a small number of representative plots can be identified as recurring proxies in a specific landscape.

Optical remote sensing methods measure properties of the uppermost surface layer. Soil properties are however variable in all three spatial dimensions. The studies confirmed that the vertical distribution of soil moisture is crucial for the interpretation of maps derived from optical remote sensing data. It can therefore be concluded that only a combination of multiple datasets allows for a thorough assessment of soil property states in the field. Remote sensing methods are needed since they provide comprehensive datasets that are collected simultaneously and offer comparability among locations. Complementary in-situ measurements are however necessary to relate surface properties to vertical profiles of the variables.

The remote sensing methods applied in this interdisciplinary study formed the basis for generating new insights in surface processes taking place at the test site. Spatiotemporal heterogeneities in surface soil moisture and roughness were quantified, while evidence for substrate movements was given based on substrate specific reflectance characteristics and changes in microtopography. For the scales under consideration, the remote sensing methods delivered missing data for a comprehensive qualitative understanding of the spatiotemporal erosion patterns in the field when being linked with precipitation patterns.

Inter-relationships between precipitation, infiltration, runoff and erosion are beginning to be understood well enough to be quantified in effective erosion and landscape development models (Kirkby 2001). Merritt et al. (2003) give an overview of common erosion and sediment transport models, which differ greatly in their complexity, scale and aims. As a general conclusion, the authors identified the lack in sufficient spatially distributed input

data to drive these models as one of the major reasons for the inapplicability of physics-based models. Due to the progress in technology and method development, remote sensing technologies increasingly provide a mean to overcome data shortages inhibiting the application of simulation models and development of further applicable models.

2 Future research

This thesis analyzed the role of two different remote sensing approaches for the quantification of distinct soil properties in the context of surface process analysis with an emphasis on soil erosion. Several interesting issues and challenges for follow-up research were identified during this study.

The study area allowed for the development and assessment of data collection and analysis methods due to its specific characteristics, but does not fully represent a typical landscape suffering from land degradation as represented for example by the Badland systems in the Mediterranean (Gallart et al. 2002). The potential of the approaches when being applied in other regions of the world needs yet to be evaluated. Dryland regions suffer from soil erosion according to a common scheme (Bull and Kirkby 2002), but each region has its specific characteristics and makes the adaptation of erosion monitoring and modelling approaches necessary (Kirkby 2001). The questions need to be answered whether the proposed methods can be applied likewise in different, potentially larger and more remote regions of the world from a practical point of view and in which way their successful application can deliver further insights into surface processes understanding.

Soil erosion is particularly damaging in terms of economical costs when agricultural areas are affected. This study focused on the analysis of soil properties and surface processes of sandy substrates, while agricultural soils are much more diverse in their physical and chemical properties. The applicability of the developed quantification models in agricultural areas is therefore of high socio-economical interest. The effects of soil properties like color and clay mineral abundance as well as crop residues on the NSMI are particularly interesting, but unknown so far. Future studies on this issue are planned covering the agricultural landscape around Demmin in northeast Germany (Gerighausen and Borg 2007), applying the NSMI for HyMap data from 2004. For the in-situ laser scanning approach, the impact of increased roughness on the quality of the data as well as the choice of locRMSH-indices needs special attention. Preliminary analyses performed

with the laser scanner in Saxony showed its potential for quantifying surface roughness also in tilled fields, which will be further evaluated in the future.

The results from this thesis promote the use of remote sensing technologies and quantification methods as a tool for the quantification of soil surface properties. The link to underlying processes could be demonstrated exemplary, but needs to be quantified more systematically in multi-disciplinary studies involving expertise from hydrology, soil science and geomatics. Soil surface processes are likely to vary among and within study areas, since surface property changes are highly sensitive towards multiple external factors. An interesting question to be answered is therefore how to deal with this heterogeneity when datasets cover only parts of the study area, but information is needed for entire landscapes. Other studies on soil properties undermine the potential of geostatistical methods to relate point measurements to two-dimensional coverage (Burgos et al. 2008). The detailed multi-temporal observation of small-scale proxy sites (as erosion plots or micro-catchments) for representing typical soil property and process patterns seams to be an efficient way of getting an overall picture, but has to be assessed for each landscape individually, while the uncertainties involved with such an approach need to be quantified.

With respect to future remote sensing studies at the catchment scale applying airborne sensors, challenges like heterogeneous atmospheric conditions, pollution, as well as high spatial variability in covariate land cover properties on the ground remain. When applying spaceborne sensors like EnMap in the future, low signal-to-noise ratios and BRDF effects are further objects of investigation. A combination of new, sophisticated methods and multiple remote and in-situ sensor types seems necessary either to remove disturbing side-effects or to quantify and model them adequately. Airborne sensors exhibiting various technologies are also used for the measurement of surface topography. The combination of multi-scale roughness indices and their visualization in form of spatial maps can be seen as a similarly fruitful approach to capture surface heterogeneities at the catchment scale (Carbonneau et al. 2004).

Soil erosion is an indicator of land degradation taking place in many regions of the world and will likely be accelerating when trends in climate change, land use patterns and population pressure are continuing (Müller 2007). A thorough understanding of the underlying surface processes, their relation to soil properties and spatiotemporal dynamics are of crucial importance for identifying appropriate countermeasures. Although monitoring land degradation in a holistic approach makes the analysis of long-term

datasets necessary, substantial processes playing crucial roles for degradation can be registered in shorter time spans (Bai et al. 2008). The recent technological developments in remote sensing promise better opportunities to monitor environmental phenomena, and the methods developed in the scope of this thesis have the potential to help developing an increased understanding of soil processes in future case studies.

References

Abrahams, A.D., Li, G., & Parsons, A.J. (1996). Rill hydraulics on a semiarid hillslope, southern Arizona. *Earth Surface Processes and Landforms, 21*, 35-47.

Adeel, Z., Safriel, U., Niemeijer, D., & White, R. (2005). *Ecosystems and Human Well-being: Desertification Synthesis*, Millennium Ecosystem Assessment. Washington, DC: World Resources Institute.

Angström, A. (1925). The albedo of various surfaces of ground. *Geografiske Annales, 7*.

Babaev, A.G. (1999). Desert Problems and Desertification in Central Asia: The Researches of the Desert. Berlin: Springer-Verlag.

Bach, H., & Verhoef, W. (2003). Sensitivity studies on the effect of surface soil moisture on canopy reflectance using the radiative transfer model GeoSAIL. *IEEE 2003 International Geoscience and Remote Sensing Symposium Proceedings*, 3 (pp. 1679–1681).

Bai, Z.G., Dent, D.L., Olsson, L., & Schaepman, M.E. (2008). *Global assessment of land degradation and improvement 1: identification by remote sensing*. Rome/Wageningen: FAO/ISRIC.

Baumgardner, M.F. (1985). Reflectance properties of soils. *Advances in Agronomy, 38*, 1-44.

Beck, R.H., Robinson, B.F., McFee, W.H., & Peterson, J.B. (1976). Info. Note 081176. Lab. Applic. Remote Sensing. Purdue University, West Lafayette.

Ben-Dor, E., & Banin, A. (1994). Visible and near-infrared (0.4-1.1μm) analysis of arid and semiarid soils. *Remote Sensing of the Environment, 48*, 261-274.

Ben-Dor, E., Irons, J.R., & Epema, G.F. (1999). Soil reflectance. In Rencz, A.N. (Ed.) *Remote Sensing for the Earth Sciences: Manual of Remote Sensing* (pp. 111-188). New York: Wiley & Sons.

Ben-Dor, E., Taylor, R.G., Hill, J., Dematte, J.A.M., Whiting, M.L., Chabrillat, S., & Sommer, S. (2008). Imaging spectrometry for soil applications. *Advances in Agronomy, Vol 97* (pp. 321-392).

Ben-Hur, M., & Wakindiki, I.I.C. (2004). Soil mineralogy and slope effects on infiltration, interrill erosion, and slope factor. *Water Resources Research, 40*, 1-8.

Berger, M., Kerr, Y., Font, J., Wigneron, J.-P., Calvet, J.-C., Saelh, K., Lopez-Baeza, E., Simmonds, L., Ferrazzoli, P., Van Den Hurk, B., Viterbo, P., Waldteufel, P., Petitcolin, F., Van De Griend, A., Attema, E., & Rast, M. (2003). *Measuring the moisture in the Earth's soil with ESA's SMOS mission*, ESA Bulletin.

Berk, A., Anderson, G.P., Acharya, P.K., Hoke, M.L., Chetwynd, J.H., Bernstein, L.S., Shettle, E.P., Matthew, M.W., & Adler-Golden, S.M. (2003). *MODTRAN 4 Version 3 Revision 1 Users's Manual*. Hanscom Air Force Base, MA: Air Force Research Laboratory.

Bertuluzzi, P., Caussignac, J.M., Stengel, P., Morel, G., Lorendeau, J.Y., & Pelloux, G. (1990). An automated, noncontact laser profile meter for measuring soil roughness in situ. *Soil Science, 149*, 169-178.

Beven, K.J. (2002). Runoff Generation in Semi-arid Areas. In Bull, L.J. & Kirkby, M.J. (Eds.), *Dryland Rivers: Hydrology and Geomorphology of Semi-Arid Channels* (pp. 57-105). Wiley & Sons.

Biemelt, D. (2000). Bestimmung der Grundwasserneubildung auf Offenlandbereichen der Lausitzer Bergbaufolgelandschaft. *PhD-Thesis*, Universität Cottbus.

Bogrekci, I., & Lee, W.S. (2004). The effects of soil moisture content on reflectance spectra of soils using UV-VIS-NIR spectroscopy. 7th International Conference on Pr*ecision Agriculture*, Minneapolis.

Bryant, R., Moran, M.S., Thoma, D.P., Holifield Collins, C.D., Skirvin, S., Rahman, M., Slocum, K., Starks, P., Bosch, D., & González Dugo, M.P. (2007). Measuring surface roughness height to parameterize radar backscatter models for retrieval of surface soil moisture. IEEE Geoscience and Remote Sensing Letters, 4, 137-141.

Bryant, R., Thoma, D., Moran, M., Holifield Collins, C., Goodrich, D., Keefer, T., Paige, G., Williamd, D., & Skirvin, S. (2003). Evaluation of hyperspectral, infrared temperature and radar measurements for monitoring surface soil moisture. Proceedings First Interagency Conference on Research in the Watersheds., 27-30 October 2003, Benson, Arizona (pp. 528-533).

Bull, L.J., & Kirkby, M.J. (2002). Dryland River Characteristics and Concepts. In Bull, L.J. & Kirkby, M.J. (Eds.), *Dryland Rivers: Hydrology and Geomorphology of Semi-Arid Channels* (pp. 3-15). Wiley & Sons.

Burgos, P., Madejon, E., Perez-de-Mora, A., & Cabrera, F. (2008). Horizontal and vertical variability of soil properties in a trace element contaminated area. *International Journal of Applied Earth Observation and Geoinformation, 10*, 11-25.

Capehart, W.J., & Carlson, T.N. (1997). Decoupling of surface and near-surface soil water content: a remote sensing perspective. *Water Resources Research, 33*, 1383-1395.

Carbonneau, P.E., Lane, S.N., & Bergeron, N.E. (2004). Catchment-scale mapping of surface grain size in gravel bed rivers using airborne digital imagery. *Water Resources Research, 40*.

Chabrillat, S., Kaufmann, H., Merz, B., Mueller, A., Bens, O., & Lemmnitz, C. (2003). Development of relationships between reflectance and erosion modeling: test site preliminary field spectral analysis. *3rd EARSeL Workshop on Imaging Spectroscopy*, Herrsching (pp. 165-172).

Chabrillat, S., Pinet, C., & Ceuleneer, G. (2000). Ronda peridotite massif: methodology for its geological mapping and lithological discrimination from airborne hyperspectral data. *International Journal of Remote Sensing, 21*, 2363-2388.

Clark, R.M., & Roush, T.L. (1984). Reflectance spectroscopy: quantitative analysis techniques for remote sensing applications. *Journal of Geophysical Research, 89*, 6329-6340.

Cloutis, E.A. (1996). Hyperspectral geological remote sensing: evaluation of analytical techniques. *International Journal of Remote Sensing, 17*, 2215-2242.

Cocks, T., Jenssen, R., Stewart, A., Wilson, I., & Shields, T. (1998). The HyMap airborne hyperspectral sensor: The system, calibration and performance. *1st EARSeL Workshop on Imaging Spectroscopy*, Zurich.

Daughtry, C.S.T., Hunt, E.R., & McMurtrey, J.E. (2004). Assessing crop residue cover using shortwave infrared reflectance. *Remote Sensing of Environment, 90*, 126-134.

De Vries, A.C., Kustas, W.P., Ritchie, J.C., Klaassen, W., Menenti, M., Rango, A., & Prueger, J.H. (2003). Effective aerodynamic roughness estimated from Effective aerodynamic roughness estimated from airborne laser altimeter measurements of surface features. *International Journal of Remote Sensing, 24*, 1545-1558.

Desir, G., & Marin, C. (2007). Factors controlling the erosion rates in a semi-arid zone (Bardenas Reales, NE Spain). *Catena, 71*, 31-40.

Doerr, S.H., Shakesby, R.A., & Walsh, R.P.D. (2000). Soil water repellency: its causes, characteristics and hydro-geomorphological significance. *Earth Science Reviews, 51*, 33-65.

Engman, E.T. (2000). Soil moisture. In Schultz, G.A. & Engman, E.T. (Eds.), *Remote Sensing in Hydrology and Water Management*. Berlin: Springer.

Eshel, G., Levy, G.J., & Singer, M.J. (2004). Spectral Reflectance Properties of Crusted Soils under Solar Illumination. *Soil Sci Soc Am J, 68*, 1982-1991.

Farrand, W.H., & Harsany, J.C. (1995). Discrimination of poorly exposed lithologies in imaging spectrometer data. *Journal of Geophysical Research, 100*, 1565-1578.

Flanagan, D.C., Huang, C., Norton, L.D., & Parker, S.C. (1995). Laser scanner for erosion plot measurements. *Transactions of the ASAE, 38*, 703-710.

Gallart, F., Solé, A., Puigdefàbregas, J., & Lázaro, R. (2002). Badland Systems in the Mediterranean. In Bull, L.J. & Kirkby, M.J. (Eds.), *Dryland Rivers: Hydrology and Geomorphology of Semi-Arid Channels* (pp. 299-326). Wiley & Sons.

Gerighausen, H., & Borg, E. (2007). Derivation of synthetic endmembers for linear unmixing to improve parameter estimation for soil erosion modelling in agricultural ecosystems. In Reusen, I. & Cools, J. (Eds.) *5th EARSeL SIG IS Workshop "Imaging Spectroscopy: Innovation in Environmental Research"*, Bruges, Belgium.

Gerstengarbe, F.-W., Badeck, F., Hattermann, F., Krysanova, V., Lahmer, W., P., L., Stock, M., Suckow, F., Wechsung, F., & Werner, P.C. (2003). *Studie zur klimatischen Entwicklung im Land Brandenburg bis 2055 und deren Auswirkungen auf den Wasserhaushalt, die Forst- und Landwirtschaft sowie die Ableitung erster Perspektiven*, PIK Summary Report. Potsdam: PIK.

Goetz, A.F.H., & Curtiss, B. (1996). Hyperspectral imaging of the Earth: Remote analytical chemistry in an uncontrolled environment. *Field Analytical Chemistry and Technology, 1*, 67-76.

Goetz, A.F.H., Vane, G., Solomon, J.E., & Rock, B.N. (1985). Imaging Spectrometry for Earth Remote Sensing. *Science, 228*, 1147-1153.

Goldshleger, N., Ben-Dor, E., Benyamini, Y., & Agassi, M. (2004a). Soil reflectance as a tool for assessing physical crust arrangement of four typical soils in Israel. *Soil Science, 169*, 677-687.

Goldshleger, N., Ben-Dor, E., Benyamini, Y., & Agassi, M. (2004b). Soil reflectance as a tool for assessing physical crust arrangement of four typical soils in Israel. *Soil Science, 169*, 677-687.

Goldshleger, N., Ben-Dor, E., Benyamini, Y., Agassi, M., & Blumberg, D.G. (2001). Characterization of soil's structural crust by spectral reflectance in the SWIR region (1.2-2.5 µm). *Terra Nova, 13*, 12-17.

Goldshleger, N., Ben-Dor, E., Benyamini, Y., Blumberg, D., & Agassi, M. (2002). Spectral properties and hydraulic conductance of soil crusts formed by raindrop impact. *International Journal of Remote Sensing, 23*, 3909-3920.

Govers, G., Takken, I., & Helming, K. (2000). Soil roughness and overland flow. *Agronomie, 20*, 131-146.

Green, R.O., Eastwood, M.L., Sarture, C.M., Chrien, T.G., Aronsson, M., Chippendale, B.J., Faust, J.A., Pavri, B.E., Chovit, C.J., Solis, M.S., Olah, M.R., & Williams, O. (1998). Imaging spectroscopy and the Airborne Visible Infrared Imaging Spectrometer (AVIRIS). *Remote Sensing of Environment, 65*, 227-248.

Hanschke (2002). Kartierungsbericht im Tagebau Welzow-Süd / Fläche WW 0 42-H14. (pp. 4-18)

Haubrock, S.N., Chabrillat, S., Kuhnert, M., Hostert, P., & Kaufmann, H. (2008a). Surface soil moisture quantification and validation based on hyperspectral data and field measurements. *Journal of Applied Remote Sensing*, accepted.

Haubrock, S.N., Chabrillat, S., Lemmnitz, C., & Kaufmann, H. (2008b). Surface soil moisture quantification models from reflectance data under field conditions. *International Journal of Remote Sensing, 29*, 3-29.

Haubrock, S.N., Kuhnert, M., Chabrillat, S., & Kaufmann, H. (2008c). Spatiotemporal variations of soil surface roughness from in-situ laser scanning. *Catena*, submitted.

Heimovaara, T.J. (1994). Frequency Domain Analysis of the Time Domain Reflectometry Waveforms -1. Measurement of the Complex Dielectric Permittivity of Soils. *Water Ressources Research, 30*, 189-199.

Howden, S.M., Crimp, S.J., & Stokes, C.J. (2008). Climate change and Australian livestock systems: impacts, research and policy issues. *27th Biennial Conference of the Australian-Society-of-Animal-Production/68th Annual Conference of the New-Zealand-Society-of-Animal-Production*, Jun 24-27, Brisbane, AUSTRALIA (pp. 780-788).

Huang, C., & Bradford, J.M. (1990). Portable laser scanner for measuring soil surface roughness. *Soil Sci. Soc. Am. J., 54*, 1402-1406.

Huang, C., & Bradford, J.M. (1992). Applications of a laser scanner to quantify soil microtopography. *Soil Sci. Soc. Am. J., 56*, 14-21.

Huang, C., Gascuel-Odoux, C., & Cros-Cayot, S. (2002). Hillslope topographic and hydrologic effects on overland flow and erosion. *Catena, 46*, 177-188.

Huang, C., White, I., Thwaite, E.G., & Bendeli, A. (1988). A noncontact laser system for measuring soil surface topography. *Soil Sci. Soc. Am. J., 52*, 350-355.

Huemmrich, K.F. (2001). The GeoSail model: a simple addition to the SAIL model to describe discontinuous canopy reflectance. *Remote Sensing of Environment, 75*, 423-431.

Jester, W., Klik, & A. (2005). Soil surface roughness measurement - methods, appicability, and surface representation. *Catena, 64*, 174-192.

Karnieli, A., Kokaly, R.F., West, N.E., & Clark, R.N. (1999). Remote sensing of biological soil crusts. In Belnap, J. & Lange, O.L. (Eds.), *Biological soil crusts: structure, function, and management* (pp. 431-455). Berlin: Springer.

Khanna, S., Palacios-Orueta, A., Whiting, M.L., Ustin, S.L., D., R., & Litago, J. (2007). Development of angle indexes for soil moisture estimation, dry matter detection and land-cover discrimination. *Remote Sensing of Environment, 109*, 154-165.

Kirkby, M. (2001). Modelling the interactions between soil surface properties and water erosion. *Catena, 46*, 89-102.

Knapp, A.K., Fay, P.A., Blair, J.M., Collins, S.L., Smith, M.D., Carlisle, J.D., Harper, C.W., Danner, B.T., Lett, M.S., & McCarron, J.K. (2002). Rainfall variability, carbon cycling, and plant. *Science, 298*, 2202-2205.

Krüger, G., Erzinger, J., & Kaufmann, H. (1998). Laboratory and airborne reflectance spectrometric analyses of lignite overburden dumps. *Journal of Geochemical Exploration, 64*, 47-65.

Kruse, F.A. (1997). Regional Geologic Mapping along the Colorado Front Range from Ft Collins to Denver using the Airborne Visible/Infrared Imaging Spectrometer (AVIRIS). *12th Thematic Conference Applied Geologic Remote Sensing*, Nov.17-19 Environmental Research Institute of Michighan (ERIM), Ann Arbor, MI.

Kuhnert, M., Haubrock, S., Lemmnitz, C., Thoss, H., Bens, O., Chabrillat, S., & Güntner, A. (2004). Surface and near-surface processes in a microscale catchment – combining pedological, hydrological and remote sensing data. *Progress in surface and subsurface water studies at the plot and small basin scale - Euromediterranean Conference*, Turin.

Lemmnitz, C., Kuhnert, M., Bens, O., Güntner, A., Merz, B., & Hüttl, R.F. (2007). Spatial and temporal variations of soil water repellency and their influence on surface runoff. *Hydrological Processes, 22*, 1976-1984.

Lobell, D., & Asner, G. (2002). Moisture effects on soil reflectance. *Soil Sci. Soc. Am. J., 66*, 722-727.

Marker, M., Angeli, L., Bottai, L., Costantini, R., Ferrari, R., Innocenti, L., & Siciliano, G. (2008). Assessment of land degradation susceptibility by scenario analysis: A case study in Southern Tuscany, Italy. *Geomorphology, 93*, 120-129.

Marques, M.J., Bienes, R., Perez-Rodriguez, R., & Jimenez, L. (2008). Soil degradation in Central Spain due to sheet water erosion by low-intensity rainfall events. *Earth Surface Processes and Landforms, 33*, 414-423.

Massonnet, D., & Feigl, K.L. (1998). Radar interferometry and its application to changes in the earth's surface. *Reviews of Geophysics, 36*, 441-500.

Merritt, W.S., Letcher, R.A., & Jakeman, A.J. (2003). A review of erosion and sediment transport models. *Environmental Modelling & Software, 18*, 761-799.

Monteith, J.L. (1965). Evaporation and environment. *Symposium of the Society for Experimental Biology XIX*, (pp. 205-234).

Müller, C. (2007). Climate change and global land-use patterns - quantifying the human impact on the terrestrial biosphere. Hamburg: Max-Planck-Institut für Meteorologie.

Muller, E., & Décamps, H. (2000). Modeling soil moisture - reflectance. *Remote Sensing of Environment, 76*, 173-180.

Nadler, A., Dasberg, S., & Lapid, I. (1991). Time Domain Reflectometry Measurements of Water Content and Electrical Conductivity of Layered Soil Columns. *Soil Sci. Soc. Am. J., 55*, 938-943.

Okin, G.S., & Roberts, D.A. (2001). Remote Sensing in arid regions: challenges and opportunities. In Ustin, S. (Ed.), *Remote Sensing for Natural Resource Management and Environmental Monitoring*. Wiley & Sons.

Penman, H.L. (1956). Estimating evaporation. *Trans. Amer. Geophys. Union, 37*, 43-46.

Planet, W.G. (1970). Some comments on reflectance measurements of wet soils. *Remote Sensing of the Environment, 1*, 127-129.

Porporato, A., Daly, E., & Rodriguez-Iturbe, I. (2004). Soil water balance and ecosystem response to climate change. *Am. Nat., 164*, 625-632.

Profeti, G., & Macintosh, H. (1997). Flood management through Landsat TM and ERS SAR data: a case study. *Hydrological Processes, 11*, 1397-1408.

Römkens, M.J.M., Helming, K., & Prasad, S.N. (2001). Soil erosion under different rainfall intensities, surface roughness and soil water regimes. *Catena, 46*, 103-123.

Römkens, M.J.M., Prasad, S.N., & Whisler, F.D. (1990). Surface sealing and infiltration. In Anderson, M.G. & Burt, T.P. (Eds.), *Process Studies in Hillslope Hydrology* (pp. 127–172). Chichester: Wiley.

Römkens, M.J.M., Wang, J.Y., & Darden, R.W. (1988). A laser microreliefmeter. *Transactions of the ASAE, 31*, 408-413.

Scheffer, F., & Schachschabel, P. (2002). *Lehrbuch der Bodenkunde*. Heidelberg: Spektrum Akademischer Verlag.

Schmid, T., Schack-Kirchner, H., & Hildebrand, E. (2004). A case study of terrestrial laser scanning in erosion research: calculation of roughness and volume balance at a logged forest site. In Thies, M., Koch, B., Spiecker, H. & Weinacker, H. (Eds.) *ISPRS working group 8/2 'Laser-Scanners for Forest and Landscape Assessment'*, Freiburg (pp. 114-118).

Schodlok, M.C. (2004). Quantitative Analysen magmatischer Gesteine mittels reflexionsspetroskopischer Infrarot-Messungen. *PhD-Thesis*: Universität Potsdam.

Shepard, D. (1968). A two-dimensional interpolation function for irregularly-spaced data. *23rd National Conference ACM*, (pp. 517-524).

Solé-Benet, A., Calvo, A., Cerda, A., Lazaro, R., Pini, R., & Barbero, J. (1997). Influences of micro-relief patterns and plant cover on runoff related processes in badlands from Tarbernas (SE Spain). *Catena, 31*, 23-38.

Steffen, W., Sanderson, A., Tyson, P.D., Jäger, J., Matson, P.A., Moore III, B., Oldfield, F., Richardson, K., Schellnhuber, H.J., Turner II, B.L., & Wasson, R.J. (2004). *Global Change and the Earth System*. Berlin: Springer Verlag.

Sunshine, J.M., Pieters, C.M., & Pratt, S.F. (1990). Deconvolution on mineral absorption bands: an improved approach. *Journal of Geophysical Research, 95*, 6955-6966.

Ustin, S.L., Roberts, D.A., Gamon, J.A., Asner, G.P., & Green, R.O. (2004). Using imaging spectroscopy to study ecosystem processes and properties. *Bioscience, 54*, 523-534. In English.

van der Meer, F. (2004). Analysis of Spectral Absorption Features in Hyperspectral Imagery. *International Journal of Applied Earth Observation and Geoinformation, 5*, 55-68.

van Wesemael, B., Poesen, J., de Figueiredo, T., & Govers, G. (1996). Surface roughness evolution of soils containing rock fragments. *Earth Surface Processes and Landforms, 21*, 399-411.

Verhoef, W., & Bach, H. (2007). Coupled soil-leaf-canopy and atmosphere radiative transfier modeling to simulate hyperspectral multi-angular surface reflectance and TOA radiance data. *Remote Sensing of Environment, 109*, 166-182.

Vincente-Serrano, S.M., Pons-Fernandez, X., & Cuadrat-Prats, J.M. (2004). Mapping Soil Moisture in the Central Ebro River Valley (Northeast Spain) with Landsat and NOAA Satellite Imagery: a Comparison with Meteorological Data. *International Journal of Remote Sensing, 25*, 4325-4350.

Vitousek, P.M., Mooney, H.A., Lubchenco, J., & Melillo, J.M. (1997). Human domination of Earth's ecosystems. *Science, 277*, 494-499.

Wang, X.M., Chen, F., Hasi, E., & Li, J.C. (2008). Desertification in China: An assessment. *Earth-Science Reviews, 88*, 188-206.

Watson, R.T., Moss, R.H., & Zinyower, M.C. (1998). *The Regional Impacts of Climate Change: An Assessment of Vulnerability*.Cambridge University.

Weidong, L., Baret, F., Xingfa, G., Bing, Z., Qingxi, T., & Lanfen, Z. (2003). Evaluation of Methods for Surface Soil Moisture Estimation from Reflectance Data. *International Journal of Remote Sensing, 24*, 2069-2083.

Weidong, L., Baret, F., Xingfa, G., Qingxi, T., Lanfen, Z., & Bing, Z. (2002). Relating Soil Surface Moisture to Reflectance. *Remote Sensing of Environment, 81*, 238-246.

Wendling, U., Fuchs, G., & Müller-Westermeier, G. (1999). *Mittlere jährliche Verdunstungshöhe als Gras-Referenzverdunstung*.Bundesministerium für Umwelt.

Whiting, M.L., Li, L., & Ustin, S.L. (2004). Predicting Water Content using Gaussian Model on Soil Spectra. *Remote Sensing of Environment, 89*, 535-552.

Wisotzky, F., & Obermann, P. (2001). Acid mine groundwater in lignite overburden dumps and its prevention - the Rhineland lignite mining area (Germany). *Ecological Engineering, 17*, 115-123.

WRB, I.W.G. (2006). *World Reference Base for Soil Resources*, World Soil Reports. Rome: FAO.

Zhang, Y., & Wegehenkel, M. (2006). Integration of MODIS data into a simple model for the spatial distributed simulation of soil water content and evapotranspiration. *Remote Sensing of Environment, 104*, 393-408.